EnergyChem 4 (2022) 100073

Contents lists available at ScienceDirect

EnergyChem

journal homepage: www.sciencedirect.com/journal/energychem

Crystalline Porous Materials-based Solid-State Electrolytes for Lithium Metal Batteries

Luyi Chen [1], Kui Ding [1], Kang Li [1], Zhongliang Li, Xueliang Zhang, Qifeng Zheng [*], Yue-Peng Cai [*], Ya-Qian Lan [*]

School of Chemistry, South China Normal University, 55 West Zhongsan Rd., Guangzhou 510006, Guangdong, China

ARTICLE INFO

Keywords:
Crystalline porous materials
Solid-state electrolytes
Lithium metal batteries
High energy density

ABSTRACT

The ever-growing market for electric vehicles and grid-scale energy storage is boosting the development of high energy density lithium metal batteries (LMBs). Solid-state electrolytes (SSEs) are not only nonflammable to overcome the intrinsic drawbacks of liquid electrolytes, but also mechanically strong enough to suppress the growth of lithium dendrites, whose development could greatly promote the safety and performance of LMBs. Crystalline porous materials (CPMs) with high surface area, adjustable pores, ordered channels, and versatile functionality have not only provided a promising structural platform for designing fast ionic conducting materials, but also offered great opportunities for manipulating their physicochemical and electrochemical properties, which have shown great potential to fabricate high-performance SSEs and have become an emerging research direction in recent years. In this review, the latest progress of CPMs-based SSEs for LMBs, including pristine CPMs and CPMs-based composites, is systematically summarized. By discussing the pioneer work, both merits and issues arising from CPMs are emphasized as well as an outlook for the development of CPMs-based SSEs with high-performance and reliable safety are presented.

1. Introduction

Lithium-ion batteries (LIBs) have been widely used in our daily life as the power source for various portable electronics over the past decades.[1–3] To fulfill the ever-growing market for electric vehicles and meet the requirement for grid-scale energy storage, batteries with high energy density, reliable safety, and long cycle life have attracted intensive research interests.[3–6] The lithium metal with high theoretical capacity (3860 mAh g^{-1}) and lowest redox potential (-3.04 V versus the standard hydrogen electrode, SHE) has been recognized as an ultimate anode for high energy batteries.[7–9] Unfortunately, the application of lithium metal as the anode faces critical challenges, which are mainly arising from the utilization of highly volatile and flammable liquid organic electrolytes, as well as the side reactions with liquid electrolytes and growth of lithium dendrites, causing battery degradation and safety hazards.[10–13]

Replacing conventional liquid electrolytes with solid-state electrolytes (SSEs) can readily address these concerns along with lithium metal batteries, since the SSEs are not only nonflammable to overcome the intrinsic drawbacks of liquid electrolytes (i.e., leakage, volatility, and flammability), but also mechanically strong enough to suppress the growth of lithium dendrites.[14–17] In addition, solid/solid interfaces between the SSEs and electrodes are expected to slowing the side reactions, which would lead to improved coulombic efficiency and cycle life for lithium metal batteries.

Up to now, SSEs can be classified into three categories: inorganic solid electrolytes, solid polymer electrolytes (SPEs), and their composites.[16–20] Inorganic solid electrolytes, such as oxides (e.g., $Li_7La_3Zr_2O_{12}$, LLZO) and sulfides (e.g., Li_6PS_5Cl), generally possess high ionic conductivity, high ionic transference number, excellent mechanical robustness, and high safety.[20] For instance, the Kano's group reported a sulfide-based SSE, i.e. $Li_{9.54}Si_{1.74}P_{1.44}S_{11.7}Cl_{0.3}$, with a extremely high ionic conductivity of 25 mS cm^{-1}.[21] However, most inorganic solid electrolytes are still facing many challenges, such as air instability, poor processability, and large interfacial impedance. SPEs, such as PEO and poly(vinylidene fluoride) (PVDF), have great advantages of lightweight, high flexibility, ease of large-scale manufacturing, and low interfacial impedance, while their low ionic conductivity and

* Corresponding authors
E-mail addresses: qifeng.zheng@m.scnu.edu.cn (Q. Zheng), caiyp@scnu.edu.cn (Y.-P. Cai), yqlan@njnu.edu.cn (Y.-Q. Lan).
[1] L. Chen, K. Ding, and K. Li contributed equally to this work.

https://doi.org/10.1016/j.enchem.2022.100073

Available online 23 March 2022

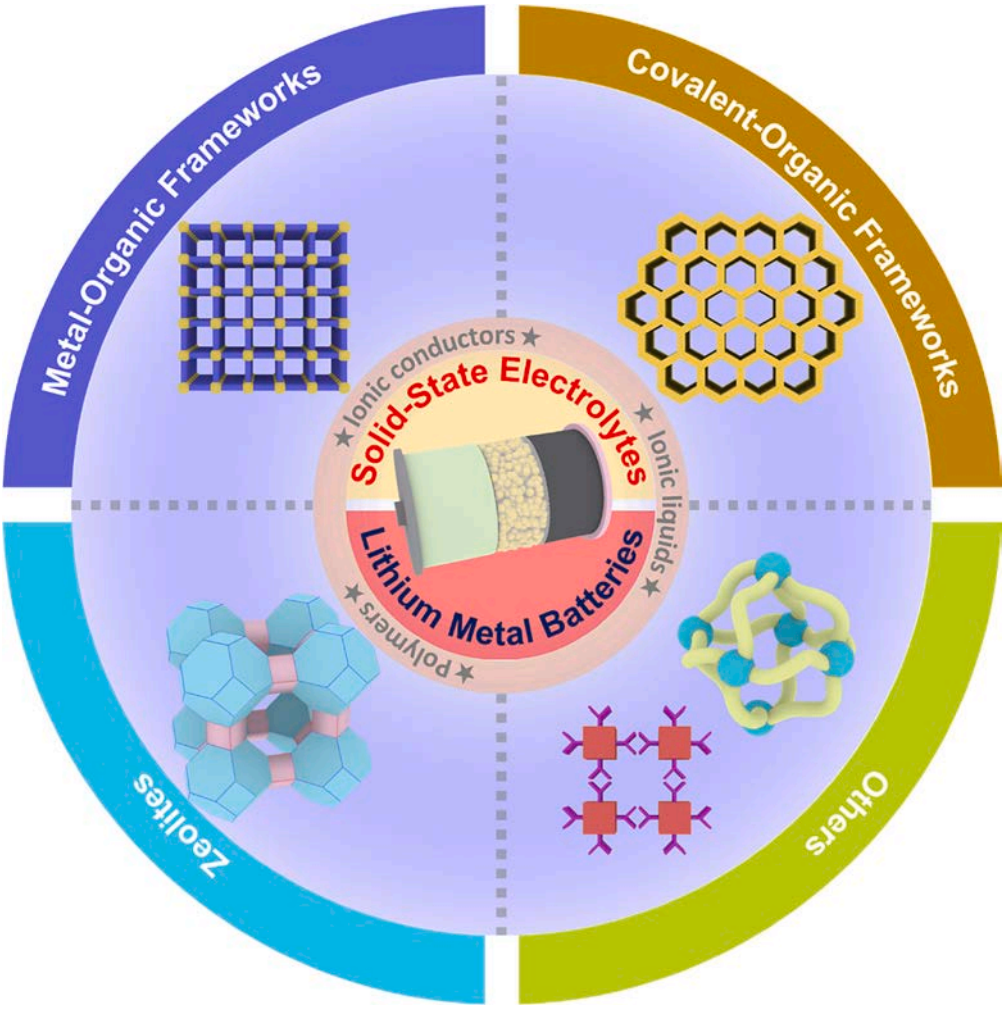

Scheme 1. Schematic illustrations of crystalline porous materials-based solid-state electrolytes for lithium metal batteries

poor mechanical strength hinder their practical applications.[22–24] Combining inorganic fillers with polymer matrix to form composite SSEs has been considered to be one of the most effective strategy to alleviate these issues to certain degree because it combines the advantages of inorganic and polymer electrolytes while overcoming their disadvantages.[17]' [19] Hence, to achieve an excellent performance for high energy density lithium metal batteries, the researchers have been delicated to optimizing the compositions/structures of the above-mentioned SSEs systems as well as exploring new SSEs fromulations.[25–27]

Over the past few decades, crystalline porous materials (CPMs), including metal-organic frameworks (MOFs), covalent-organic frameworks (COFs), zeolites, porous organic cages (POCs) and hydrogen-bonded organic frameworks (HOFs), have received tremendous development in the fields of gas separation and adsorption, catalysis, drug delivery, energy storage and so on, owing to their well-defined porous structures and facial functionality.[28–32] More recently, the application of CPMs in SSEs have emerged as a new research hotspot and attracted considerable attention due to their merits of insulativity, high surface area, adjustable pores, ordered channels, and surface functionality, which offers great opportunities for manipulating the physicochemical properties of the resulting CPMs-based SSEs (**Scheme 1** and **2**).[26–27]' [32–33]

Briefly, the merits of CPMs for SSEs can be summarized as follows: (i) the high surface areas of CPMs could offer sufficient contact with other components, thus reducing the interfacial resistance and promoting the ion transport; (ii) the adjustable pores (i.e., pore size, pore shape, and pore polarity) of CPMs could act as ion sieves that preferentially promote Li^+ transfer; (iii) the periodical crystalline structure with ordered channels of CPMs allows for the homogeneous Li^+ plating during the charging-discharging process, preventing the growth of lithium dendrites and improving the cycling stability; (iv) the variabilities of chemical compositions and surface functionalities have bestowed CPMs with high designability to accommodate the requirement of SSEs.

On account of the above-mentioned merits of CPMs, the periodical crystalline structure with aboundent active sites, including open metal sites (OMS) and ionic frameworks, is critical for the Li-ion conduction based on Lewis acid-base reaction. For most of CPMs, the cationic sites of the framework could anchor the anions to release more free Li^+ and reduce the Li^+ migration barrier, therefore the Li^+ conduction is through hopping involving neighboring site within the ordered channels. Furthermore, the Li^+ conductive segments could be assemble into the framework through the covalent bond or coordination, making for the Li^+ transport more fast. CPMs with such type of the Li^+ transport mechanism can be classfied as Lewis acidic conductors. The other type of CPMs is single ion conductors, of which the anions are immobilized by covalently linked to the framework, where the Li^+ transport is based on the complexation and dissociation reactions between the Li^+ and anions. CPMs with such type of the Li^+ transport mechanism can be considered as Lewis basic conductors, where the lithium transference number can reach as high as 1.

In this review, we will first systematically summarize the latest progress of CPMs-based SSEs for LMBs, including pristine CPMs and

Scheme 2. The timeline for crystalline porous materials-based solid-state electrolytes.

CPMs with other components (e.g., ionic liquid, polymer, and inorganic filler), for which both merits and issues arising from CPMs will be emphasized. In the end, an outlook for the development of CPMs-based SSEs with high-performance and reliable safety will be presented from the fundamental mechanism understanding, rational desgin, and controllable synthesis.

2. MOF-based SSEs

MOFs, also known as porous coordination polymers (PCPs), are a kind of star porous crystalline material with reticular chemistry, which are constructed by metal ions/clusters and organic ligands with high surface area, high porosity, adjustable porous structures, and intrinsic insulation. Recently, it has shown great potential for the application of MOFs as filler into SSEs, and the merits of this method are summarized as following (Fig. 1): (i) The high surface area of MOFs could improve the interfacial contact with electrodes and electrolytes and then endow SSEs with a low resistance. (ii) The custom-made porous chemistry of MOFs based on various metal nodes and ligands (including particle size, pore size, framework chemistry) could be seen as a robust platform to optimal the electrochemical performance of SSEs. (iii) The abundant microporous within the order channel of MOFs could be helpful for Li^+ to form a homogenous flux through a convenient pathway and further be beneficial to guide the uniform plating/stripping during the charge/discharge process. (iv) The functionality or modification from the organic ligands would anchor anions through strong adsorption and further enhance Li^+ transportation. (v) The homogenous sites on the surface of order channels would be prefer to immobilize anion based on Lewis acid-base interaction, resulting in high Li^+ transference number.

In this review, we outline the progress of MOF-based SSEs in lithium metal batteries as the following categories: (1) MOF ionic conductors; (2) MOF/ionic liquid-based SSEs; (3) MOF/polymer-based SSEs; (4) MOF/multicomponent-based SSEs.

2.1. MOF ionic conductors

In this section, we describe the recent advances in MOF ionic conductors, in which there are two main strategies: MOF incorporated with lithium salts and anionic MOF.

2.1.1. MOF incorporated with lithium salts

Usually, the active sites of the adopted ligands are almost participated in the coordination with metal center nodes formatting secondary building units and no longer accessible for binding with the extra guest cation. Oligobenzoates and polybenzoates are a significant class of compounds in design multifunctional MOFs, such as UIOs, MILs, HKUSTs, and some other MOFs. In term of the intrinsic merits of polybenzoates, Long's group consecutively developed a series of promising MOF ionic conductor,[34–35] such as Mg_2(dobdc), and Mg_2(dobpdc) adopted with **H_2bdc, H_4dobdc**, and **H_4dobpdc**, respectively. As in Mg_2(dobdc), one-dimensional hexagonal channels with diameters of about 14 Å that are lined with coordinatively unsaturated Mg^{2+} cation sites were realized. The authors speculated that the presence of OMS could facilitate the uptake of a lithium alkoxide, resulting in a higher ionic conductivity (up to 3.1×10^{-4} S cm^{-1} at 300 K.). Then, the alkoxide anions were simultaneously favor to bind the Mg^{2+} of the framework, and pinned inside the channels leaving the freedom Li^+ to move. Further, the OMS coordinating nucleophilic anions and absorbing more electrolyte, could inhibit the migration of nucleophilic anions and then be favor to facilitate cation mobility, which was proved in another attractable work of Mg_2(dobpdc) (Fig. 2**a**). Also, both the pore size (13 and 21 Å) and the anion basicity of magnesium salts, *i.e.*, PhO^-, $MePhO^-$, CF_3PhO^-, and $TFSI^-$, had been demonstrated as the crucial factors on the charge transport properties MOF electrolytes. That is to

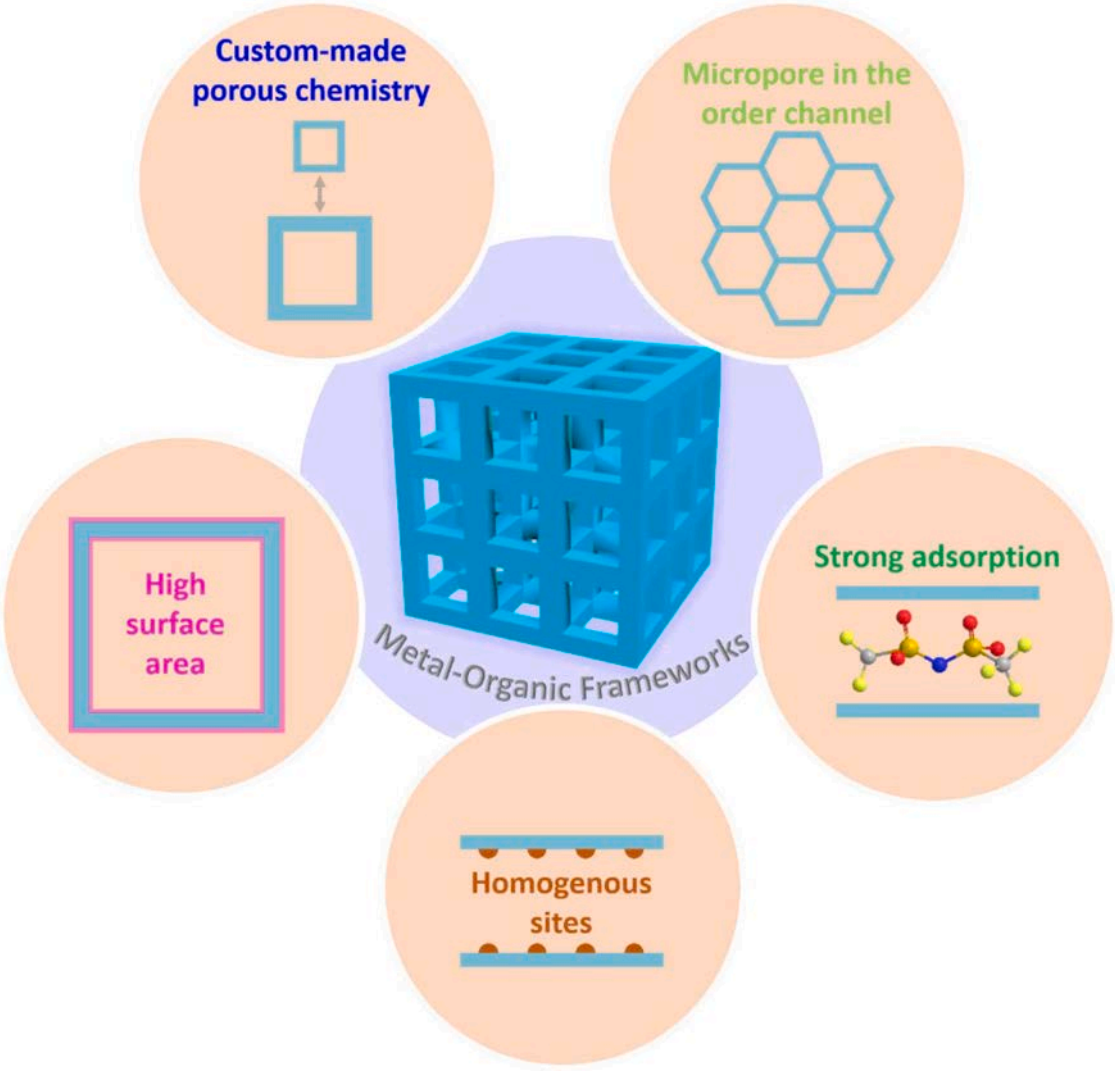

Fig. 1. Schematic illustration for the merits of MOFs as filler into SSEs.

say, the bigger pore size resulted more pore volume and contained more magnesium salts within the channels, and a less coordinating anion of magnesium salts exhibited much higher concentration within the framework. Further, a UIO-66 ($Zr_6O_4(OH)_4(bdc)_6$, consisting of ($Zr_6O_4(OH)_4(O_2CR)_{12}$ clusters and **H_2bdc** organic ligands, was modification of lithium *tert*-butoxide (LiO^tBu) to obtain the LiO^tBu grafted UIO-66 and exhibited a high Li^+ conductivity of 1.8×10^{-5} S cm^{-1} at room temperature and a low active energy of 0.18 eV, which was also reported by Long's group.[36] They further revealed that grafting ^{t}BuO$^-$ anions in the channels were shielded by the bulky aliphatic group, resulting in a weaker interaction with the charge-balancing Li^+ ion than that of free ^{t}BuO$^-$ anions (ladened in the channels) and consequently a higher ionic conductivity.

Recently, Zettl and colleagues also developed a MIL-121 post-modifying with the lithiation of LiAc, which was flexible and consisting of aluminum centers linked by pyromellitic acid (1,2,4,5-benzenetetracarboxylic acid, **H_4btec**).[37] The free carboxylic units within 1D channels of activated MIL-121 were ion-exchanged facilely with Li^+ or Na^+ ions through soaking with liquid electrolyte, and the Arrhenius plots results demonstrated the activation energy of Li^+ and Na^+ ions were 0.28 and 0.36 eV, respectively, which was consistent with further observed by broadband impedance spectroscopy and by ^{7}Li and ^{23}Na NMR spin-lattice relaxation. Moreover, the ^{1}H NMR definitely proved that the Li^+ is responsible for ionic conductivity rather than the protons. In addition, the authors confirmed both the solid conducting MOF framework and the soaking electrolyte inside the pores leading compatible interfacial effect would be the prerequisite of reaching high Li^+ conductivity.

Two heterometallic ionic conductor MOFs (EHU1(Sc, M)) had been designed employing scandium (Sc^{3+}) as trivalent ions, alkaline metals (Li^+ or Na^+) as monovalent ions, and pyrimidine-4,6-dicarboxylic acid (**H_2pmdc**) as organic ligands (Fig. 2**b**), resulting an ordered distribution of alkaline ions among the crystal structure, which was reported by Cepeda and colleagues.[38] They demonstrated that partially replacing Sc^{3+} by doping with Cd^{2+} and Mn^{2+} could achieve high ionic conductivity and reduce the activation energies. Additionally, loading alkaline electrolyte salt to increase the charge carriers through the soaking procedure could further enhance ionic conductivity and decrease the activation energies, without destroy the pristine crystal structure.

Lu's group investigated that the cations of the 3rd period ((Na^+, Mg^{2+}, and Al^{3+}) and the first group (Li^+, Na^+, K^+, and Cs^+), with various Stokes radii and ionic solvation shell thickness, were infiltrated into MOF (MIL-100(Al)) framework to form SSEs and remarkably influenced ion-transport behaviors (Fig. 2**c**).[39] The Mg-MOF displayed an ionic conductivity of 1.0×10^{-3} S cm^{-1} and a low activation energy of 0.2 eV.

2.1.2. Anionic MOF

Usually, the active sites of the adopted ligands are almost

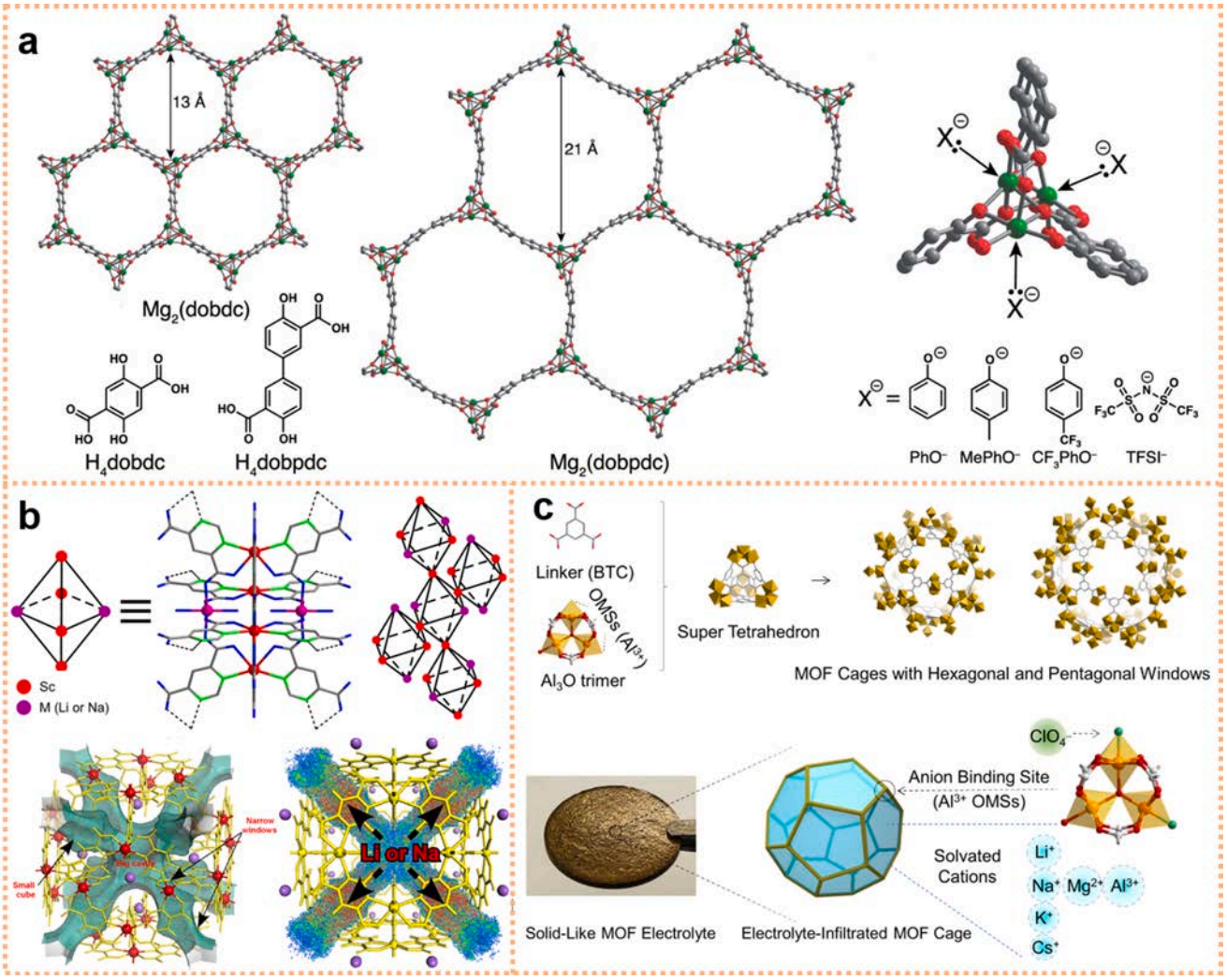

Fig. 2. (a) Structures as viewed along the *c*-axis of the organic frameworks of Mg_2(dobdc) and Mg_2(dobpdc) and a close-up of the open coordination sites at the vertices of the pore that interact with nucleophilic guest species: PhO^- = phenolate, $MePhO^-$ = methylphenolate, CF_3PhO^- = 4-trifluoromethylphenolate, and $TFSI^-$ = bis(tri fluoromethanesulfonyl)imide. Reproduced with permission.[35] Copyright 2014, Royal Society of Chemistry. (b) Arrangement of the β-cage fraction, junction of β-cages, and schematic illustration for ion conduction of EHU1(Sc, M). Reproduced with permission.[38] Copyright 2015, American Chemical Society. (c) Schematic illustration for forming MIL-100(Al) and photograph of SSE containing different cations while the anions are complexed to OMSs. Reproduced with permission.[39] Copyright 2016, American Chemical Society.

participated in the coordination with metal center nodes formatting secondary building units and no longer accessible for binding with the extra guest cation. Duan's and colleagues designed a highly electronegative carboxyl-decorated anionic MOF (InOF) based on [1,1′:4′,1″-terphenyl]-2′,3,3″,5,5′,5″-hexacarboxylic acid ligands (**H_4THBA**), which possessed 12 negative sites originating from secondary building units and exposed carboxyl group on the ligand (Fig. 3**a**).[40] The obtained InOF showed a high Li^+ conductivity of 1.49×10^{-3} S cm^{-1}, which could be ascribed to the abundant electronegative sites facilitating the hopping of ions in channels. Analogously, Hong and colleagues synthesized six anionic metal-organic frameworks based on the ionic interaction of alkali metals with 2,2′-disulfo-4,4′-oxidibenzoic acid (**M_2dsoba**, M^+ = Na^+, K^+, Cs^+), resulted in higher ionic bonding dimension and reached high ionic conductivity (up to 1.25×10^{-3} S cm^{-1}) (Fig. 3**b**).[41]

Moreover, Panda and colleagues reported, with two ligands of 4,4'-bipyridine and zigzag naphthalenediimide ligands accoutered with two terminal sulfonate groups (**NDIDS**), a strategy of not post-synthetically modified MOF ($Cu_2(BPY)_2$(NDIDS)) (Fig. 3**c**).[42] Inspired by the multifunction of NDIDS, synchronously binding gust Li^+ ions with its carbonyl and uncoordinated sulfonate oxygen atoms and anchoring ClO_4^- anions with π-acidic NDIs. The resulted $Cu_2(BPY)_2$(NDIDS) could take up 20 wt% $LiClO_4$ and reache a million-fold higher bulk ionic conductivity than that of the pristine material and a remarkably low activation energy (0.167 eV), which could be attributed to Li^+ ions inside the channels hopping from one binding site to another.

Unlike the strategy of immobilize anion into the framework materials, Yaghi's group initiatively designed a three-dimensional MOF (MOF-688) with 4-connected tetrahedral tetrakis(4-formylphenyl) methane (**TFPM**) building units by imine condensation (Fig. 4**a**).[43] The intrinsically anionic framework from highly charged Anderson type polyoxometalates displayed high ionic conductivity of 3.4×10^{-4} S cm^{-1} at 20°C, a high t_{Li+} of 0.87, and low interfacial resistance of 353 Ω against metallic lithium. The model Li||LFP cells could be work at room temperature at the current density of about 0.2 C.

Interestingly, Dincă's group proposed a strategy of reversible phase transition (single crystal to single crystal transition) upon reaction with stoichiometric amounts of halide or pseudohalide salts in the secondary building units of MIT-20 with tubular pores, which was synthesized through the solvothermal reaction between $CuCl_2 \bullet 2H_2O$ and **H_2btdd** in DMF solvent, inducing an anionic framework from a neutral one (Fig. 4**b**).[44] When the halide/pseudohalide anions could be bound to

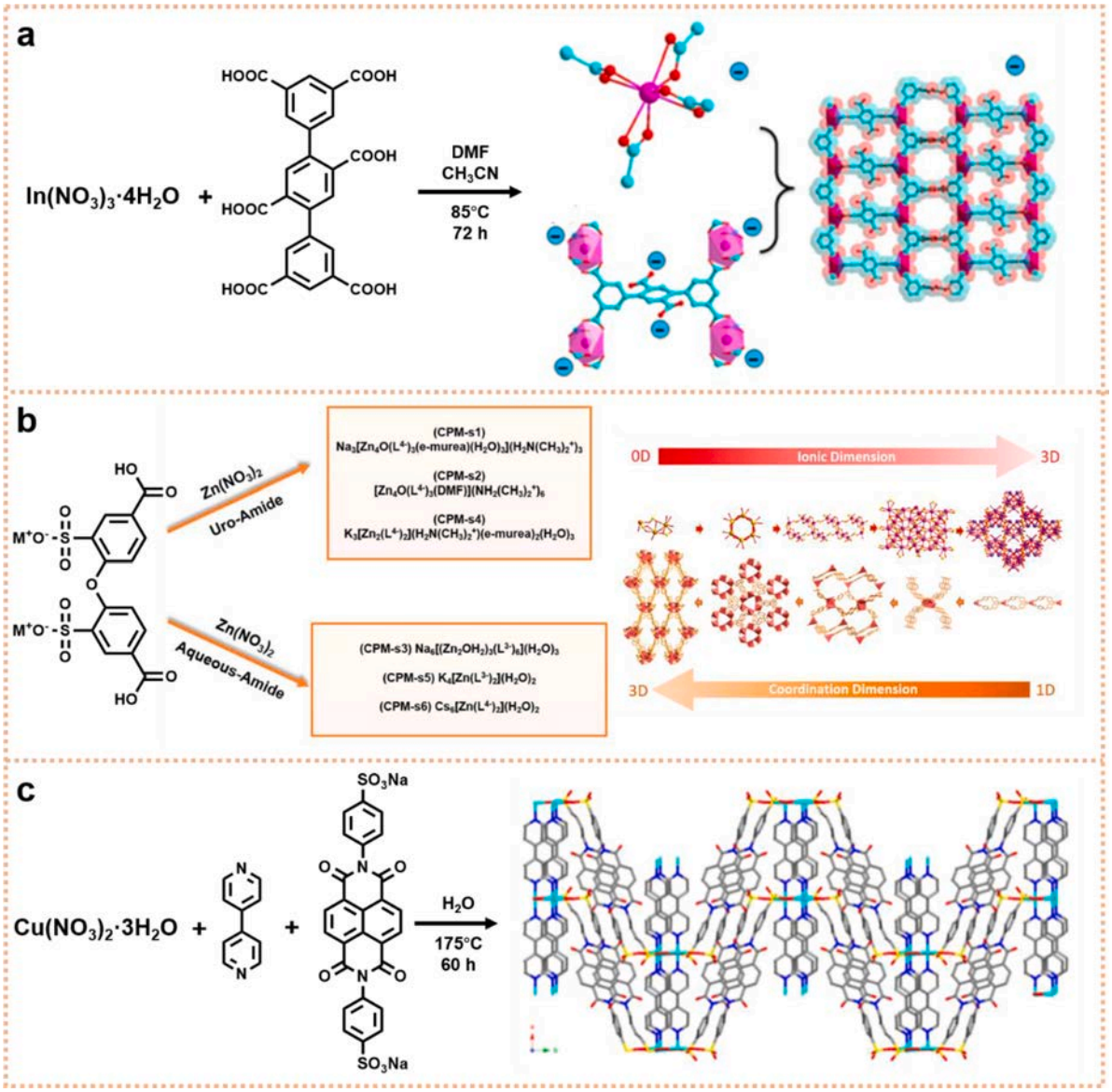

Fig. 3. (a) Schematic illustration and X-ray crystal structure for InOF. Reproduced with permission.[40] Copyright 2021, American Chemical Society. (b) Synthetic design for constructing CPMs. Reproduced with permission.[41] Copyright 2020, American Chemical Society. (c) Schematic illustration and X-ray crystal structure for $Cu_2(BPY)_2(NDIDS)$. Reproduced with permission.[42] Copyright 2019, American Chemical Society.

the square pyramidal Cu centers and thus stationary, the mobile cations could be moved freely within the one-dimensional pores as single-ion solid electrolytes, which t_{Li+} could reach at 0.69. The obtained Li^+-loaded materials displayed high ionic conductivity of 4.4×10^{-5} S $cm^{-1}$and further reached at 4.8×10^{-4} S cm^{-1} due to the addition of $LiBF_4$ providing nonstoichiometric Li^+ ions. Further, from the same group, another type of tetrakis(4-tetrazolylphenyl)methane (**H_4ttpm**) was choose to design a anonic Cu-azolate metal-organic framework (MOF-MX_n) through the single crystal to single crystal transition immobilizing anions within the framework (**Fig. 4c**).[45] The obtained MOF-MX_n, which presented abundance of OMS leading amounts of stoichiometric halides, loaded a high density of mobile Li^+, Mg^{2+}, and Al^{3+} and further endowed maximal cation transference numbers and facilitated the ionic transport by suitably immobilized anion. Thus, t_{Li+} and ionic conductivity in MOF-LiCl could be up to 0.69 and 2.4×10^{-5} S cm^{-1}, respectively.

Recently, due to the limitation of optional ligands, Wu's group designed a MOF single lithium-ion conductor (UIO-66-LiSS) via covalently immobilizing anions to the framework of UIO-66, which was different from the anions coordinating with the OMS in the method of abovementioned post-synthesized modification with lithium salt (**Fig. 4d**).[46] Grafting 4-styrenesulfonate anion groups onto the framework of UIO-66 and further ion-exchange reaction with LiOH, the resulted UIO-66-LiSS showed a high atomic concentration of Li (up to 4.7 mol %), ionic conductivity of 6.0×10^{-5} S cm^{-1} at 25°C, and an electrochemical stability window of 5.2 V. Profitting from the nano-wetted interfaced with ethylene carbonate (EC) and propylene carbonate (PC), ionic conductivity could be further improved to 7.8×10^{-4} S cm^{-1} from that of pristine UIO-66-LiSS and a high t_{Li+} of 0.88 could be realized. The implemented Li||LFP cells exhibited the first discharge capacity of 127 mAh g^{-1} and a capacity retention of 88.1% after 100 cycles.

Moreover, Tolbert's group firstly reported Lewis acid-based anionic aluminum metal-organic framework (Al-Td-MOF-1) *via* anionic tetrahedral AlO_4 secondary building units (**Fig. 4e**).[47] The resulted Al-Td-MOF-1 exhibited the best described topologically of a uninodal 6-coordinated *snp* rod net and unidirectional pore channels with a square window aperture of $\approx 5 \times 5$ $Å^2$, which was consisting of

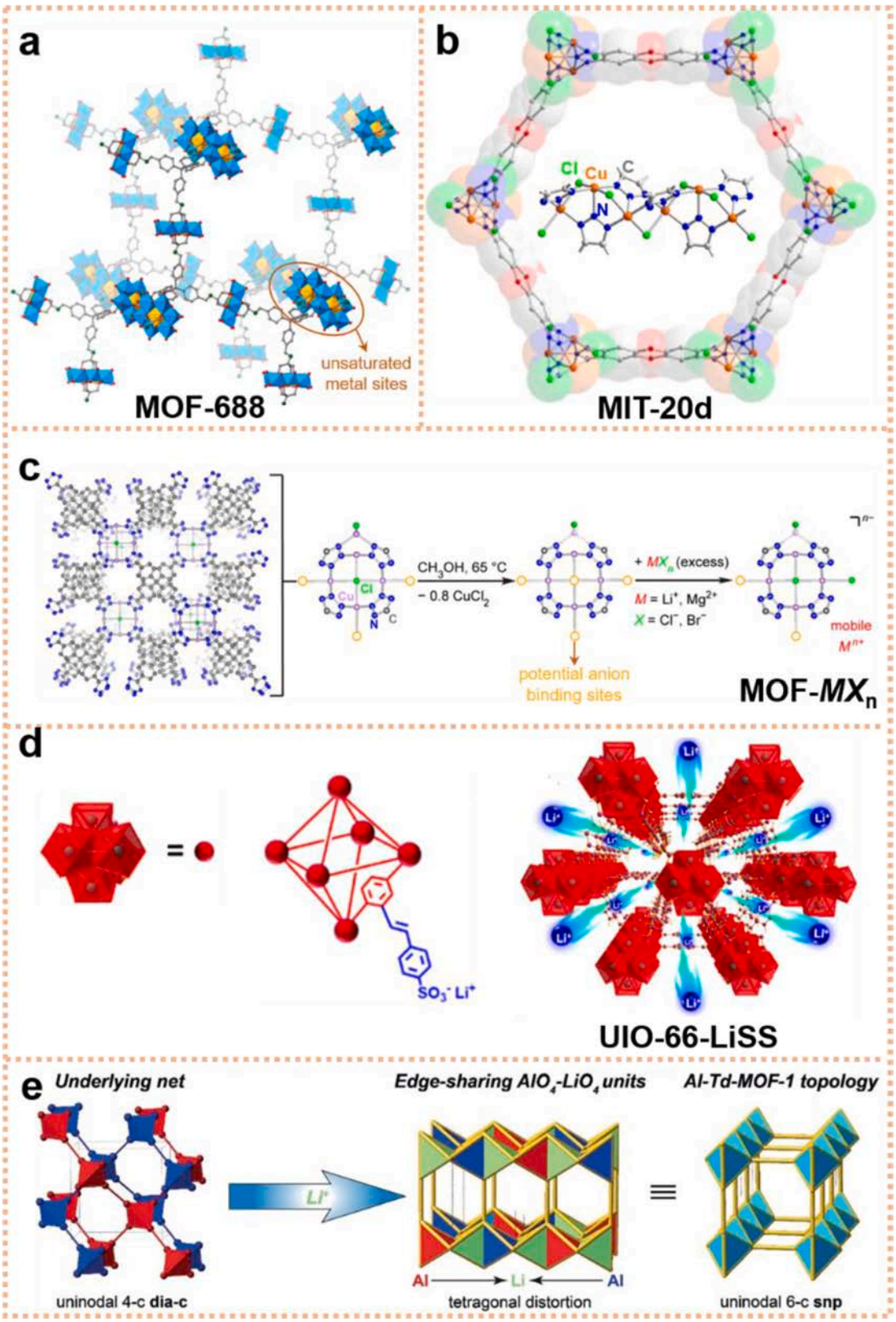

Fig. 4. (a) Schematic illustration and structure of MOF-688. Reproduced with permission.[43] Copyright 2019, American Chemical Society. (b) X-ray crystal structures of MIT-20 and MIT-20d. Reproduced with permission.[44] Copyright 2017, American Chemical Society. (c) Schematic illustration of MOF-MX_n. Reproduced with permission.[45] Copyright 2019, American Chemical Society. (d) Schematic illustration and Li^+ ion transport mechanism for UIO-66-LiSS. Reproduced with permission.[46] Copyright 2020, American Chemical Society. (e) The underlying net and topologically relevant of Al-Td-MOF-1. Reproduced with permission.[47] Copyright 2018, Wiley-VCH.

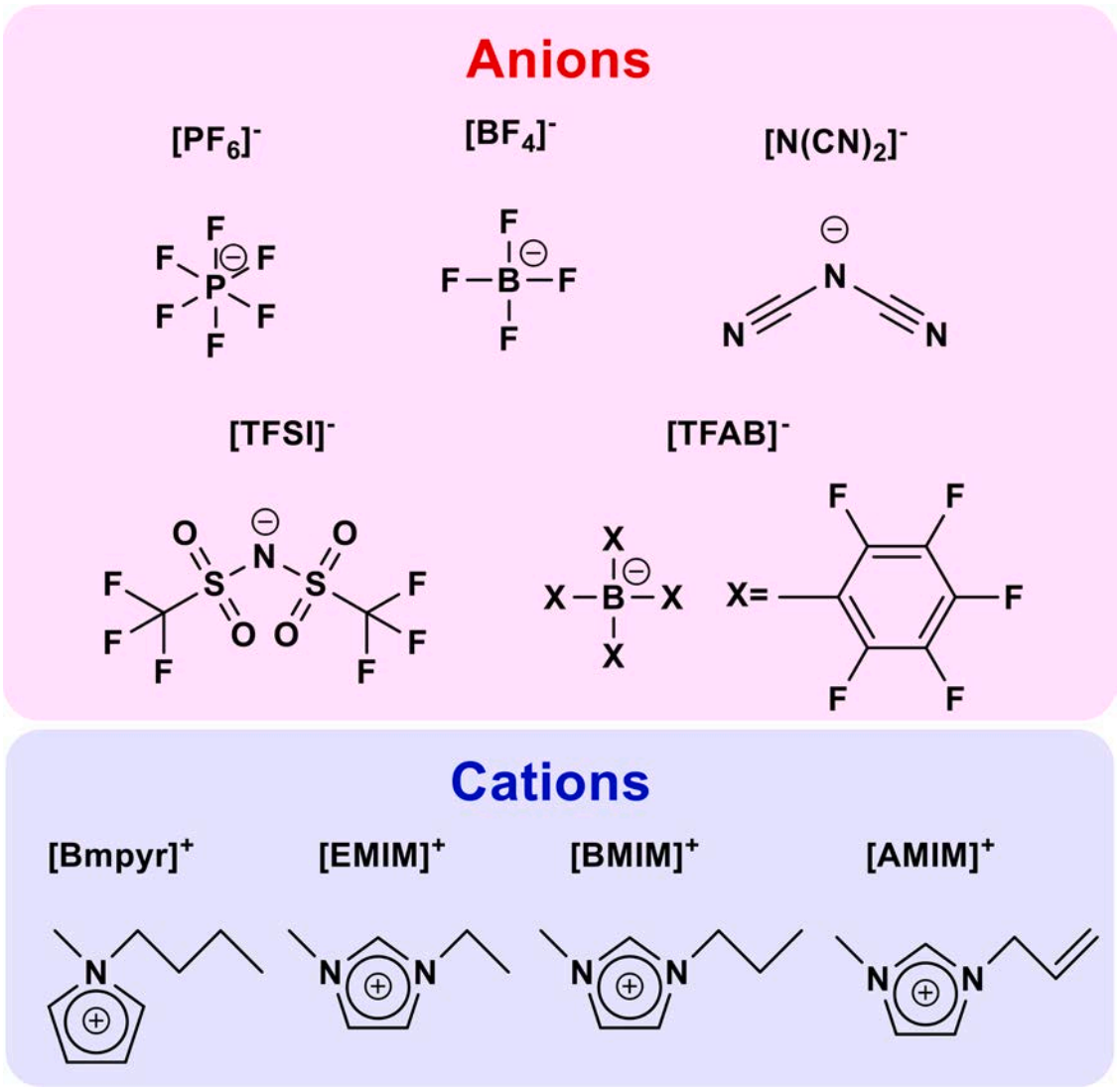

Fig. 5. The structural formula of anions and cations for mentioned ILs in this review.

one-dimensional chains of alternating edge-sharing AlO_4 and LiO_4 tetrahedral sites. They further demonstrated that, excepting from the high Li^+ loading, the crystallinity with highly periodic channel is also important to boost the number of mobile charge carriers, leading to an effective single-ion solid electrolyte with an ionic conductivity of 5.7×10^{-5} S cm^{-1}.

In contract to the above MOF ionic conductors, Biradha's group firstly presented a kind of porous carboxylate based Li-MOF (Li-AOIA and Li-TMCA) *via* the solvothermal reaction of $LiNO_3$ with 5,5'-(anthracene 9,10-diylbis(methylene)bis(oxy))diisophthalic acid (**H_4AOIA**) and 5,5'-(((2,3,5,6-tetramethyl-1,4-phenylene)bis(methylene))bis(oxy))diisophthalic acid (**H_4TMCA**).[48] Especially, doping of lithium salts to provide adequate amount of mobile Li^+, activated Li-AOIA possessing OMS in 1D rectangular channels along the *c-axis* achieved ionic conductivity of 1.09×10^{-5} S cm^{-1} at 25°C and low activation energy of 0.18 eV.

2.2. MOF/ionic liquid-based SSEs

Ionic liquids (ILs), which usually are salts with the melting points below 100°C composing organic cations of organic/inorganic ions, have attracted enormous attention of researcher's community as a promising candidate in the fields of chemical synthesis, catalysis, separation, and extraction, especially as safe electrolyte in application of energy storage.[49–55] Despite its many advantages, such as, low vapor pressure, high electrochemical and thermal stability, high ionic conductivity, and nonflammability, the higher melting points comparing with liquid electrolyte is the one of most significant hinders for the widely use of ILs. Up to now, there are two type of MOF/Ionic liquid-based SSEs described as following: MOF filled with ILs and MOF grafting ILs. In this review, the mentioned ILs are listed as shown in **Fig. 5**.

2.2.1. MOF filled with ILs

In order to fill ILs into the micro-/mesopore of MOF, it's primarily necessary to illuminate the relationship between the loading ratio of ILs and its corresponding ionic conduction. Comparing with most of the confined ILs that are a simple function of the surface-to-volume of the host porous silica,[56] the ionic conductivity of IL confined mesoporous MOF (PCN-777) with appropriate filling ratio was superior to bulk-IL, which has been demonstrated by Kitagawa's group.[57]

ZIF-8 (also named as MAF-4, which was discovered by Chen's group [58] and Yaghi's group in 2006[59]), is a kind of MOF with aperture and cavity diameter of 0.34 and 1.3 nm, respectively. As a pioneering work, Kitagawa's group successfully employed [EMIM][TFSI] as the gust ionic liquids into the ZIF-8 as the host materials, and demonstrated that nano confined [EMIM][TFSI] experienced an anomalous phase-transition

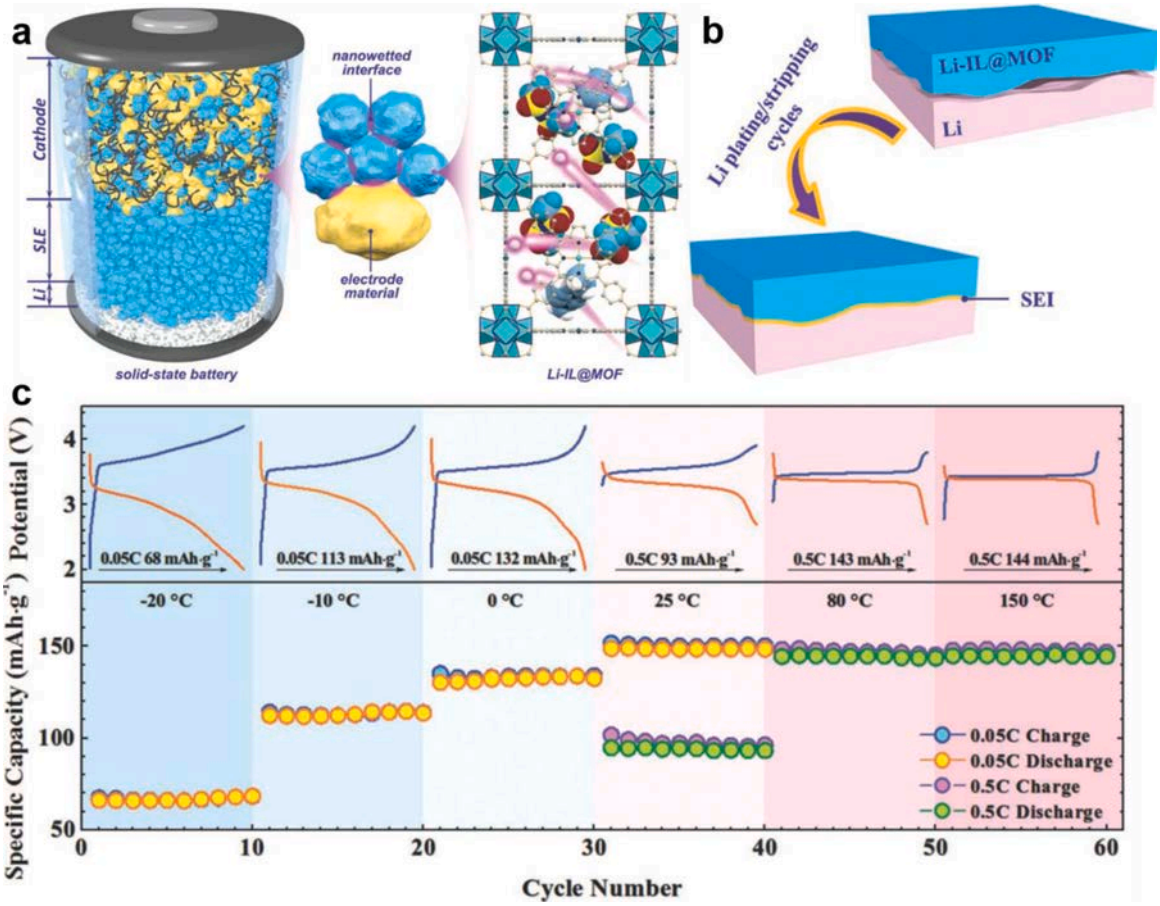

Fig. 6. (a) Schematic illustration for the architecture and nanowetted interfacial mechanism, (b) schematic illustration for the improved interfacial contact during Li-plating/stripping, and (c) temperature-dependent cyclability of MOF-525/IL SSE. Reproduced with permission.[64] Copyright 2018, Wiely-VCH.

behavior leading to low freezing and melting points, in which no freezing transition down to 123 K compared with bulk [EMIM][TFSI] freezing at 231 K.[60] As following, Wondraczek's group further demonstrated that impregnating the sodium-salt-containing IL ([$Na_{0.1}EMIM_{0.9}$][TFSI]) into the micropore of partially amorphization ZIF-8 by the ball-milling technology showed a Na^+-ionic conductivity of about 2×10^{-4} S·cm^{-1} at room temperature, an activation energy as low as 0.26 eV, and with enhanced stability under ambient conditions.[61] Also in the same protocol, Tuffnell and coworkers exhibited that, due to the high porous volume, although the mesopores of ZIF-8 incorporated more IL than that of the micropores, the microcrystalline pores afforded a long range, continuous and minimal tortuosity ion pathways, which was more helpful for facilitating ionic conduction than that in the discontinuous mesopores.[62] Further, to improve the processability of nanoscale ZIF-8, Tu and co-workers developed a method of filling Li-[EMIM][TFSI] into PP membrane with distributed ZIF-8 nanoparticles, in which ZIF-8 nanoparticles could be uniformly distributed both on the surface and in the interior of PP membrane resulting in more like to inhibit the dendrite growth and more affinitive for Li-conductor.[63] The as-obtained SSE exhibited an improved ionic conductivity of 2.09×10^{-4} S cm^{-1} at 25°C, a t_{Li+} of 0.45. And Li||LFP cells showed an initial discharge capacity of 157.9 mA h g^{-1} and a capacity retention of 91.23% after 450 cycles at 0.2 C.

In 2018, Pan's group proposed MOF/IL SSE based on MOF-525 loading with [$Li_{0.2}EMIM_{0.8}$][TFSI], which was firstly applicated in rechargeable battery system (**Fig. 6**).[64] With an aperture size of 12 × 7 Å, MOF-525, which was firstly synthesized by Yaghi's group,[65] could confine $[EMIM]^+$ and $[TFSI]^-$ ions and be capable of allowing Li^+ transportation within the channels. They firstly demonstrated a unique nanowetted interfacial mechanism with a dense morphology, which was formed between the adjacent nanocrystals leading to good compatibility with cathodic electrode and lithium metal anode. Finally, the Li||LFP cells with a high active loading of 25 mg cm^{-2} and a thickness of 20 μm were achieved and could work over a wide temperature range between -20 to 150°C.

Due to the nanometer-scale leading to increased specific surface area and surface tension and improved interfacial contact between electrodes and electrolytes, Guo's group adopted UIO-66 ladening Li-IL (LiTFSI in [EMIM][TFSI]) to prepared UIO-66/IL SSEs (**Fig. 7a**), which exhibited a ionic conductivity of 3.2×10^{-4} S cm^{-1} and a t_{Li+} of 0.33 at 25°C when the weight ratio of UIO-66/Li-IL is 15/16.[66] Besides, the obtained Li||LFP cells showed the initial discharge capacity of 130.2 mAh g^{-1} and maintained 130.4 mAh g^{-1} after 100 cycles at 0.2 C, and the initial discharge capacity of 119 mAh g^{-1} with a retention of 94% after 380 cycles at 1 C. Further, Arumugam's group designed a UIO-66/IL SSE based UIO-66 grafting a lithium sulfonate group (UIOSLi) with [EMIM][TFSI].[67] Benefitting from improved ionic conduction by the lithium sulfonate group and suppressing the penetration of polysulfide species of UIOSLi (the pore size ≈ 6-12 Å), the resulted ionic conductivity of UIO-66/IL SSE reached 3.3×10^{-4} S cm^{-1} at room temperature and the relevant Li||S cells (Li_2S_6 as the catholyte) showed a capacity retention of 84% after 250 cycles with a capacity-fade rate of 0.06% per cycle. This method had been further demonstrated also by Arumugam's group that it was successful to design another type of UIO-66/IL SSE based on a UIO-66 grafting with sodium sulfonic group (UIOSNa) lading with a sodium-based ionic liquid (sodium bis(trifluoromethylsulfonyl)imide in 1-*n*-butyl-1-methylpyrrolidinium bis(trifluoromethylsulfonyl)imide [Bmpyr][TFSI]).[68] Moreover, as shown in **Fig. 7b**, a kind of core-shell

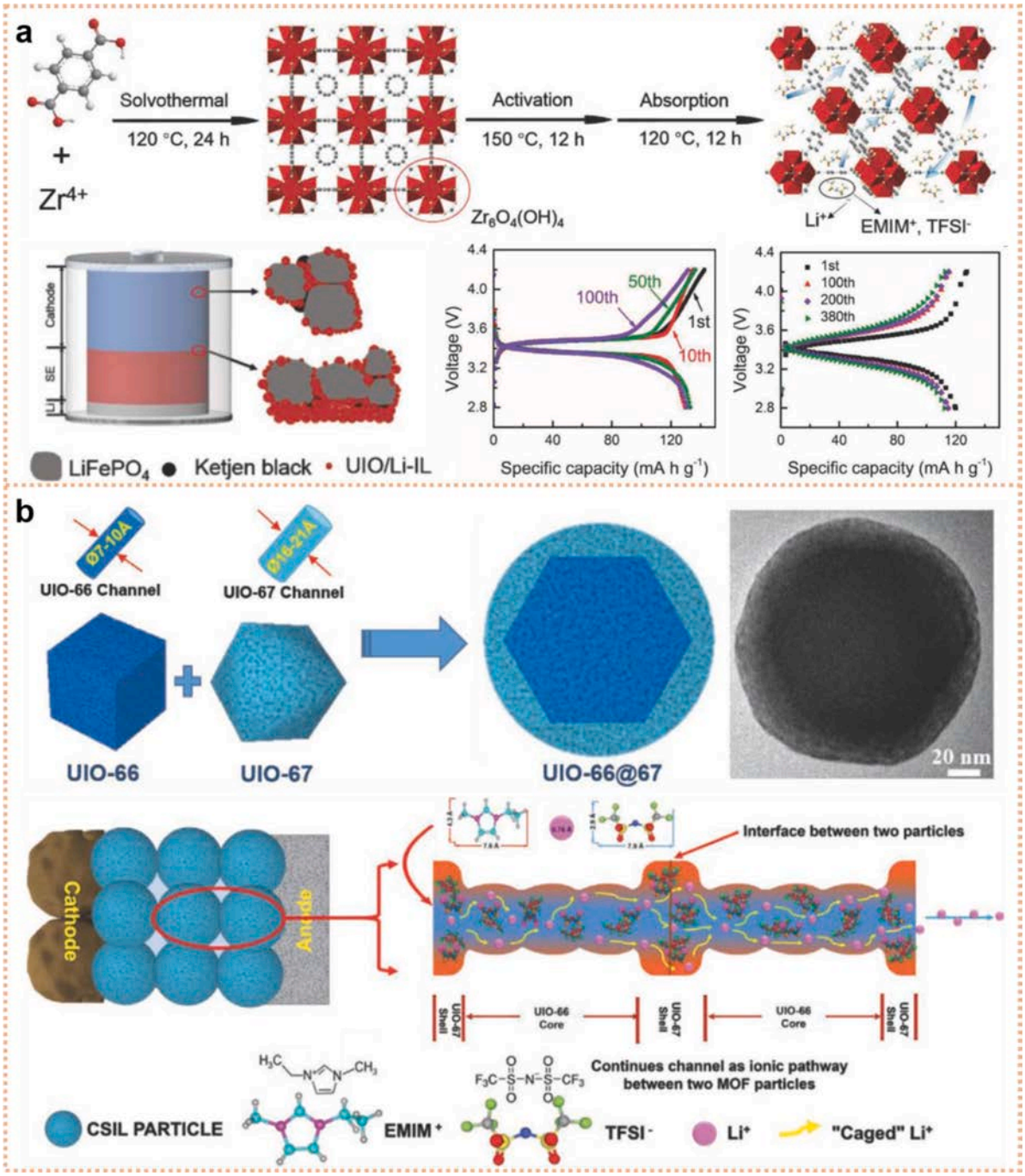

Fig. 7. (a) Preparation process, schematical structure, and plots of cell potential versus specific capacity for Li||LFP cells at 0.2 and 1.0 C of UIO/IL SSE. Reproduced with permission.[66] Copyright 2019, Wiely-VCH. (b) Schematic preparation of continued channel within the adjacent particles and nanowetted interfacial mechanism of core-shell UIO-66@67/IL SSE. Reproduced with permission.[69] Copyright 2021, Wiely-VCH.

MOF-in-MOF (UIO-66@67) incorporating with [EMIM][TFSI]was employed to fabricate core-shell ionic liquid-solid electrolyte (CSIL), which was reported by Mai's group.[69] The core UIO-66 possessed a smaller pore size (8 Å) than that of UIO-67 (1.6-2.1 nm), which is bigger than that of ionic liquid ions ($[EMIM]^+ \approx 7.9$ Å and $[TFSI]^- \approx 7.6$ Å), and simultaneously confined ionic liquid ions and improved Li^+ transport. With a particle size of about 150 nm, UIO-66@67 spheric morphology could furnish excellent platform for building ionic conductors and facilitating Li^+ transport by the face-sharing among adjacent crystals, resulting an ionic conductivity of 2.1×10^{-3} S cm^{-1} and a t_{Li+} of 0.63 at room temperature. The Li||Li cells showed a small polarization (less than 28 mV) for more than 1000 h at 1 mA cm^{-2}. The Li||LFP cells displayed the capacities of 163.8, 163.6, 162.3, 160.8, 159, 156, and 162.6 mAh g^{-1} at different rates of 0.2, 0.4, 0.6, 0.8, 1.0, 1.5, and 0.2 C at 25°C, respectively. What is more, a flat operating voltage plateau with a small polarization (0.055 V) could be observed.

Considering of the size of the $TFSI^-$ and $EMIM^+$ in ionic liquid, Bae's group employed HKUST-1 with angstrom-scale pores to restrict $TFSI^-$ through a weaken coordination in the 3D channels and further improve mobilization of Li^+ to construct HKUST/IL SSE, which was good for low interfacial contact between electrodes and electrolytes.[70] At almost the same time, a class of dense thin films of surface-mounted metal--organic frameworks (SURMOFs) was chosen as the solid substrate for investigating the IL mobility exclusively in the MOF pores, which was

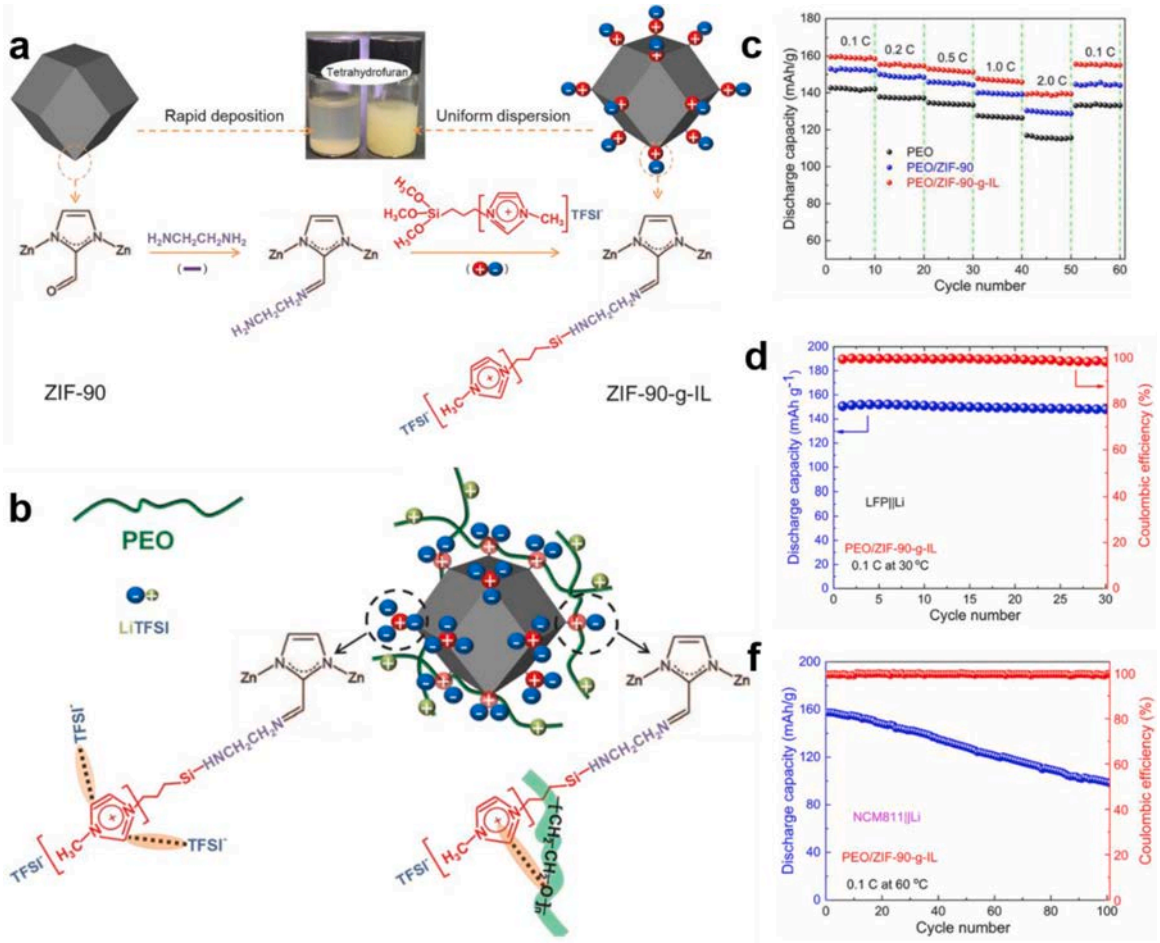

Fig. 8. (a) Schematical preparation of ZIF-90-g-IL nanoparticle, (b) schematic of synthesis of ZIF-90-g-IL nanofillers with PEO chains and LiTFSI, (c) rate capabilities of Li||LFP cells using PEO, PEO/ZIF-90 and PEO/ZIF-90-g-IL SPEs at 60°C, cycling performance and (d) at 0.1C under 30°C for Li||LFP cells and (e) at 0.1 C under 60°C for NMC||Li using PEO/ZIF-90-g-IL SPEs. Reproduced with permission.[74] Copyright 2021, Elsevier.

reported by Heinke's group.[71] SURMOFs was firstly synthesized by growing HKUST-1 in a layer-by-layer (LBL) fashion on glass substrates with deposited interdigitated gold electrodes, and then [$Li_{0.2}BMIM_{0.8}$][TFSI] was loaded into the channels of HKUST-1. They further unveiled a complex conduction mechanism based on experiment results and molecular dynamics (MD) simulations: at low and medium concentrations of IL loading, Li^+ conduction displayed the Grotthuss-like mechanism, in which the charge was transported by coordinated hopping of Li^+ ions between the adjacent anions and was also limited by the distance between the [TFSI] anions in this work. While at high IL loadings, due to the relatively large organic cations and anions and the narrow MOF channels, it resulted a field-induced bunching and immobilization behavior with decreasing the ionic conductivity. It is worth to mention here that the Grotthuss-like mechanism, also known as proton jumping mechanism, refers to the shuttling of protons through the cooperation of neighboring water molecules based on the hydrogen bond network,[72] has been widely accepted as Li^+ transport mechanism in the liquid electrolytes.

Furthermore, in order to investigate the diffusion coefficients of electrons and ions within conductive framework, Morris's group adopted a series of metallocene-doped M-NU-1000 (M=Fe, Ru, Os) thin films into two different electrolytes ([TBA][PF_6] and [TBA][TFAB]) for the application of chronoamperometry experiments.[73] The as-results revealed that there were three different stages of the relative contribution of electron and ion diffusion during the electrochemical transformation: the initial stage of rapid electron diffusion along the crystal-solution boundary, the second stage of diffusion of electrons and ions within the bulk MOF, and the final stage of conversion dominated only by the diffusion of ions. They further discovered that rapidly self-exchanging molecular moieties of MOF would be improved the electron diffusion in both PF_6^- and $TFAB^-$. On the other side, because of the low degree of ion-pair association between $TFAB^-$ and the metallocenium ion, the ion diffusion coefficient of $TFAB^-$ was higher than that of PF_6^-, which was further leading to a faster mobility through the MOF pores.

2.2.2. *MOF grafted with ILs*

For the above-mentioned laden method through weak coordination with ionic liquid ions, it was difficult to ensure an ideal loading and to fill into the inside cavity of each micropores. Thus, grafting ionic liquid ions onto the MOF skeleton would be seen as a more effective strategy for immobilizing ionic liquid anions, since the anions were firmly anchored at the skeleton or on the surface of MOF based on the strong covalent-bond rather than through weak coordination. Recently, Deng's group presented a novel MOF surface grafting with imidazole ionic liquid containing siloxane groups (ZIF-90-g-IL), which was synthesized through consecutive -NH_2 modification and dehydration condensation reaction, was chosen as MOF/PEO/IL-based SSE nanofiller giving rise to the uniform distribution interfaces between ZIF-90-g-IL and PEO matrix (**Fig. 8**).[74] Taking the rigid feature into consideration, ZIF-90-g-IL could prevent the reorganization of PEO segments to reduce the crystallinity, leading to more amorphous regions, which would be favor to facilitating ion transport and show higher ionic conductivity. The uniform distribution resulting from surface grafting ILs and the electrostatic

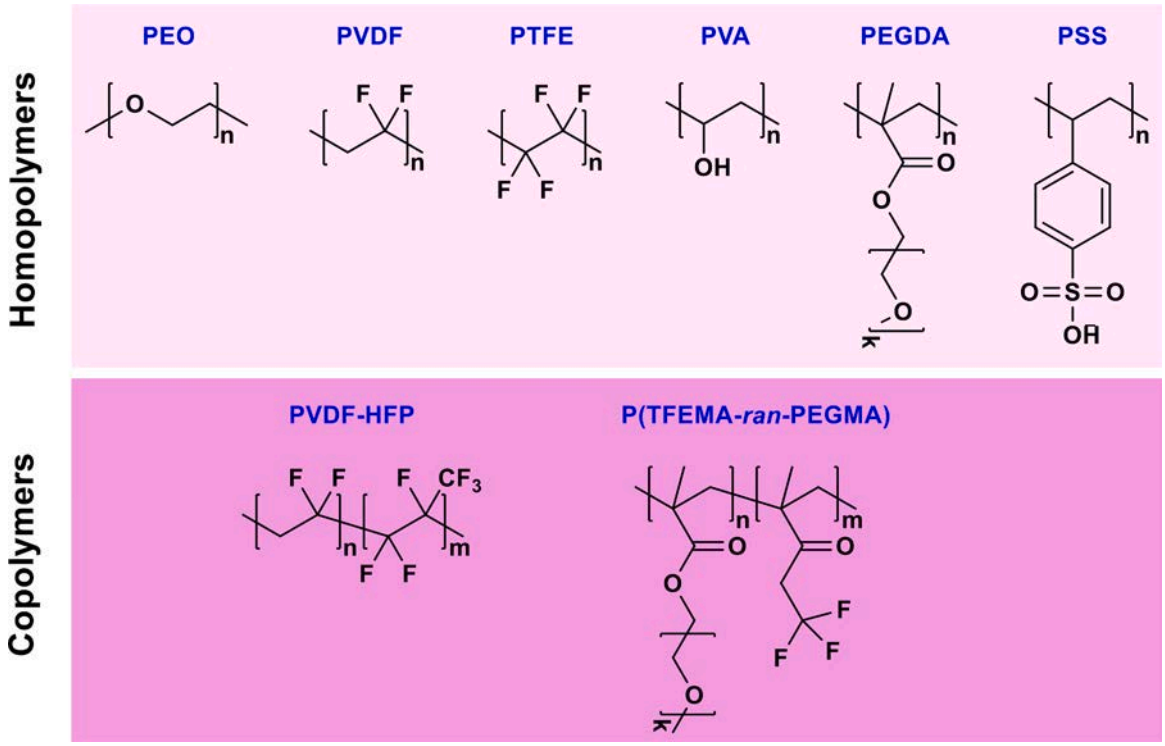

Fig. 9. Common polymer matrix used in the synthesis of MOF/Polymer-based SSEs in this review.

reaction among ILs with the ester groups of PEO could also hinder the reorganization of PEO chains, inducing a low crystallinity of PEO and high ionic conductivity. Moreover, ZIF-90-g-IL could be used as a cross-linking point for releasing the stress from one groaned polymer chains to other polymer chains, which was helpful to suppress the growth of lithium dendrites. Noteworthily, even though the surficial negativity, the Lewis acidic site from the ZIF-90-g-IL was demonstrated that could still absorb the $TFSI^-$ anions and improve Li^+ transference. The resulted Li||LFP cells exhibited a capacity of 101 mAh g^{-1} after 500 cycles at 2 C under 60°C and a capacity retention of 97.4% after 30 cycles at 0.1 C under 30°C. This SSE was also worked for Li||NCM811 cells with a capacity of 99 mAh g^{-1} after 100 cycles at 0.1 C under 60°C.

2.3. MOF/polymer-based SSEs

Polymer electrolytes, possessing lightweight, plasticity, and processible interfacial contact with electrode, became the promising candidate for ion conducting material, which showed great potential in the field of energy storage/conversion.[75–77] However, their low ionic conductivity, poor mechanical properties, and thermal instability hinder their further development.[78] To achieve high performance solid-state battery, a prospective strategy for design MOF-based SSEs with polymer (denoting as MOF/polymer-based SSEs) has been developed. Normally, MOF/Polymer-based SSEs combine the advantages of MOFs (high surface area, periodical porous structure, precise porous chemistry, and active OMS) and those of polymers (flexibility and adjustable interfacial chemistry). Within this strategy, high specific surface area of MOFs can facilitate contact with polymer and further reduce electrochemical resistance, anchoring anions into MOFs framework can improve Li^+ transfer and increase ionic conductivity, and order porous channel can be good for uniform Li^+ transport resulting in homogeneous Li^+ plating/stripping and further hindering the growth of lithium dendrites. While polymer electrolytes can offer a pathway for ion to be moved, provide hopping sites for ion transport *via* segmental motion, and further boost Li^+ transport with the incorporation of MOFs.

Moreover, in view of cost-effective and processing technology of battery package, polymer matrixes are suitable for solid electrolyte for the large-scale solid-state batteries with good interfacial contact.[24,79] Up to now, numerous types of MOFs have been chosen to design MOF/polymer-based SSEs. We summarize the progress of two different types of polymer matrixes in this section (Fig. 9), including homopolymer, such as polyethylene oxide (PEO), poly(vinylidenefluoride) (PVDF), poly(tetrafluoroethylene) (PTFE), poly(vinyl alcohol) (PVA), poly(ethylene glycol) diacrylate (PEGDA), polystyrene sulfonate (PSS), and some other copolymers, like poly(vinylidene fluoride-*co*-hexafluoropropylene) (PVDF-HFP), ploy(trifluoroethyl methacrylate-*ran*-poly(ethylene glycol) methacrylate) (P(TFEMA-*ran*-PEGMA)).

2.3.1. MOF/homopolymer-based SSEs

2.3.1.1. MOF/PEO-based SSEs. Among of abovementioned polymer electrolytes, PEO has become one of the most widely used polymeric matrix for design MOF/Polymer-based SSEs. PEO has been chosen to construct SSE in cooperating with MOF as early as 2013. As a representative example, Liu's group pioneeringly reported a kind of MOF/PEO-SSEs with MOF-5, PEO, and LiTFSI through an *in-situ* method (**Fig. 10a**).[80] In comparison with *ex-situ* method, the *in-situ* method could result in more uniform distribution and less agglomeration of MOF-5, then improve the ionic conductivity of MOF/PEO-SSE. When the molar ratio of PEO/LiTFSI was set at 10:1 with 10 wt% MOF-5, MOF-5/PEO SSE exhibited a high Li^+ conductivity (3.16×10^{-5} S cm^{-1} at 25°C). They speculated that the interaction of Lewis acidic sites on MOF-5 with PEO chains and LiTFSI will simultaneously restrain the crystallization of PEO and accelerate Li^+ conduction through the conductive phase configuration of PEO:LiTFSI. Moreover, the three-dimensional pore of MOF-5 could adsorb trace solvent, which further boosts the Li^+ conductivity.

Wang's group proposed a type of MOF/PEO-SSEs based on ZIF-8, which was formed by combining Zn^{2+} with 2-methylimidazole organic ligands and showed exceptional chemical and thermal stability and a pore size at angstrom scale (0.34 nm) (**Fig. 10b**).[81] The reason of the obtained MOF/PEO-SSEs could be attributed to the following: i) The

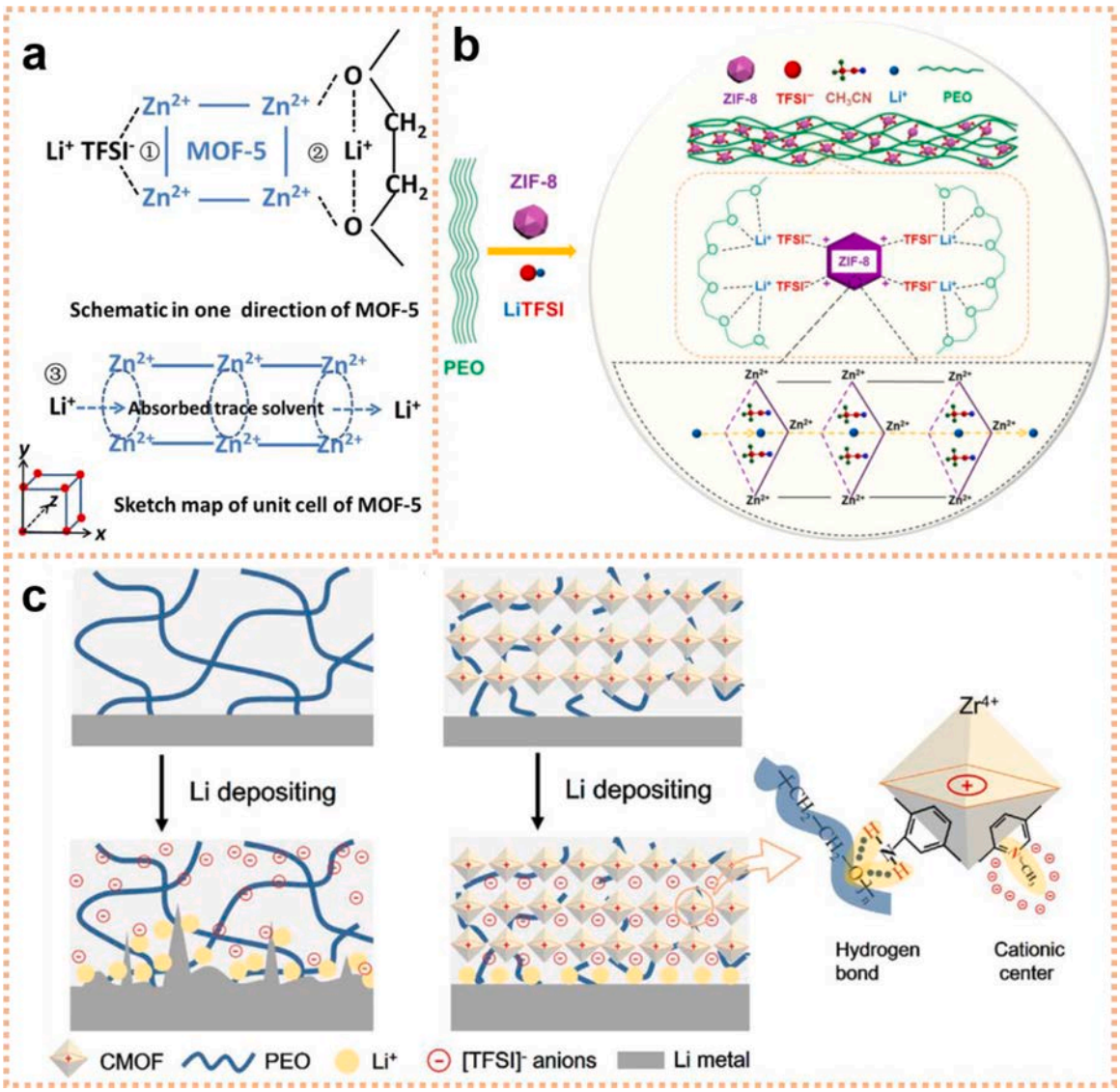

Fig. 10. MOF/PEO-based SSEs. (a) Schematic illustration of MOF-5/PEO-SSE: interaction of unsaturated metal sites on the surface of MOF-5 with LiTFSI and PEO chains and ionic transport within the pore canals of MOF-5. Reproduced with permission.[80] Copyright 2013, Elsevier. (b) Schematic of Li^+ ions conductive mechanism for ZIF-8/PEO-SSE. Reproduced with permission.[81] Copyright 2020, Spring Nature. (c) Schematic of Li^+ deposition behavior with pure PEO (containing LiTFSI) and UIO-66-NH_2/PEO SSE. Reproduced with permission.[82] Copyright 2019, Elsevier.

nanoscale size of ZIF-8 was benefiting for the form of good interfacial compatibility between the electrolyte and electrode resulting from the uniform dispersion in PEO matrix. ii) ZiF-8 acted as a solid plasticizer hindering the crystallizing of PEO, reducing the glass transition temperature and increasing the amorphous phase, which was induced to enhance the segment movement of PEO chains and benefitting for high ionic conductivity and high t_{Li+}. iii) The strong Lewis acidic sites of ZIF-8 were combined with the PEO main leading to the physic crosslinks, which was in favor of enhanced mechanical strength and the inhibition of Li dendrite growth, and further reducing the polarization during charge-discharge process. Besides, it was noteworthy that, due to the strong absorption of the microporous structure, the trace solvent with ZIF-8 was nonnegligible factor to improve the ionic conductivity.

As a representative example of UIO-66, Sun's group developed a novel cationic metal-organic framework (CMOF) through the nucleophilic substitution of grafted pyridine N based on UIO-66-NH_2, which was adopted to immobilizes anions and guide Li^+ uniform distribution for constructing MOF/PEO-SSEs (**Fig. 10c**).[82] They found that the hydrogen bong between -NH_2 group of CMOF and the ether oxygen of PEO could extend the electrochemical window to 4.97 V. Besides high specific surface of CMOF, the anions were forcibly adsorbed on the surface of CMOF by electrostatic interaction, resulting in a t_{Li+} of 0.72 and uniform Li plating/stripping without discernable dendrites. The constructed Li||LFP cells showed a capacity retention of 85.4% after 300 cycles at 1 C. Especially, Li||LFP cells exhibited an initial coulombic efficiency of 94.1% at 0.1 C and a capacity retention of 81.2% after 100 cycles, which was charged to 4.4 V. Moreover, Qing and colleagues further demonstrated that, comparing with UIO-66-NO_2, the electrostatic effect and the pore polarity of UIO-66-NH_2 had facilitated remarkably the bind with Li^+, the dissociation of Li^+ from PEO segments, and the deposition of dendrite-free lithium.[83] In addition, the strategy of UIO-66-NH_2 *in-situ* grown on the surface of silica nanoparticle had been demonstrated to enhance ionic conductivity and suppressthe growth of lithium dendrites.[84]

In 1999, HKUST-1 was initiatively synthesized by Chui and colleagues,[85] which was a kind of highly porous metal coordination polymer with a pore size of 1 nm, high accessible porosity of about 40%, high thermal stability (240°C), and abundant OMS. In view of the good compatibility resulting well dispersion and the certain flame-retardancy property, Wang's group proposed a class of MOF/PEO-SSEs with

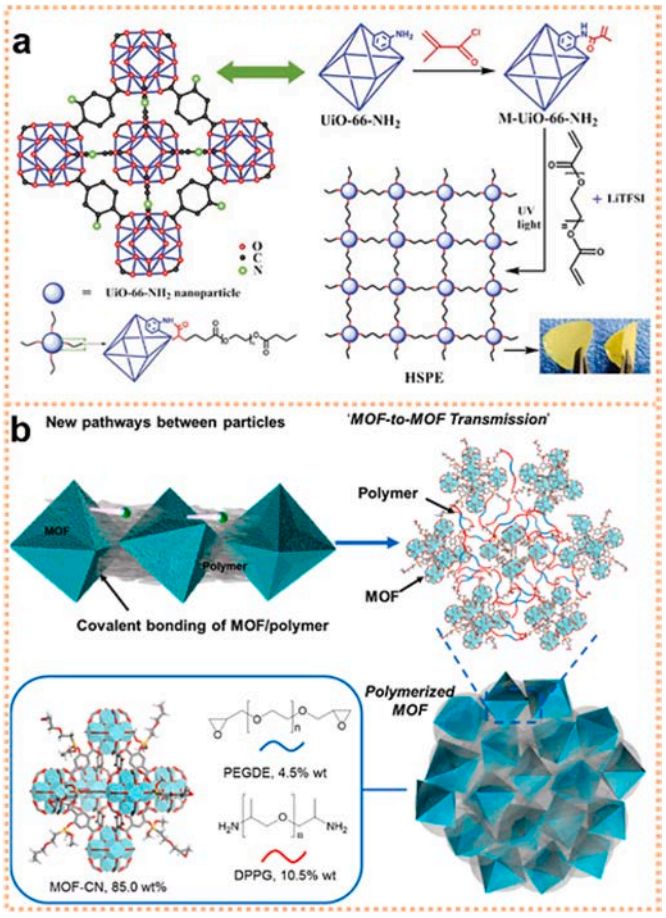

Fig. 11. MOF/PEG-based SSEs. (a) Schematical preparation of MOF/PEGDA-SSE based on UIO-66-NH_2 covalently linking PEGDA and LiTFSI. Reproduced with permission.[94] Copyright 2018, Royal Society of Chemistry. (b) Schematic illustration of design MOF/PEGDA-SSEs through a bioinspired strategy. Reproduced with permission.[95] Copyright 2020, American Chemical Society.

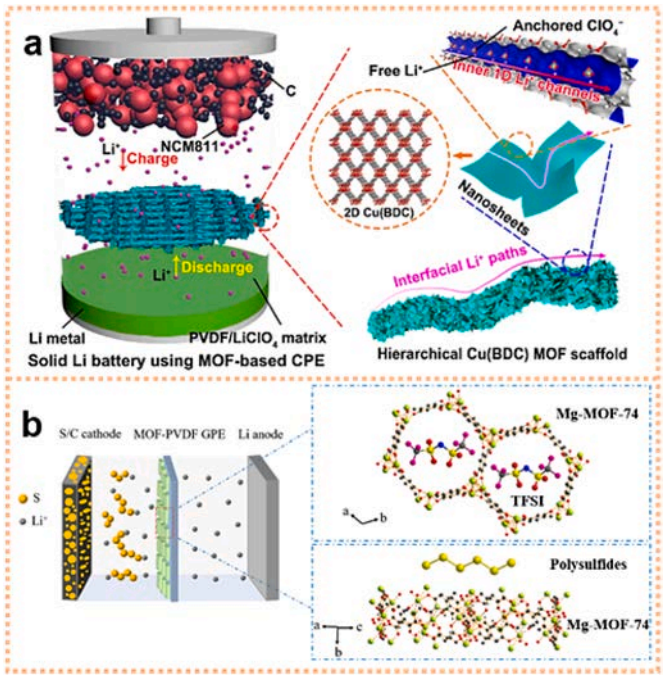

Fig. 12. MOF/PVDF-based SSEs. (a) Schematic illustration of the 3D Cu(BDC)/PVDF-based SSE.[99] Reproduced with permission. Copyright 2019, American Chemical Society. (b) Schematic illustration of MOF/PVDF-based SSE with anions immobilized for the lithium-sulfur battery.[100] Reproduced with permission. Copyright 2021, American Chemical Society.

activated HKUST-1, which could also act as an additivity with multi-function, such as, reduced the glass transition temperature point (T_g), captured ions ($TFSI^-$) to facilitate lithium transference number, enhanced the mechanical property, effectively improved the electrochemical performance, and possessed the fire safety.[86]

Zhang and co-workers demonstrated that a nanorod-like Al-MOF was helpful to synchronously suppress the crystallization of PEO and weak the interaction of among PEO chains, leading to enhanced ionic conductivity and improved electrochemical stability.[87] Meanwhile, the micrometer scale length forming a 3D-network and the microporous structure could further enhance the transport of Li^+, resulting in the ion conductivity of 2.09×10^{-5} S cm^{-1} at 30°C and 7.11×10^{-4} S cm^{-1} at 60°C, and a t_{Li+} of 0.46. Further, a similar work was reported by Stephan's group where a type of Al-based MOF (Al-TPA-MOF) with a Lewis acid center interacted with the anion of LiTFSI was chosen to design MOF/PEO-based SSEs.[88] Thus, both Li||S and Li||LFP cells exhibited specific capacities exceeding 800 and 130 mAh g^{-1}, respectively. Liu's group had reported a series of MOF/PEO-based SSEs for Li||S batteries with MIL-53(Al).[89] It's noteworthy that the strong Lewis acid from MIL-53(Al) could adsorb abundant $TFSI^-$ groups leading to an electronegativity of MIL-53(Al), which could reject polysulfide anions through the electrostatic reaction resulting in hindering polysulfide dissolution.

Moreover, Ni-based MOF had been demonstrated one of promising candidates to design MOF/PEO-based SSEs by Stephan's group, in which Ni_3-$(BTC)_2$ was synthesized through Ni salt and 1,3,5-benzene tricarboxylate and was employed with LiTFSI.[90] Further, ultrathin nanosheet-like Ni-based MOFs (NMS) with a high aspect ratio were demonstrated that it's effectively hampered the crystallization of PEO region and thus boosted the Li^+ passport by Han and co-workers.[91] Besides, the Lewis acid-base interaction of between the surface-coordinated unsaturated Ni atoms of NMS and $TFSI^-$ could facilitate the dissociation of LiTFSI and further reach a high t_{Li+} of 0.378. The assembled Li||LFP cells showed a high reversible capacity of 130 mAh g^{-1} at 0.1 C and 30°C for 50 cycles. Moreover, a series of MOF/PEO-SSE were designed in this simple strategy with some other metal-based MOFs, such as Mg-TMA[92] and Ce-MOF[93].

2.3.1.2. MOF/PEG-based SSEs. Comparing with linear polymers, crosslinked polymers often have enhanced mechanical properties due to the three-dimensional interwork, which can be more conducive to suppress the growth of lithium dendrite. Zhang's group firstly reported a MOF/PEGDA-SSE based on UIO-66-NH_2 covalently linking PEGDA and LiTFSI (**Fig. 11a**).[94] The UIO-66-NH_2 linked with PEGDA as carbon-carbon double bonds could form a space grid structure and avoid aggregation, which could provide additional Li^+ transport channels and effectively adsorb the impurities from the electrochemical reduction process to further improved ionic conductivity. The ionic conductivity of as-prepared MOF/PEGDA-SSE could reach 4.31×10^{-5} S cm^{-1} at 30°C and the assembled Li||LFP cells exhibited superior low/high temperature performance, of which the initial discharge capacity is 140 mA h g^{-1} with the retention of specific capacity is 121 mA h g^{-1} after 100 cycles at 0.2 C (28°C) and the discharge capacity reaches 110 mA h g^{-1} at 2 C (60°C). Likewise, Huang's group designed a kind of MOF/PEGDA-SSEs through a bioinspired strategy, in which surficial function MOF (MOF-CN) from UIO-66-2OH was used to cross-link with poly(ethylene glycol) diglycidyl ether (PEGDE) with diamino-poly (propylene glycol) (DPPG) *via* an *in-situ* ring-opening reaction (**Fig. 11b**).[95] On account of the covalent-bond between MOF-CN and polymer matrixes, the obtained MOF/PEGDA-SSE showed a low

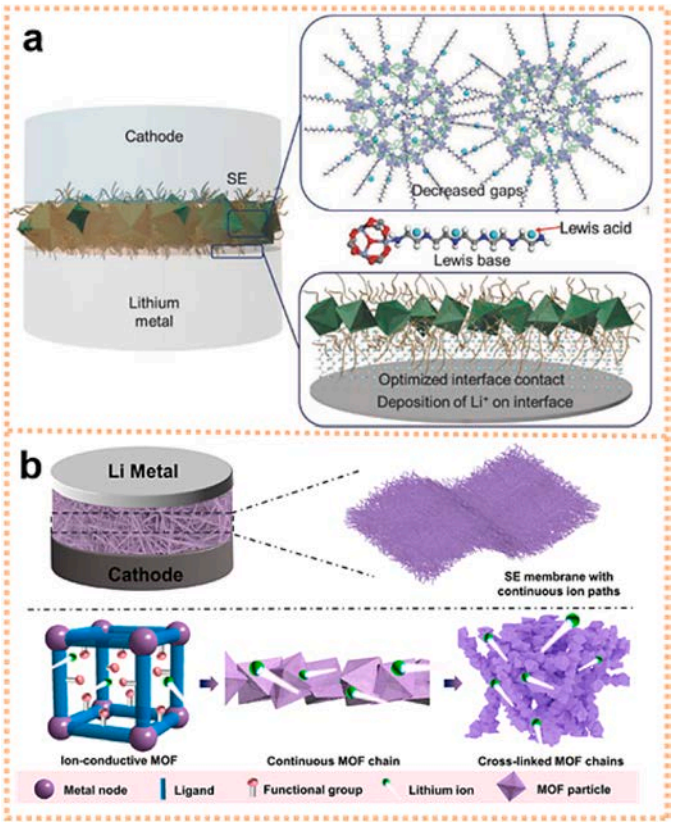

Fig. 13. MOF/PVDF-HFP-based SSEs. (a) Schematic illustration of the molecular-scale interface engineering strategy of MOF with long chain Lewis base.[114] Reproduced with permission. Copyright 2020, Wiely-VCH. (b) Schematic structure of flexible cross-linked MOF chains as SSE and Synthesis of cross-linked MOF Chains on BC skeleton. Reproduced with permission.[115] Copyright 2021, American Chemical Society.

interface resistance (34.0 Ω) and a high t_{Li+} (0.8). The resulted Li||LFP cells presented specific capacities of 153, 150, 144, and 130 mAh g^{-1} at 0.2, 0.5, 1, and 2 C, respectively. Further, Zn||$NH_4V_4O_{10}$ cells also showed excellent capacity and cyclic performances.

Recently, Wang's group reported a king of SSEs, with an ionic conductivity of 9.96 × 10^{-5} S cm^{-1} at 30°C, based on methoxy poly (ethylene glycol) acrylate through *in-situ* UV polymerization compositing with ZIF-8.[96] The resulted Li||LFP cells showed a capacity of 116 mAh g^{-1} at 0.5 C and 30°C and a retention of 89.4% after 150 cycles with the average coulombic efficiency of 99.9%. In contract to linear polymers, cross-linking polymers possess a higher mechanical property. Thus, Sun's group design a sort of SSEs composting with thiol-branched poly(ethylene glycol) diacrylate (PEGDA) with an ionic conductivity of 2.26 × 10^{-4} S cm^{-1} at 25°C and good mechanical strength (9.4 MPa)/toughness (≈ 500%), which was prepared by covalently cross-linking UIO-66-NH-MET, tetrakis (3-mercaptopropionic acid) pentaerythritol (PETMP) and PEGDA.[97] Then, high electrochemical window (>5.4 V), low interfacial impedance (<550 Ω), and t_{Li+} of 0.44 were achieved. In consequence, Li||Li cells could be stable up to 1300 h and Li||LFP cells demonstrated a capacity of 143.7 mAh g^{-1} at 0.5 C with a retention of 85.6% after 500 cycles.

2.3.1.3. MOF/PVDF-based SSEs. On account of the merits of high relative permittivity (8.3), high melting temperature (172°C), high tensile strength (up to 50 MPa), and large voltage window (4.5 V), PVDF had been seen as another one of the most promising candidate polymer matrixes for SSEs.[98] Yaghi's group firstly designed Li^+ exchange MOF-688, which was further mixed PVDF to form a membrane separator with a macroporous cellulose support.[43] The obtained MOF/PVDF-SSE gave give high ionic conductivity (3.4 × 10^{-4} S cm^{-1} at 20°C), a high t_{Li+} (0.87), and low interfacial resistance (353 Ω), due that most of charges within MOF-688 were carried by Li^+. Finally, the Li|| LFP cells presented the initial discharge capacity of 125 mAh g^{-1} with the capacity retention of 96% after 200 cycles at 30 mA g^{-1}. Further, Gao's group developed a kind of MOF/PVDF-SSEs based of PVDF and Mg-MOF-74, which had a high pore size of 10.2 Å and abundant Lewis acidic sites for immobilizing polysulfides anions and encage $TFSI^-$ anions of LiTFSI (**Fig. 12a**).[99] The obtained MOF/PVDF-SSE was favor to a uniform Li^+ flux and further facilitate homogenous lithium plating/stripping to form stable SEI film.

In order to enhance limited ionic conductivity and insufficient mechanical strength of polymer matrix, Yu and co-workers' adopted layered MOF (Cu(BDC)), which possessed a 1D Li^+ channel and was *in situ* growth on a nonwoven fabric to form a 3D continuous structure, to construct MOF/PVDF-SSE composing of PVDF and $LiClO_4$ (**Fig. 12b**).[100] DFT results proved that, due to the lower adsorption energy of the ClO_4^-, the OMS from Cu(BDC) could anchor the ClO_4^- and further release the Li^+ resulting fast Li^+ pathways. Meanwhile, the 3D continuous structure could boost the mechanical strength of MOF/PVDF-SSE and improve the interfacial contact of Cu(BDC) and PVDF, simultaneously. Finally, Li||NCM811 cells achieved a high reversible capacity of 164 mAh g^{-1} with coulombic efficiency of 99.4% after 80 cycles at 0.1 C (30°C).

Although PVDF possessed high electric constant and strongly polar C-F bonds, the absence of interaction with Li^+ and poor interfacial stability restrained PVDF-based SSEs further application in energy storage. Thus, Kang and co-workers reported a kind of single-ionic conducting SSE (PL/UIOLiTFSI) using anionic functional MOF (LiUIO-66), which was covalently linked the trifluoromethanesulfonyl group (Tf).[101] Because of the strong electron-absorption of O=S=O and the charge delocalization of nitrogen atom in Tf from the inside pore of LiUIO-66, the resulted PL/UIOLiTFSI showed an ionic conductivity (2.07 × 10^{-4} S cm^{-1} at 25°C) and a high t_{Li+} (0.84). Finally, Li||Li cells showed an excellent cycle stability and low polarization voltage, and Li||LFP cells maintained a capacity retention (97.0%) after 500 cycles at 25°C and simultaneously exhibited high-rate performance at 0°C.

2.3.1.4. MOF/PTFE-based SSEs. PTFE, as the most stable polymer, has been widely used as binder in the preparation of electrodes.[102] Shen and colleagues firstly designed a series of MOF, such as HKUST-1, UIO-(66/67), MIL-100-(Al/Cr/Fe), and MOF-5.[103] And six types of pseudo-SSEs were prepared based on the above MOFs pressing into dense pellets with PTFE and further soaking in the $LiClO_4$-PC solution (LPC). The authors further demonstrated that large pore channel would allow more effective solvation of the lithium ion, the OMS coordinating with anions would be essential for Li^+ transport, and the strong acidity of OMS were also favor to the dissociation of ion pairings and improvement ion transport. Based on Grotthuss-like mechanism, Cu-MOF-74 was chosen to design MOF/PTFE-based SSEs *via* this same strategy, which was reported by Yuan and coworkers.[104]

Dong's group prepared a kind of quasi-SSEs based on the matrix film of ZIF-8/PTFE impregnating into organic liquid electrolyte (1 M $LiPF_6$ in EC/DMC/EMC).[105] Profiting from the hybrid features of inorganic ZIF-8 nanoparticles and organic PTFE within the matrix film, the as-prepared quasi-SSEs exhibited good thermal stability (up to 350°C), which was much higher than the boiling point of the liquid electrolyte solvents (90°C for DMC, 107°C for EMC, 160°C for EC) and the melting point of PE/PP based Celgard membrane (135°C for PE, 165°C for PP). And the ionic conductivity at 25°C and t_{Li+} of the as-prepared quasi-SSEs reached 10^{-4} S cm^{-2} and 0.52, respectively. Then, Li||LCO cells exhibited an initial discharge capacity of 135 mAh g^{-1} at 50 mA g^{-1} and the remaining capacity of 119 mAh g^{-1} after 100 cycles. Further, Liu and co-workers developed a new MOF/PTFE-SSE based on PTFE and hollow

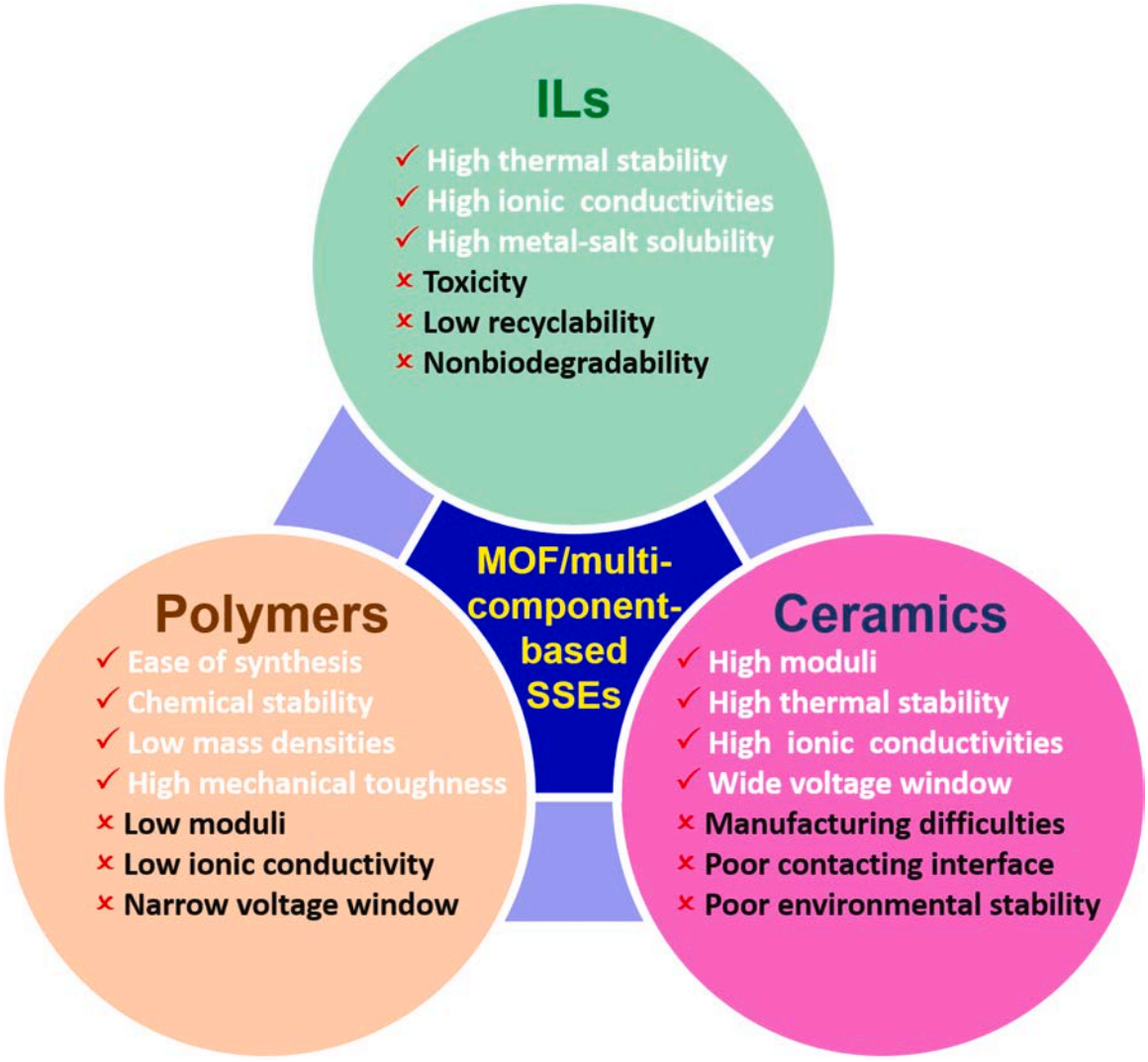

Fig. 14. The design rationale of MOF/multicomponent-based SSEs including ILs, polymers, or/and ceramics.

MOF (ZIF-67@ZIF-8) with a $LiPF_6$ solution, in which could store more Li^+ and facilitate Li^+ transport through the wall of the special hollow structure.[106] The ionic conductivities of as-prepared MOF/PTFE-SSE were 3.44×10^{-4}, 1.35×10^{-3}, and 4.98×10^{-3} S cm^{-1} at -20, 25, and 100°C, respectively. Thus, Li||LFP cells achieved the initial discharge capacity of 116 mA h g^{-1} with the capacity retention of 89.1% after 100 cycles.

Recently, in consideration of the features of grain boundary-free and isotropic characteristics within the glassy MOF, Xu's group developed a kind of glassy ZIF-4/PTFE based SSE with lean Li content (0.12 wt%) and miniscule amount of solvent (19.4 wt%).[107] Thus, a remarkable ion conductivity of 1.61×10^{-4} S cm^{-1} was achieved at 30°C, and a capacity of 101 mAh g^{-1} was kept after 500 cycles at 1 C was also demonstrated for Li||LFP cells.

2.3.1.5. MOF/PVA-based SSEs. Due to excellent chemical stability, good mechanical property, high processibility, and nontoxicity, PVA had also been seen as one of the most promising candidates to study.[108] Lu *et al.* fabricated a series of MOF/PVA-SSEs based on UIO-66 particles containing OMS and PVA through a simple electrospinning technique.[109] Except the high specific surface and order pore channels, the OMS from MOF particles could also effectively immobile anions and further modulate the transport of Li^+. The strong chemical bond between dangling carboxylic acid groups of MOF and hydroxyl groups of PVA could lead to a crosslinking-like structure, which could reduce the contact resistance and improve Li^+ transport. Thus, t_{Li+} of the as-prepared MOF/PVA-SSE could reach 0.79 at 30°C, and both graphite||NCM and LTO||LFP full cells exhibited improved rate capability and cycling durability.

2.3.1.6. MOF/PSS-based SSEs. Single-ion conducting polymers are a class of the polymer backbone with tethered anions *via* a covalent bond and with associated counterions. As an representative work, Chen's group reported a simple method to construct membrane-like materials based on polystyrene sulfonate (PSS) threaded MOF (HKUST-1) through an *in-situ* confinement conversion process.[110] The as-prepared membranes (PSS@HKUST-1-6.7), with uniquely 3D sulfonate networks, showed high Li^+ conductivity capability (5.53×10^{-4} and 1.89×10^{-3} S cm^{-1} at 25 and 70°C, respectively) and high Li^+ flux (6.75 mol m^{-2} h^{-1}). Moreover, due to the size sieving effects and the affinity differences of the sulfonate groups towards alkaline and alkaline-earth metal ions, the PSS@HKUST-1-6.7 membrane presented excellent selectivity for Li^+ over Na^+, K^+, and Mg^{2+} with binary ion separation factors of 35, 67, and 1815, respectively.

2.3.2. MOF/copolymer-based SSEs

Comparing with homopolymer, copolymer based on the polymerization of two or more different types of monomers, usually possess

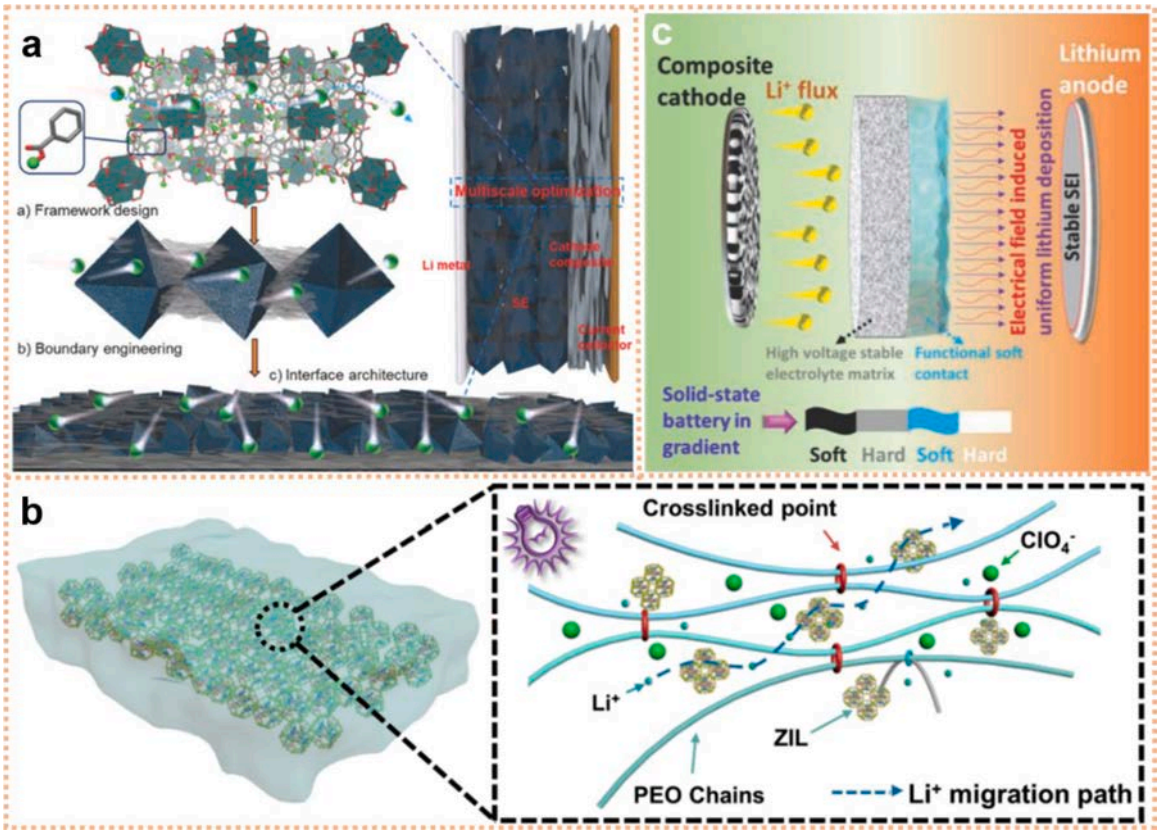

Fig. 15. Schematic illustration of (a) UIO-SO_3H/IL/PVDF SSE based on the multiscale optimization strategy. Reproduced with permission.[119] Copyright 2020, Royal Society of Chemistry. (b) Design ZIF/IL/PEO SSE based on the Li^+ transport mechanism of "chain-ZIL-chain". Reproduced with permission.[121] Copyright 2020, American Chemical Society. (c) Configuration of the solid-state battery based on the "soft-hard-soft-hard" mechanism.[127] Reproduced with permission. Copyright 2020, Wiley-VCH.

diverse properties combining from the indigenous monomers into a single backbone. Recently, the following two different class copolymers have been attracted increasing research attention.

2.3.2.1. MOF/PVDF-HFP-based SSEs. Due to the high degree of crystallinity, the main chain of PVDF could not provide enough free volume to mobile Li^+ resulting in a low conductivity.[111] PVDF-HFP, which was a class of copolymer based on the random copolymerization of two different monomers (VDF and HFP), had a higher conductivity than that of PVDF owing to the CF_3 pendant group from the HFP monomers providing steric hinderance to generate amorphous domains. Furthermore, apart from the abovementioned merits of PVDF, PVDF-HFP could adsorb more electrolyte and have lower solubility in acetone and lower melting temperature. Lu's group developed a kind of MOF/PVDF-HFP-SSEs based on UIO-66 containing OMS and PVDF-HFP, which simultaneously possessed high ionic conductivity (up to 10^{-3} S cm^{-1}) and t_{Li+} (0.66) at room temperature, and low activation energy (<0.1 eV).[112] Thus, Li||LFP, Li||NCM523, and LTO||LFP cells were implemented and all exhibited improved electrochemical performances. Similarly, Zhang's group adopted a series of ion conductive MOF (Zr-MA-M (M = Li^+, Na^+, K^+, Zn^{2+})) with -SH groups functionalized in small pores and metal ions adsorbed on the thiol groups to prepare MOF/PVDF-HFP-SSEs (SE-Zr-MA-M).[113] Both the -SH groups in pores and metal ions adsorbed on the thiol groups could boost the ion transport resulting high ionic conductivity (the ion conductivities of Zr-MA-Li^+ achieved at 6.62×10^{-4} S cm^{-1}) and high t_{Li+} (0.63). Besides, low interfacial resistance and wide electrochemical window up (4.6 V) could be also realized. Thus, the obtained Li||LFP cells showed 152.5 mA h g^{-1} at 0.2 C with a small polarized voltage (0.08 V), stable cyclic properties and remarkable rate performances. Later on, the same group further discovered ion conductive MOF decorated with a long chain Lewis base could be helpful for improving the interfacial contact and boosting the ionic conductivity of MOF/PVDF-HFP-SSEs (**Fig. 13a**).[114] The reasons could be attributed that the Lewis base reacting with Li^+ was directly anchored on the OMS of MOF through chemical bond and the flexuous long-chain structure could reduce the ion transport gaps between adjacent MOF nanoparticles and further improve the interfacial resistance between electrolytes and electrodes. Further, consideration of separated MOF resulting high interfacial contact for ion transport, a strategy of cross-linked MOF chains growth from the bacterial cellulose (BC) nanofibers to construct continuous ion-conductive paths was reported by Zhang's group (**Fig. 13b**).[115] Benefitting from the cross-linked MOF chains, the resulted SSEs exhibited an ionic conductivity of 7.88×10^{-4} S cm^{-1}, a t_{Li+} of 0.88 at 25°C, and a wide electrochemical window voltage up to 5.1 V.

2.3.2.2. MOF/P(TFEMA-ran-PEGMA)-based SSEs. Furthermore, Zhang's group also reported a kind of MOF/Copolymer-based SSEs based on the copolymerization of PEGMA with trifluoroethyl methacrylate (TFEMA).[116] Benefiting from relatively rigid fluorine-containing PTFEMA segments and promoting charge carrier transport of PPEGMA segments from the copolymer matrix (P(TFEMA-ran-PEGMA)), the obtained MOF/Copolymer-based SSE showed excellent flexibility, processibility, free-standing capability, and electrochemical performances, which the ionic conductivity at 30°C and t_{Li+} reached 4.31×10^{-5} S cm^{-1} and 0.51, respectively. Therefore, Li||LFP cells showed the initial discharge specific capacity of 116 mA h g^{-1} and the capacity retention of 92.2% after 25 cycles at 0.1 C (60°C).

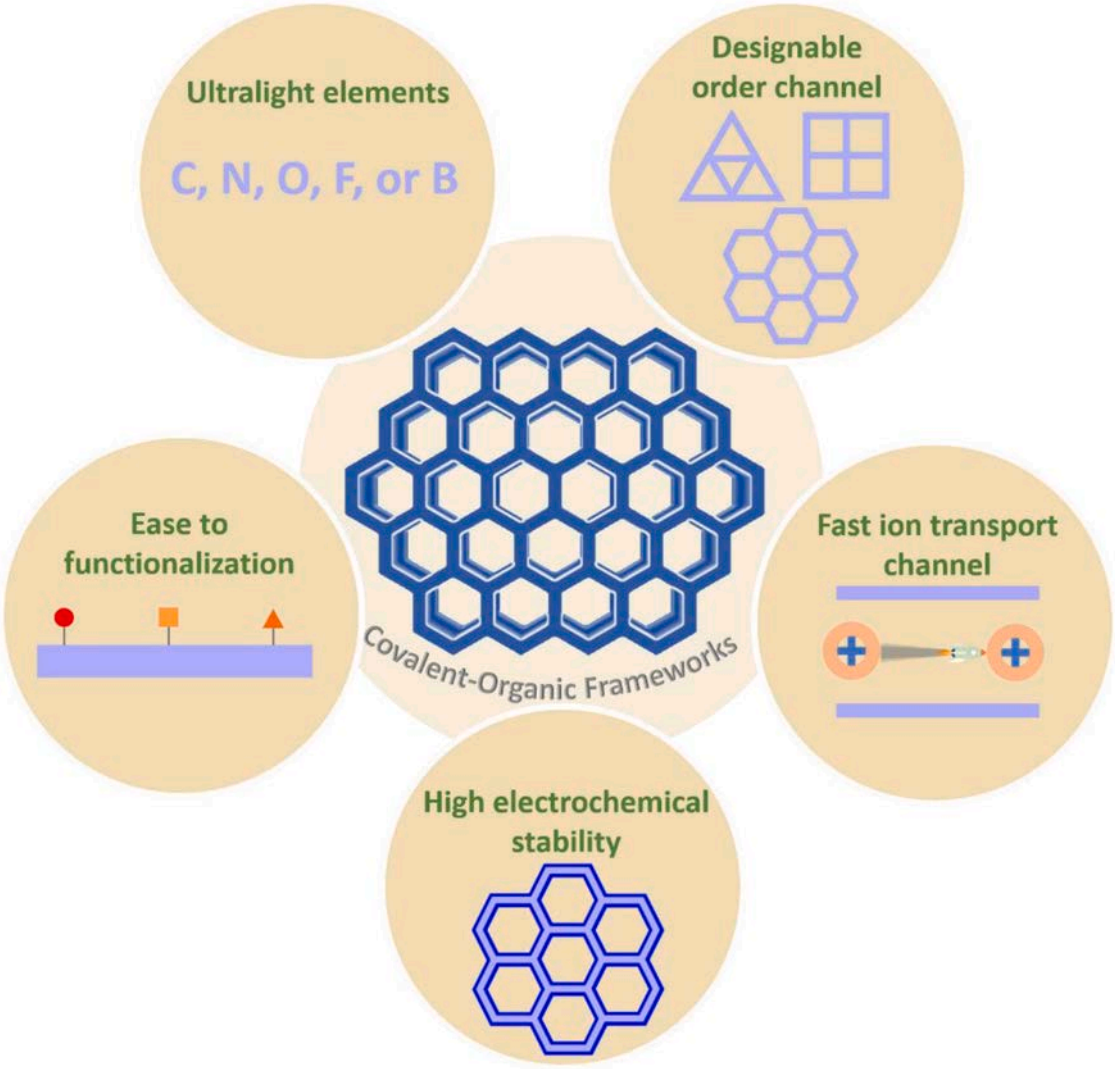

Fig. 16. Schematic illustration for the merits of COFs as filler into SSEs.

2.4. MOF/multicomponent-based SSEs

Although the recent progress of MOF ion conductors, MOF/ILs SSEs, and MOF/Polymer SSEs has been made, they still remain studied insufficiently and cannot fully meet the requirement for practical industrial applications. Especially, poor interfacial contact between electrolytes and electrodes, natural brittle feature in MOF/ILs SSEs, and low ionic conductivity and insufficient electrochemical stability for MOF/Polymer SSEs have not yet been fully resolved and should be further investigated to construct improved SSEs. With the aim of solving the above issue associating with MOF-based SSEs, it shows great potential that through the combining with multicomponent to design MOF/multicomponent-based SSEs (Fig. 14).

2.4.1. MOF/IL/polymer-based SSEs

UIO/ILpolymer SSEs: Wu and colleagues developed a pioneering work of UIO/IL/PEO-based SSEs based on UIO-66 loading with Li-IL (LiTFSI in [EMIM][TFSI]) and PEO matrix.[117] The nanostructured UIO-66 was homogenously dispersed in PEO matrix leading to a uniformly distribution and a low crystallinity of PEO, the ionic conductivity could reach to 1.3×10^{-4} S cm^{-1} at 30°C. Moreover, another similar work based on UIO-67 was reported by Liu and coworkers.[118] Consideration of the low conductivity in this method, a modified strategy was further reported by Huang's group,[119] in which Li^+ conductive UIO-66 binding Li^+ with ionogenic chemical groups, including -CO_2H, -SO_3H, and -OH, was choose to replace the pristine UIO-66 and further to design UIO/IL/PVDF-based SSEs with PVDF matrix (Fig. 15**a**). Because of the improved Li^+ transportation from a multiscale optimization strategy: molecular scale Li^+ transport within conductive UIO-66, nanoscale transport between the UIO-66's boundaries, and microscale interfacial contact from SSE and electrodes. A high ionic conductivity of 1.06×10^{-3} S cm^{-1} at 25°C would be reached. The Li||LFP cells displayed a wide temperature range from -20°C to 60°C.

ZIF/IL/polymer SSEs. Zhang and co-workers adopted a kind of hollow ZIF-8 encapsulating with Li-[EMIM][TFSI] and PEO to prepare hollow-ZIF/IL/PEO-SSE with a thickness of 50 μm, in which the hollow structure could facilitate the passage and storage of more Li-IL.[120] The ionic conductivities of as-prepared hollow-ZIF/IL/PEO-SSE reached at 1.41×10^{-4} S cm^{-1} at 25°C. When paired with NCM811 cathode, Li||NCM811 cells demonstrated an discharge capacity of 182.5 mAh g^{-1} and capacity retention of 73% after 100 cycles at 0.1 C at 60°C.

Cross-linked copolymer electrolytes with a network structure, different from most of linear polymeric matrix adopting in SSEs, can be used to increase the mechanical strength and thermal stability of polymer matrix and some unexpected property, like leading fast ion transport path. Thus, Xia and co-workers proposed a new Li^+ transport mechanism (denoted as "chain-ZIL-chain") between cross-linked PEO and ZIF-8 incorporated with Li-IL (ZIL), in which ultraviolet irradiation

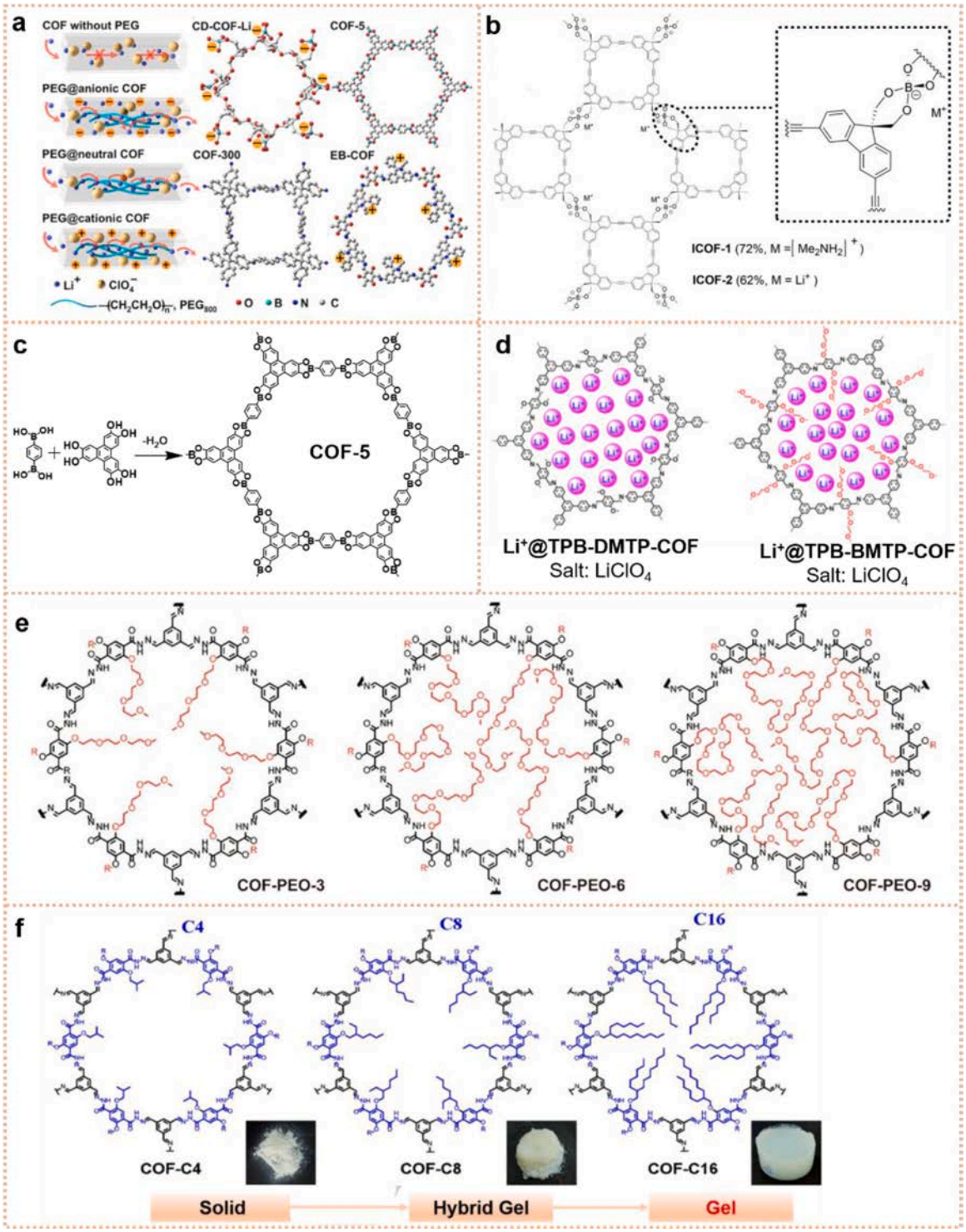

Fig. 17. (a) Structural representations of CD-COF, COF-5, COF-300, EB-COF and the schematic illustrations of Li^+ transport [129]. Reproduced with permission. Copyright 2019, American Chemical Society. (b) Structures of ICOF-1 and ICOF-2.[130] Reproduced with permission. Copyright 2016, Wiley-VCH. (c) Synthesis and structural of COF-5. (d) Structure and conductivities of two COFs grafting without and with oligomer (ethylene oxide) chains [132]. Reproduced with permission. Copyright 2018, American Chemical Society. (e) The structure of three COF-PEO-n with different numbers of PEO units.[133] Reproduced with permission. Copyright 2019, American Chemical Society. (f) The structure of COF-Cx (x=4, 8, 16) with different length of branched alkyl chains.[134] Reproduced with permission. Copyright 2022, Wiley-VCH.

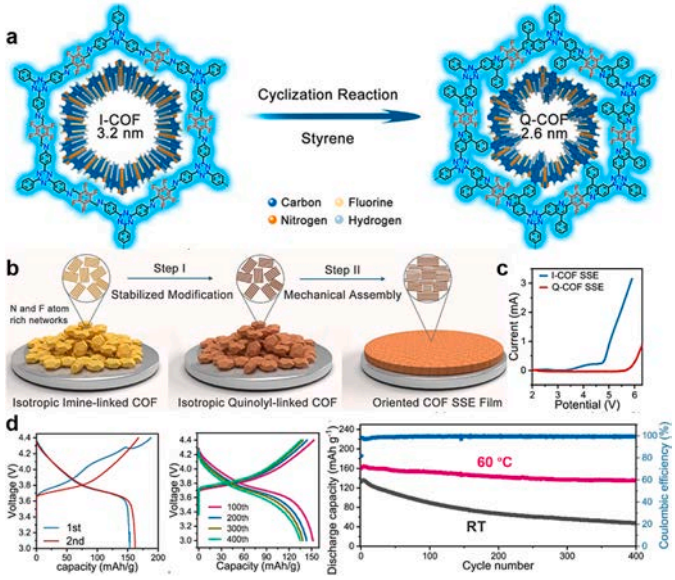

Fig. 18. (a) Synthesis of Q-COF by the cyclization reaction of I-COF. (b) Synthesis of the electrochemically stable and holistically oriented COF SSE in two steps; (c) LSV curves with the I-COF and Q-COF SSE at 1 mV s^{-1} under 60 °C; (d) All solid states Li||NMC811 cells performance with Q-COF SSE prepared at high temperature (pink) and RT (black).[135] Reproduced with permission. Copyright 2021, Wiley-VCH.

was utilized to construct cross-linked PEO matrix with 4-methylbenzophenone (MBP) as the photo initiator leading to a low crystallization and the Li^+ transport mechanism of "chain-ZIL-chain" from "chain-chain-chain" on the solid-liquid transport interface (**Fig. 15b**).[121] Thus, an ionic conductivity of 4.26 × 10^{-4} S cm^{-1} at 30°C, high t_{Li+} of 0.67, and good compatibility with lithium metal anode over 1040 h were realized.

Cu-based MOF/IL/polymer SSEs. Further, in consideration of HKUST-1 possessing 3D channels and OMS, Yuan's group designed a kind of SSEs (CPEs) through HKUST-1 encapsuled with Li-IL (LiTFSI and [EMIM][TFSI]) and PEO matrix.[122] The obtained CPE exhibited a high ionic conductivity of 1.2 × 10^{-4} S cm^{-1} than that of pure PEO electrolyte (9.76 × 10^{-6} S cm^{-1}) at 30°C. And the assembled Li||LFP cells delivered a reversible capacity of 136.2 mAh g^{-1} after 100 cycles. Further, Dutta and coworkers investigated that ionic transport behaviors of ionic liquids ([BMIM][Br] and [BMIM][BF_4]) loaded in another Cu-based MOF (CuBTC) with PEO and PVDF-HFP matrix, respectively.[123] Based on the strong interaction between Cu metal cluster of CuBTC and Br^- or BF_4^- anions, both two different SSEs containing 50 wt % IL showed ionic conductivity as high as the order of 10^{-3} S cm^{-1} at 380 K and electrochemical stability up to 6.1 V.

2.4.2. MOF/bicomponent polymer-based SSEs

Wang and co-workers precisely designed a kind of 3D asymmetric cross-linked network MOF/PI-SSE (SPE2-PI-ZIF8) consisting of in-situ polymerization of poly(ethylene glycol) diacrylate (PEGDA) and butyl methacrylate (BMA) and ZIF-8 nanoparticles modified polyamide (PI-ZIF8), which showed high ionic conductivity (4.7 × 10^{-4} S cm^{-1}) and t_{Li+} (0.68) at room temperature.[124] Furthermore, based on SPE2-PI-ZIF8, Li||Li symmetric cells exhibited cyclic stability over 800 h at current densities of 0.1 mA cm^{-2} for 0.1 mAh cm^{-2}, and Li||NCM523 cells delivered a capacity retention of 95.6% after 100 cycles at 0.5 C. This as-prepared asymmetric MOF/PI-SSE could not only suppress the growth of lithium dendrites through regulation the uniform Li^+ transport of ZIF-8 layer, but also reduce the interfacial resistance between electrodes and electrolytes through *in-situ* copolymerization of PEGDA and BMA.

Alternatively, Zheng's group developed a kind of 3D interconnected MOF network-based SSE *via* the electrospinning of PAN and several MOFs and then backfilled with PEO/LiTFSI.[125] The precise structure of 3D interconnected MOF/PAN network not only provides a continuous pathway for fast Li^+ transport among adjacent MOF particles thereby effectively increasing the ionic conductivity, but also significantly enhances the mechanical strength of the resulting SSE. Furthermore, they demonstrated that the as-obtained SSE with optimized pore size and strong cationic site from different MOFs could afford a homogeneous Li^+ flux with a t_{Li+} of 0.52 and an ionic conductivity of 2.89 × 10^{-4} S cm^{-1}. Then, Li||Li cells could be stably operated for more than 700 h. The resulting SSE is also demonstrated to enable the stable cycling of Li||LFP and Li||NCM111 cells.

2.4.3. MOF/IL/ceramic SSEs

Although SSEs were considering to be promising candidate for future solid-state battery, the processability of SSEs leaded to a potential interfacial contact issue, which would become the significant factor for hindering the further practical application, especial in the inorganic ceramics solid-electrolytes with the natural drawback of rigid and brittle. Therefore, Pan's group designed a novel type of MOF/IL/Ceramic-based SSEs (LIM) through a method of physical mixing, which were consisting inorganic ceramics ($Li_7La_3Zr_2O_{12}$, LLZO) with MOF ionic conductor based on UIO-67 loading with Li-IL (LiTFSI and [EMIM][TFSI]).[126] The loading Li-IL within the pore of UIO-67 could directly contact with the LLZO nanoparticles to form nanowetted interface, giving rise to boost Li^+ transport and contacting compatibly with lithium metal anode. Also, the obtained LIM displayed a high ionic conductivity of 1.0 × 10^{-4} S cm^{-1} with a wide electrochemical window of 5.2 V at room temperature. Therefore, through the nanowetted interfacial mechanism, the Li||LCO and Li||LFP cells showed cyclic stability with acceptable rate performance at active loadings of 15.9 and 12.4 mg cm^{-2}, respectively.

2.4.4. MOF/polymer/ceramic-based SSEs

Further, taking account of the compatibility of polymer electrolyte, a concept of bilayer heterointerface MOF/polymer/ceramic-based SSEs was proposed by Sun and co-workers,[127] in order to boosting ionic conductivity at room temperature, perfecting interfacial contact, and reducing polarization. The bilayer heterointerface SSEs with a thickness of *c.a.* 80 μm, which was consisting of a tough ion-conductive hybrid matrix of LiTFSI/PVDF-HFP/garnet-typed nanowires ($Li_{6.75}La_3Zr_{1.75}Nb_{0.25}O_{12}$, LLZN) and an interfacial soft-humid gel-like layer of PEO/PVDF-HFP/modified HKUST-1, possessed a gradient configuration of "soft-hard-soft-hard" resulting a good interfacial contact (**Fig. 15c**). The configuration, in which Li^+ could easily transport through the channels of HKUST-1 and LLZN nanowires leading to a uniform deposition, could simultaneously buffer the volume change and form a stable solid-electrolyte interface with good electrochemical stability from the reaction of multicomponent. Additionally, the intensive hydrogen bonds among the joint surface further assisted the carriers transporting across the interface, and the inorganic layer was also improved the mechanic strength of gel-like layer. Thus, an ionic conductivity of 2.00 × 10^{-4} S cm^{-1}, a t_{Li+} of 0.62, and an electrochemical window of 4.92 V would be realized, and the Li||LCO and Li||LFP cells would be worked at room temperature with high capacity and superior cycling stability. Also, the pouch cell utilizing this bilayer heterointerface SSE exhibited good flexibility and excellent durability under some extreme testing conditions.

Recently, Zhao and co-workers employed ZIF-67/PEO (ZCPL) as a protective SSE layer to prevent the redox reaction between $Li_{1.5}Al_{0.5}Ge_{1.5}(PO_4)_3$ (LAGP) and Li metal.[128] The ZCPL layer could not only infiltrate into the gap of the LAGP surface with intimate contact but also provide rich pathways for fast Li^+ transport and ensure a uniform Li^+ flow through the interface. Consequently, a much more stable interface

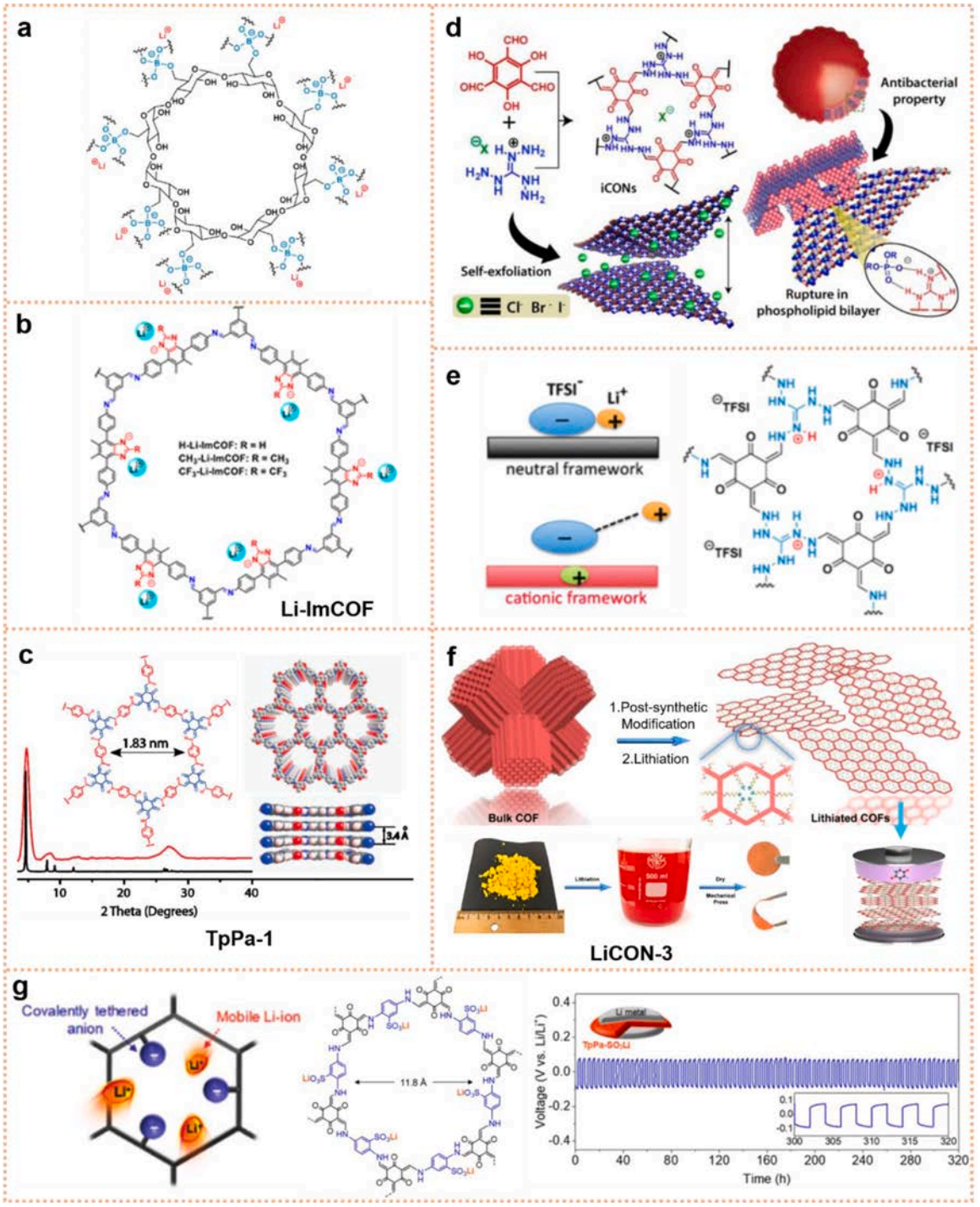

Fig. 19. (a) Synthesis of CD-COFs with different counter ions. Reproduced with permission.[136] Copyright 2017, Wiley-VCH. (b) Synthesis of ImCOFs and Li-ImCOFs and TEM images of H-ImCOF and H-Li-ImCOF. Reproduced with permission.[137] Copyright 2019, American Chemical Society. (c) Schematic representation of the synthesis of TpPa-1 and TpPa-2. Reproduced with permission.[138] Copyright 2012, American Chemical Society. (d) Synthesis of iCONs and self-exfoliation TEM images of H-ImCOF and H-Li-ImCOF. Reproduced with permission.[139] Copyright 2016, American Chemical Society. (e) Structure of the cationic COF for binding with anions as the Li^+ conductor. Reproduced with permission.[140] Copyright 2018, American Chemical Society. (f) Schematic illustration describing the fabrication of all-solid-state organic Li-ion battery using lithiated COF nanosheets. Reproduced with permission.[141] Copyright 2020, American Chemical Society. (g) Structure of solvent free TpPs-SO_3Li and Li||Li battery. Reproduced with permission.[142] Copyright 2019, American Chemical Society.

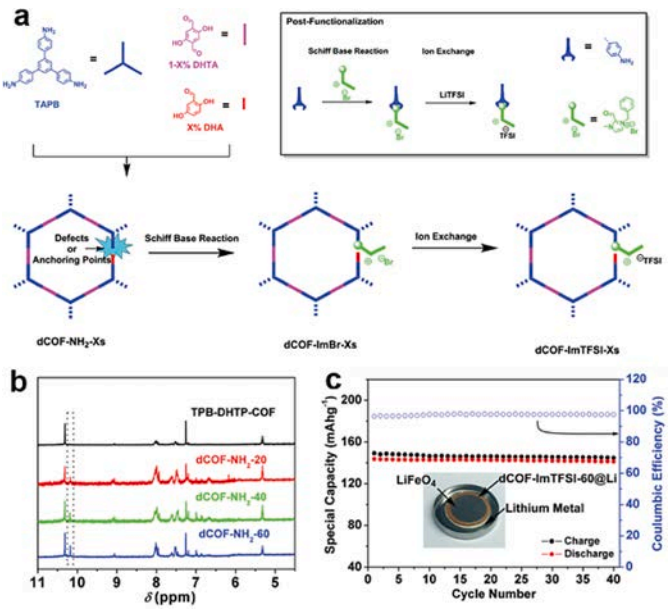

Fig. 20. (a) Synthesis of dCOF-NH_2-Xs by three-component condensation of 1, 3, 5-tri-(4-aminophenyl) benzene, 2, 5-dihydroxyterephthalaldehyde, and 2, 5-dihydroxybenzaldehyde, synthesis of dCOF-ImBr via a Schiff base reaction, and synthesis of dCOF-ImTFSI via an ion-exchange method; (b) ^{1}H NMR spectra of digested dCOF-NH_2-Xs powder, revealing its level of defects; (c) Cycling performance of Li|ImCOF-TFSI@Li|LiFePO4 at 0.1 C and 80 °C. Reproduced with permission.[143] Copyright 2020, Wiley-VCH.

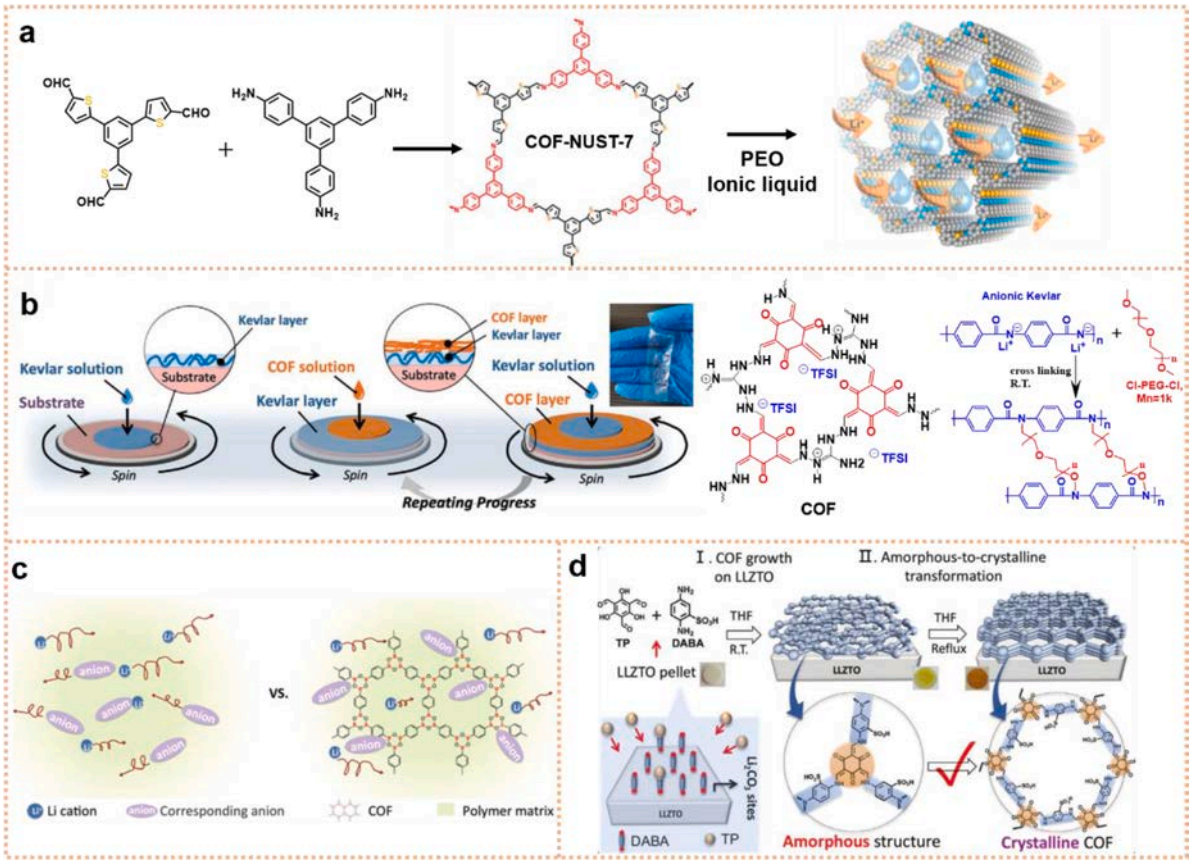

Fig. 21. (a) COF-NUST-7 based solid-state electrolytes with ion liquid and polymer PEO. Reproduced with permission.[144] Copyright 2021, American Chemical Society. (b) Schematics of layer-by-layer assembly technology and a free-standing, 500-bilayer L@K/C membrane, structural model of an exfoliated cationic COF and its homogeneous dispersion in an organic solvent and synthesis of crosslinked Kevlar and the ideal structure of its crosslinking networks. Reproduced with permission.[146] Copyright 2020, American Chemical Society. (c) Schematic diagram of SSE representing with anion adsorption capacity of boron-containing COFs or without COF. Reproduced with permission.[145] Copyright 2019, Royal Society of Chemistry. (d) Two-steps to build crystalline COF layer on LLZTO surface through the amorphous-to-crystalline conversion process. Reproduced with permission.[147] Copyright 2020, Wiley-VCH.

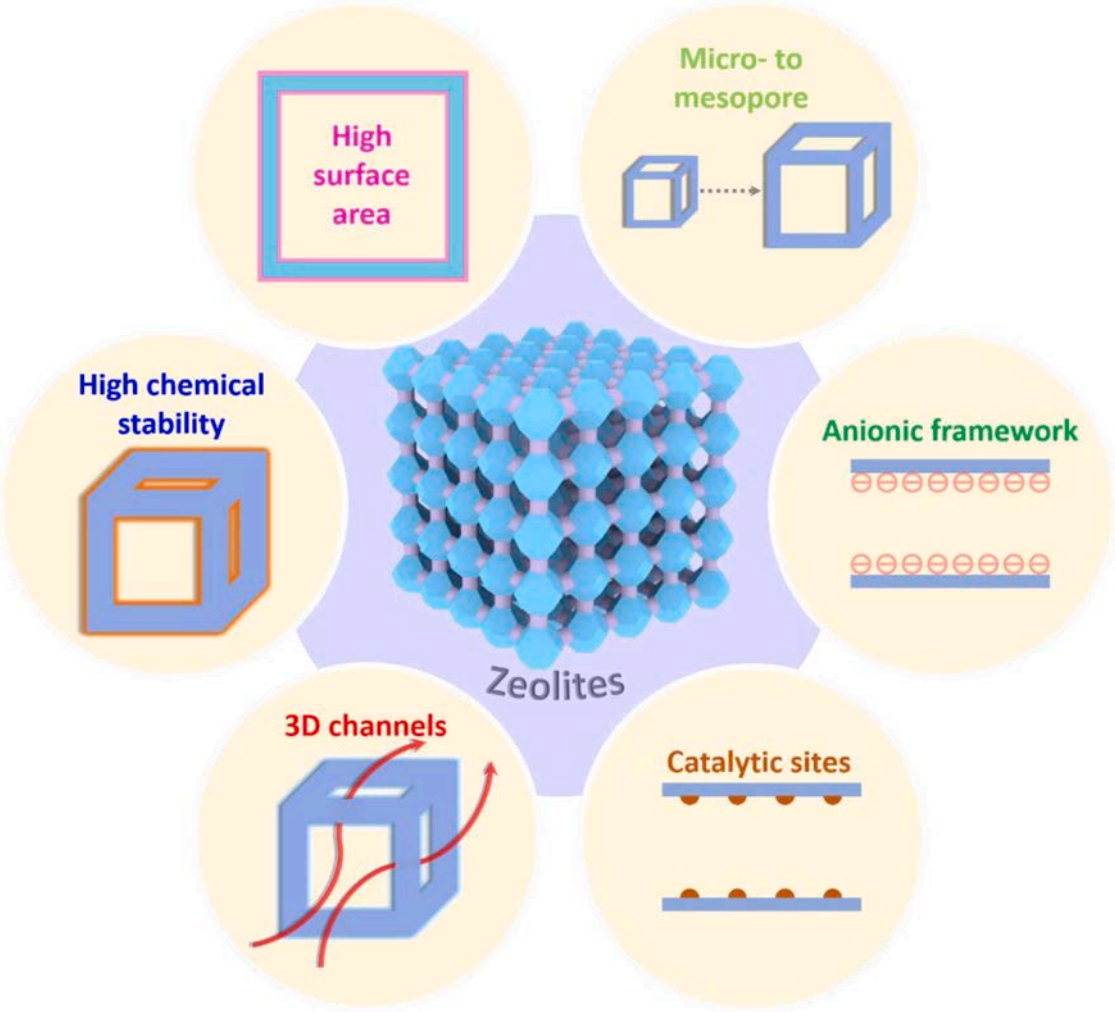

Fig. 22. Schematic illustration for the merits of zeolites as filler into SSEs.

was achieved and the Li||LFP cells also demonstrated a high initial capacity of 138 mAh g^{-1} and capacity retention of 110 mAh g^{-1} after 60 cycles at 0.1 C and 60°C.

3. COF-based SSEs

As a novel class of porous crystalline solids, COFs are characterized by their rigid stable organic frameworks and 1D periodic open channels, which make them attractive after certain modification and thus may support ionic conduction. Comparing to inorganic ion conductors such as metal oxides/sulfides, the permanent porosity, wide structural tunability, and good electrochemical stability of the COFs have bestowed the COF-based SSEs with various merits as following (Fig. 16): (i) The light weight of COFs could reduce the weight of the SSE and thereby improve the energy density of batteries. (ii) The easy functionalization of the COFs structure allows it to be modified for application in SSEs. (iii) The covalent linkages and functional groups in COFs endow the framework with high electrochemical stability. (iv) The layer-ordered porous structure of the COFs can provide fast ion transport channel and is helpful to form a homogenous Li^+ flux. (v) The designable ordered porosity could sieve anions to further improve Li^+ transference number.

The ionic conductivity of pure COFs are typically lower than inorganic SSEs, therefore in order to obtain sufficient ionic conductivity, the COFs are normally blended with other ion conductive materials covalently or non-covalently, such as ionic liquid, polymers, and ceramics. In this review, we outline the progress of COF-based SSEs in lithium metal batteries as the following categories: (1) COF ionic conductors; (2) COF/ionic liquid-based SSEs; (3) COF/polymer-based SSEs; (4) COF/ceramic-based SSEs.

3.1. COF ionic conductors

In this section, we describe the recent advances in COF ionic conductors, in which there are two main strategies: (1) COF incorporated with lithium salts and (2) ionic COF.

3.1.1. COF incorporated with lithium salts

In order to raise the ion conductivity of COF-based SSEs, some researchers have infiltrated solvents, Li salts, ionic liquid and polymer chains into the inner space of COFs, or compounded with polymers and inorganic ion conductors to boost ion conductivity.

Wang and Feng's team immersed $LiClO_4$ and PEG in an ethidium bromide derived cationic COF, as showing in Fig. 17**a**, improving the ion conductivities to 1.93 × 10^{-5} S cm^{-1} at 30°C and 1.78 × 10^{-3} S cm^{-1} at 120°C.[129] Zhang and coworkers reported a PC incorporated ICOF-2 (Fig. 17**b**) SSE with lithium-ion conductivity of 3.05 × 10^{-5} S cm^{-1} and an average Li^+ transference number of 0.80.[130] A major concern of the above research works is that the contribution to the improved ionic conduction in such COF-based solid electrolytes with added organic solvents may mainly come from the solvent rather than the COF solid medium itself. To align the intergrain channels structure,

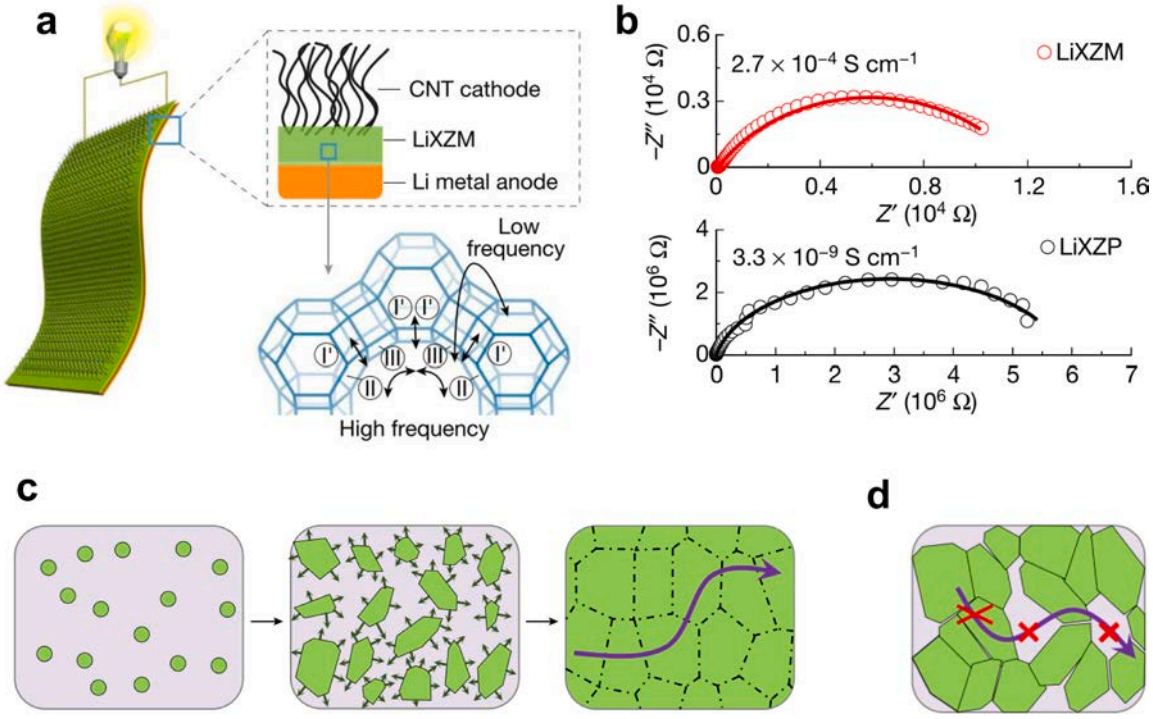

Fig. 23. Schematic and characterization of the zeolite solid electrolyte. (a) Schematic illustration of the integrated solid-state Li-air battery with C-LiXZM and the mechanism of Li ions transfer in LiX. (b) EIS spectra of LiXZM and LiXZP. (c) In situ zeolite membrane growth method adopted in this work. (d) The traditional preparation method for inorganic solid electrolytes. Reproduced with permission.[151] Copyright 2021, Spring Nature.

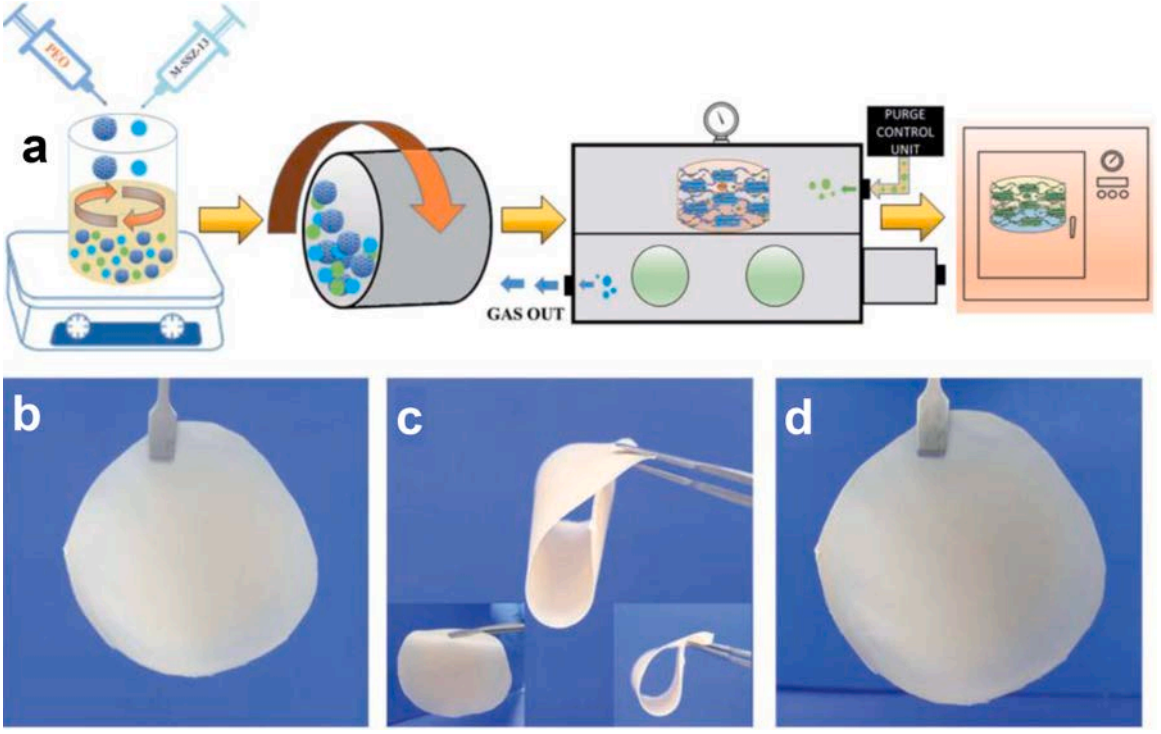

Fig. 24. Systematic representation of the synthesis of CPEs and photo images to demonstrate the flexibility and bendability of 5% MZ-CPE, (a) schematic representation of CPEs, (b) before bending, (c) bending at different angles, and (d) after bending. Reproduced with permission.[152] Copyright 2021, Royal Society of Chemistry.

Uribe-Romo and coworkers reported a mechanical stress 2D COFs (COF-5, Fig. 17**c**) for lithium ion conduction, with $LiClO_4$ infiltrated into the channels they achieved a solvent-free ion conductivity of 2.6×10^{-4} S cm^{-1} at room temperature.[131]

Additionally, incorporated polymer chains into COFs are another method to improving the ion conductivities of COFs-based SSEs. Jiang's

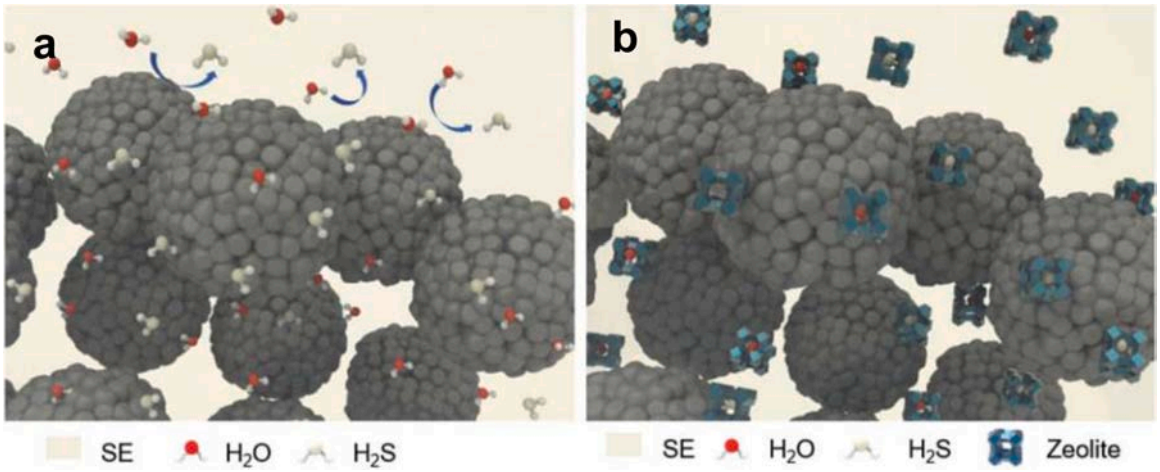

Fig. 25. Schematic illustration of composite electrode prepared with the Z-Li_6PS_5Cl solid electrolyte. (a) H_2S was generated on the surface of solid electrolytes. (b) H_2S was captured by the embedded zeolite. Reproduced with permission.[153] Copyright 2021, Royal Society of Chemistry.

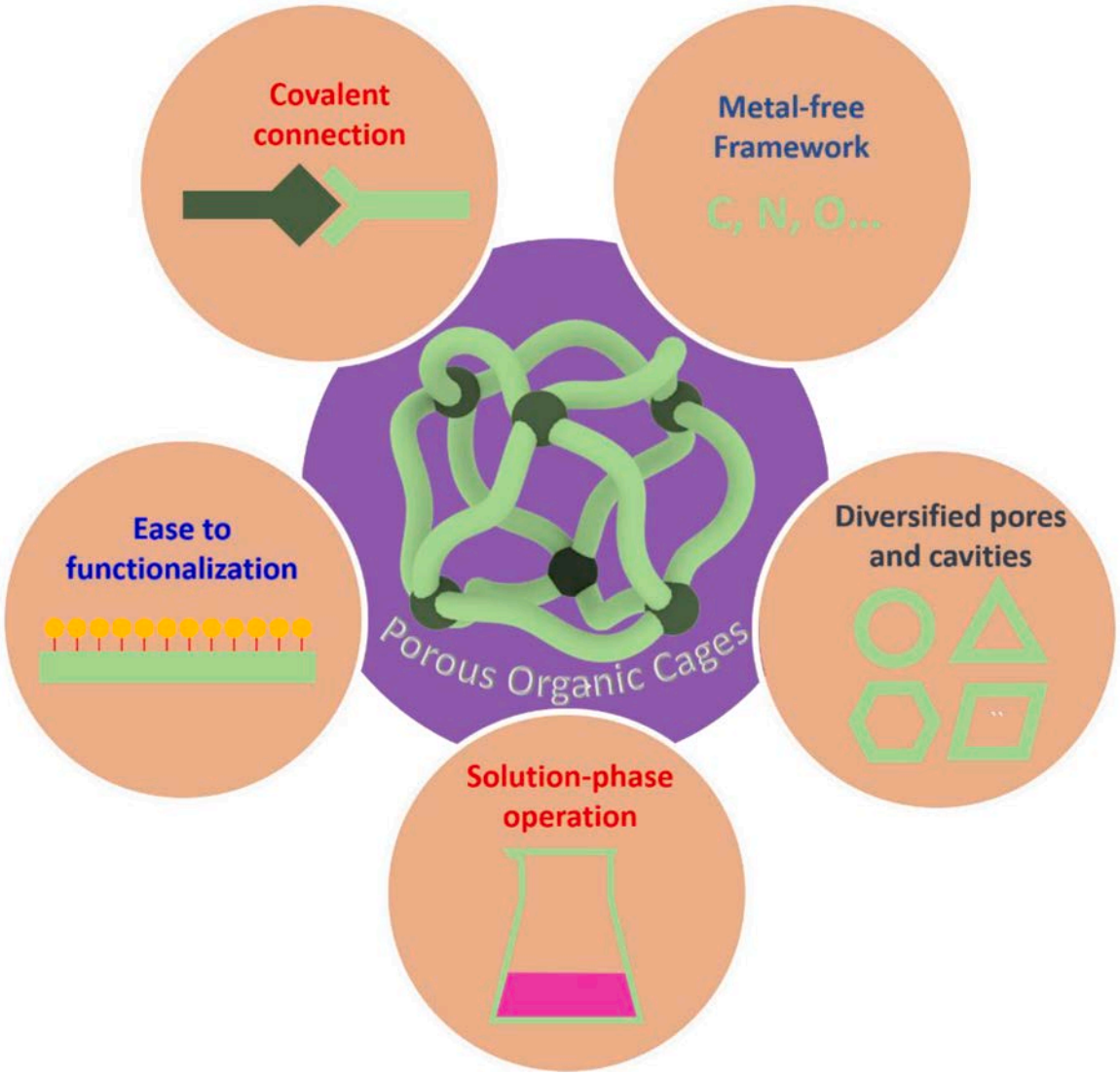

Fig. 26. Schematic illustration for the merits of POCs as filler into SSEs.

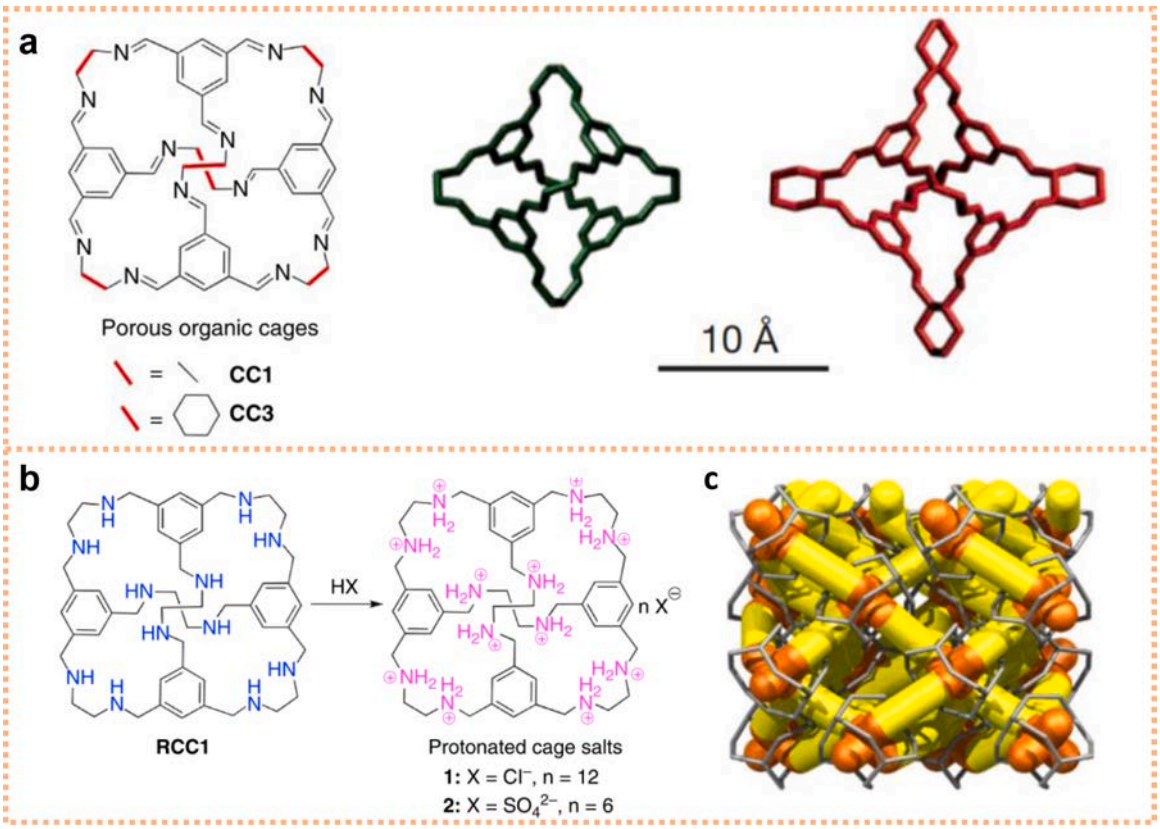

Fig. 27. Pristine organic cage and protonated cage salts. (a) Chemical and crystal structures of neutral POCs. Reproduced with permission.[154] Copyright 2009, Spring Nature. (b) Formation of cage salt materials from reduced POCs and (c) The 3D channels across the intrinsic cage cavities and the extrinsic voids between cages. Reproduced with permission.[155] Copyright 2016, Spring Nature.

group reported a polyelectrolyte COFs by integrating flexible oligo (ethylene oxide) chains onto the pore walls for lithium ion transport.[132] As showing in Fig. 17**d**, after functionalized with oligo(ethylene oxide), an ion conductivity of 6.04×10^{-6}, 2.85×10^{-5}, and 1.66×10^{-4} S cm^{-1} could be achieved at 40, 60, and 80°C, respectively. In addition, the COF skeleton itself was found to be an electrical insulator, confirming that oligomer (ethylene oxide) chain functionalization can promote lithium-ion transport.

Based on the effect of PEO chain on lithium-ion transport, Horike reported a PEO-functionalized hydrazone-linked COFs as SSEs.[133] A bottom-up self-assembly approach was applied to synthesis the rigid two-dimensional COFs with different PEO length (Fig. 17**e**). Due to the presence of PEO chain in COFs, the functionalized COFs have a high glass transition temperature of ~30°C, leading to a low ion conductivity of 6.25×10^{-10} S cm^{-1} at 30°C. By infiltrating LiTFSI into the COF pores, the SSEs achieved Li^+ conductivity 1.33×10^{-3} S cm^{-1} at 200°C. With $LiFePO_4$ cathode and COF-base SSE, the Li metal battery could present capacity greater than 120 mAh g^{-1} run for 10 cycles under a current density of 3.0 mA g^{-1} at 100°C, and the discharge efficiency was maintained above 95%.

Recently, Zhang's group stick with similar strategy introduce side chain engineering to construct gel-state COF with high processability, which overcome the processing difficulties of traditional COF powder materials (Fig. 17**f**).[134] Benefit from gelation strategy, this novel COF gel can be easily processed into gel-type electrolytes with specific mechanical property, which were further applied to assemble Li|$LiFePO_4$ batteries that exhibited high cycling stability and rate performance. The side chain gelation strategy further guides us in developing the precise molecular design and self-assemble in SSEs, suggestive of enormous potential applicability in crystalline engineering.

Xu's group reported a crystallographically oriented Q-COF-based SSE (Fig. 18), which have a remarkable ionic conductivity of 1.5×10^{-4} S cm^{-1} at 60 °C, excellent mechanical strength with a high Young's modulus of 10.5 GPa and higher decomposition voltage up to 5.6 V (versus Li^+/Li) as SSEs.[135] The COF-based SSE film was used to assemble with nickel-rich cathodes (NMC811). The all-solid-state lithium metal batteries presented a stable cycling performance over 400 cycles with high coulombic efficiency (> 99%).

3.1.2. *Ionic COF*

Ion conductors based on immobilizing anions on COFs were also proposed, due that the anions have been incorporated in COF structures can significantly improve the Li^+ transference number. For example, Feng's group synthesized a 3D anionic COF (denoted as CD-COF-Li, with Li^+ as the counter ion) with a highly crystalline structure and a Brunauer-Emmett-Teller (BET) surface area of 760 m^2 g^{-1}.[136] As showing in Fig. 19**a**, the COF was impregnated with 1.0 M $LiPF_6$ in EC and dimethyl carbonate (DMC). The SSE was fabricated by pressed into pellets, giving rise to an ion conductivity of 2.7×10^{-3} S cm^{-1} at 30°C and present excellent long-term Li ion stripping/plating stability. Zhang and coworkers reported a series of COFs with 20wt% PC incorporated single-ion conductors improved ion conductivities up to 7.2×10^{-3} S cm^{-1} and Li^+ transference number 0.81-0.93 at room temperature (Fig. 19**b**).[137] Uribe-Romo and coworkers reported a mechanical stress 2D COFs, with $LiClO_4$ incorporated TpPa-1 (Fig. 19**c**) obtained an ion conductor with an Li^+ ion conductivity of 1.5×10^{-4} S cm^{-1} at 25°C.[138]

Interestingly, introducing Lewis acidic frameworks has also been suggested to enhance the Li-ion transference number of porous crystalline ion conductors. For example, Banerjee and coworker's synthesized

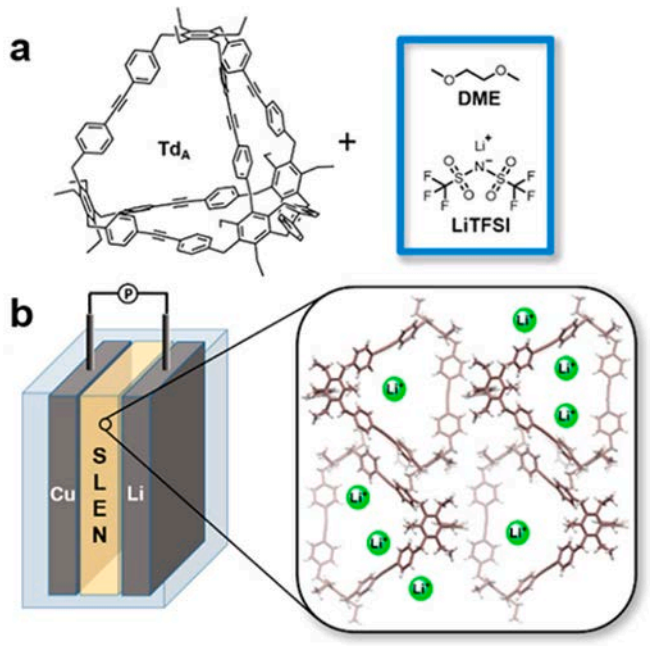

Fig. 28. Representation of POCs based solid-liquid lithium electrolyte nanocomposites. (a) Chemical structures of individual components. (b) Illustration of solid-liquid electrolyte nanocomposite half-cell configuration. Reproduced with permission.[156] Copyright 2018, American Chemical Society.

three self-exfoliated guanidinium halide based 2D ionic covalent-organic nanosheets (iCONs, **Fig. 19d**) without external stimuli.[139] On the basis of research, Chen and co-workers reported a cationic COF comprising alternatively linked triaminoguanidinium and 1, 3, 5-triformylphloroglucinol ligands which was proposed to feature π-π stacking, forming channels from the aligned pores (**Fig. 19e**).[140] It is observed that the concentration of free Li^+ ions in the resulting material is drastically increased, leading to a significantly improved Li^+ conductivity without any solvent up to 5.74×10^{-5} S cm^{-1} at 30°C and 2.09×10^{-4} S cm^{-1} at 70°C. The Li^+ transference number of 0.61 was consistent with at least a portion of the $TFSI^-$ ions being immobilized through interaction with the cationic triaminoguanidinium groups. Additionally, a respectable operating potential window of 3.8 V was measured. Loh and coworkers reported a scalable and solution-processable COF-based SSE (LiCON-3, **Fig. 19f**).[141] It achieves an ion conductivity of 10^{-5} S cm^{-1} at -40°C with a Li^+ transference number of 0.92. Furthermore, LiCON-3 as solid electrolyte and 1, 4-benzoquinone as cathode can effectively prevents the dissolution of small organic molecule and circulate stably for 500 times at a stable current density of 500 mA g^{-1} at 20°C. The advantages of exfoliated 2D COF sheets are not only the accessibility to additional free volume for ion migration, but most importantly, they also enhance the processability of the materials, which is needed for transforming SSEs into desirable sizes and dimensions. In addition, exfoliation may also improve the homogeneity of the SSEs and mitigate the poor contact between electrodes and SSE separators.

Lee's group reported a lithium sulfonated covalent-organic framework (denoted as TpPa-SO_3Li, **Fig. 19g**) as a new class of solvent-free, single lithium-ion conductors.[142] Benefiting from well-designed

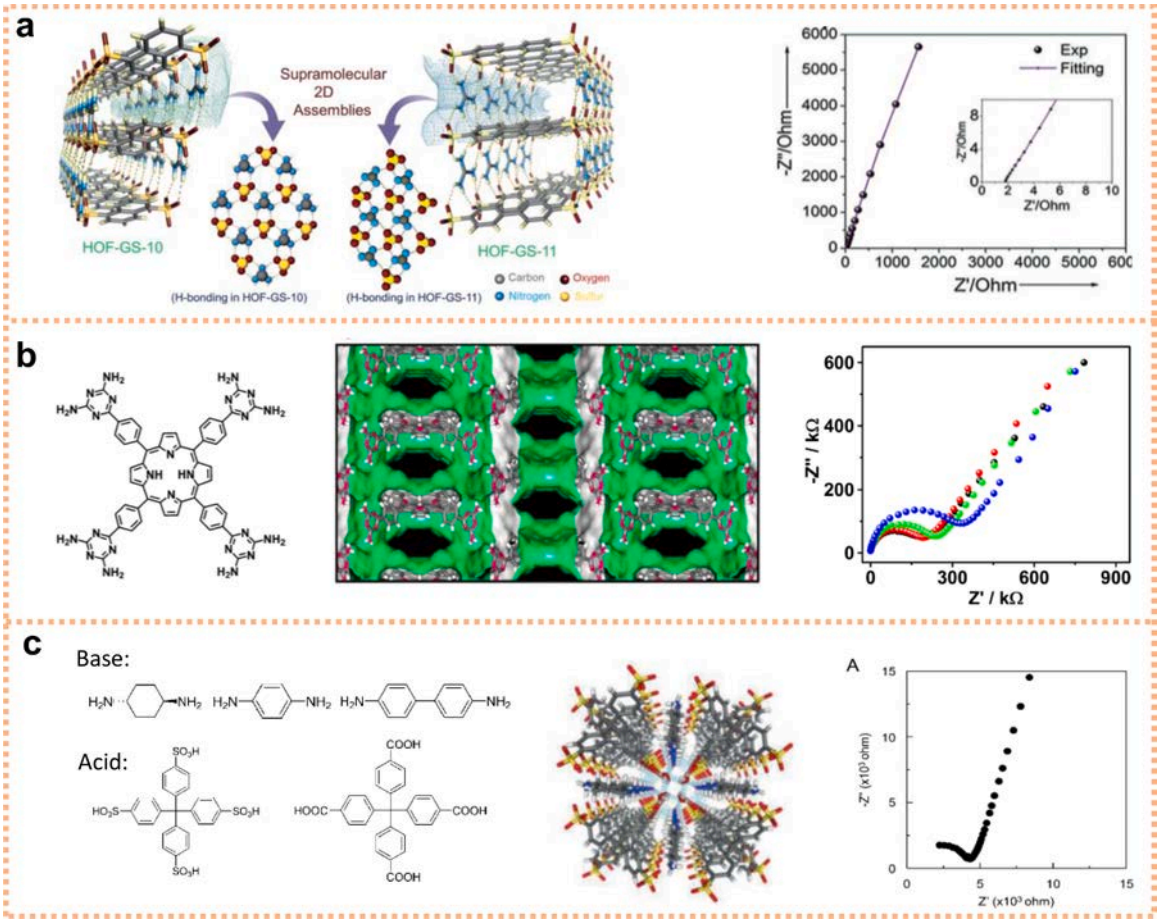

Fig. 29. HOFs structures based on variable organic components and their proton conductivity performance. (a) Arene sulfonates and guanidinium ions based HOFs. Reproduced with permission.[157] Copyright 2016, Wiley-VCH. (b) Porphyrin-based HOFs. Reproduced with permission.[158] Copyright 2016, American Chemical Society. (c) Acid-base combination based HOFs. Reproduced with permission.[159] Copyright 2018, Wiley-VCH.

directional ion channels, a high number density of lithium-ions, and covalently tethered anion groups, TpPa-SO_3Li exhibits an ionic conductivity of 2.7×10^{-5} S cm^{-1} with a lithium-ion transference number of 0.9 at room temperature without additionally incorporating lithium salts and organic solvents.

Ha and coworkers synthesized a series COFs with different defect degrees by introducing imidazolium functional groups onto the pore walls of COFs, and after ion-exchange strategy to obtain the final products (**Fig. 20**).[143] The dCOF-ImTFSI-60@Li based SSE exhibits a high ion conductivity up to 7.05×10^{-3} S cm^{-1} at 150 °C. Furthermore, Li||LFP cells display stable cycling performance as well as high coulombic efficiency under 80 °C in the voltage 2.5-4.0 V at the current density of 0.1 C.

3.3. COF/ionic liquid-based SSEs

The strategies presented above suggested that it is challenging to modulate structure to improve the COFs-based ionic conductivity. Therefore, introducing fillers is also proposed to increase the ionic conductivity. Zhang and coworkers developed doping ionic liquids and lithium salt into 1D nano-channels of COFs as SSE for high-temperature Li^+ conductivity (**Fig. 21a**).[144] The obtained COF-IL composite electrolytes exhibited excellent thermal stability up to 400°C and high Li^+ conductivity up to 2.60×10^{-3} S cm^{-1} at 120°C. In addition, the COF-IL composite electrolytes exhibited stable cycling in a solid-state Li||LFP cells with a high initial discharge specific capacity of 140.8 mAh g^{-1} at 100°C, which is more stable than PEO-based electrolytes.

3.4. COF/polymer-based SSEs

Furthermore, polymer was also introduced to compound with COFs to increase the ionic conductivity of the SSEs. Chen and coworkers reported boron-containing COF enable strong adsorption of the anions of the lithium salt, leading to a significantly enhanced Li^+ transference number of PVDF-based electrolyte (**Fig. 21c**).[145] The PDVF/H-COF-1 composited SSE exhibited 2.5×10^{-4} S cm^{-1} conductivity with 20 wt% COF additives, and remarkably decreased over potentials and enhanced rate performances. Furthermore, adjusting the structure of the polymer/COF-based composite SSEs can also maximize the properties of COF-based SSEs. For example, Chen's group reported a 7.1 μm thick heterolayered Kevlar/COF composite membrane (**Fig. 21b**) fabricated via a bottom-up spin layer-by-layer assembly technology that resulting in a highly strong and Li^+ conductive 1.62×10^{-4} S cm^{-1} at 30°C and 4.6×10^{-4} S cm^{-1} at 70°C.[146]

3.5. COF/ceramic-based SSEs

The ordered porosity of COF is conducive to balancing Li^+ bundles and can be used for electrolyte functionalization. Chen and coworkers reported a COF-based soft interfacial layer has been constructed on a garnet-type LLZTO ceramic pellet via a simple solution method (**Fig. 21d**).[147] The COF-based layer not only significantly improves the lithiophilicity of LLZTO, but also creates effective Li^+ conducting "highways" between LLZTO and Li metal anode. The solid-state full cells consisted of $LiFePO_4$ cathode, COF-modified LLZTO, and Li metal anode show excellent rate performance and cycling stability even at 2 C rate. Considering the great potential of COF materials with modular structural design, the optimized COF-based intermediate layer deserves further investigation.

Through the above discussion for recent report of COF-based SSEs, it is clear that high ionic conductivity can be achieved through simple ionization of the COFs, which greatly simplified the fabrication process compared to MOFs. Together with its lightweight and high electrochemical stability, the COF-based SSEs offer great potential to fabricate high-performance SSEs for high energy batteries.

4. Zeolites-based SSEs

Benefitted from the intrinsic one-, two-, or three-dimensional channels across the structures and cation exchange ability, zeolites meet the prerequisites to be good candidates for ion conductors and hold great potentials in the field of solid-state batteries. Thus, the conductivities of zeolites are derived from the migration of cations across the crystalline frameworks. (**Fig. 22**)

The designability and accessible structure diversity of the MOFs/COFs make them more versatile choices and functionalities than the limited structure types of zeolites. However, compared with MOF/COF-based SSEs, zeolites possess better physical and chemical stability for practical use and regeneration. More importantly, the natural ionic framework of zeolites could facilitate the ion transport, which would potentially solve the biggest challenge for SSEs (i.e., low ionic conductivity). Nevertheless, the main issues faced by zeolite-based SSEs are to synthesis high quality of crystalline phase and to solve the compatibility between the interfaces.

In the early stage, the research is mainly focused on the fundamental ionic conductivities. Kelemen et. al. measured and summarized this parameter for a series of dehydrated zeolites with variable ion content and obtained a Na-zeolite A with the best ionic conductivity value of 2.9×10^{-3} S cm^{-1} at 600 °C.[148] Munichandraiah et. al. investigated the influence of zeolite on electrochemical properties of polyethylene oxide solid electrolyte.[149] They found that with the presence of zeolite the ionic conductivity was increased from 10^{-9} S cm^{-1} to about 10^{-7} S cm^{-1} under 29 wt% zeolite contents. Meanwhile, some researchers employed spectroscopy techniques (*e.g.*, solid-state NMR) to in situ monitor the mobility of lithium ion in zeolites.[150]

Until recently, the Yu group has made great progress in this field and push forward the zeolite-based solid-state electrolyte for Li-air battery tremendously (**Fig. 23**).[151] They adopted a high-ion-conductive lithium-ion-exchanged zeolite X (LiX) membrane as the only solid electrolyte. The battery showed high safety and stability (149 cycles), high conductivity (2.7×10^{-4} S cm^{-1}), and excellent interfacial compatibility. Owing to these integrated merits and advantages, this system holds great promise for practical application in energy storage. Subsequently, Kim and co-workers functionalized a polymer electrolyte surface with SSZ-13 zeolite for all-solid-state Li-metal batteries.[152] The ionic conductivity of the composite was substantially enhanced (5.3×10^{-2} S cm^{-1}) due to the upgraded and hydrophobic surface of SSZ-13 zeolite (**Fig. 24**). Cho et. al. reported that the ZSM-5 zeolite can act as H_2S scavengers in argyrodite Li_6PS_5Cl solid electrolytes for all-solid-state batteries to improve chemical stability and suppress H_2S release in humid conditions (**Fig. 25**).[153]

5. Others

Porous organic cages (POCs) and hydrogen-organic frameworks (HOFs) are the other two common family members of CPMs. Even though the study of POCs and HOFs are mainly focus on proton conduction, nevertheless, they also possess some unique characteristics intrinsically and could potentially be used in SSEs after necessary functionalization. Therefore, the recent study of POCs and HOFs related to proton conduction were also included in this review.

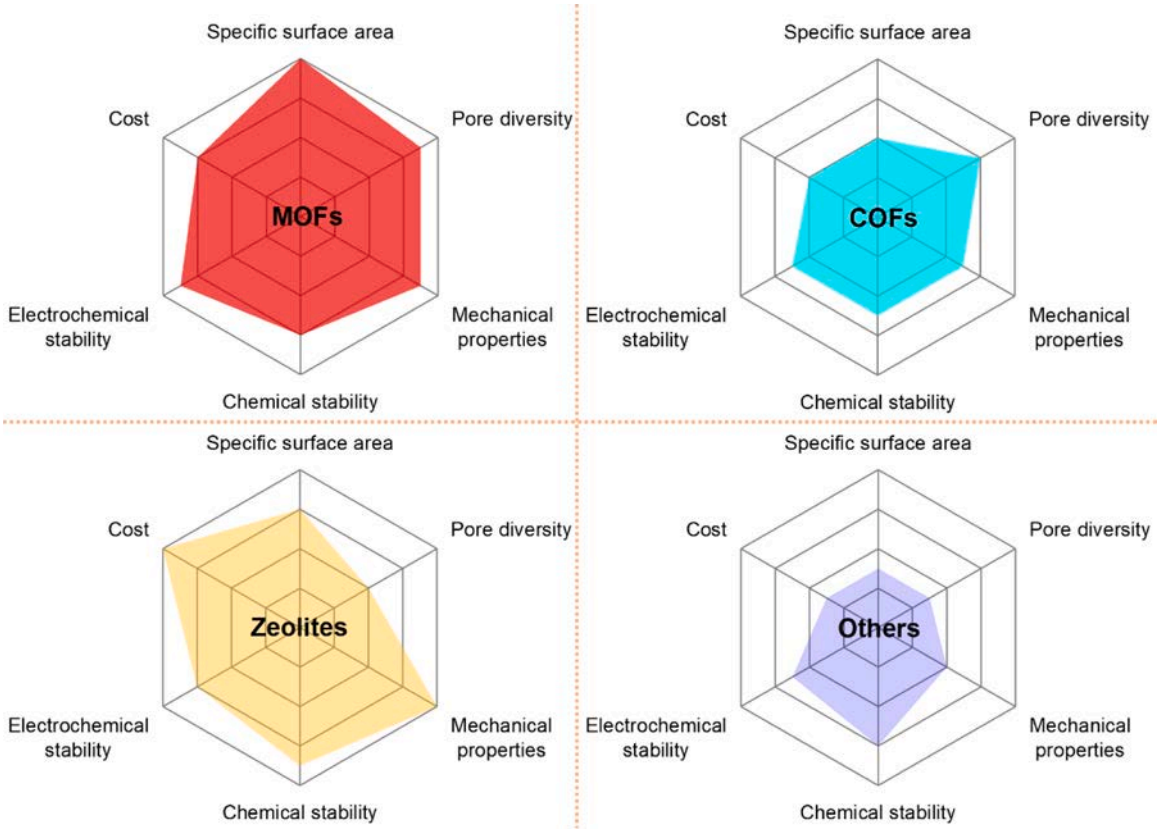

Fig. 30. Radar plots of the comprehensive performance comparisions of CMPs-based SSEs.

5.1. POCs-based SSEs

Porous organic cages (POCs) that are solely formed through covalent bonds are a new class of crystalline materials and retain their porosity via molecular packing(Fig. 26).

A representative example was developed by Cooper et. al. through dynamic imine bond between tris-aldehyde and bis-amine (Fig. 27**a**). [154] Considering the low proton conductivity performance for pristine POCs (6.4×10^{-6} S cm^{-1}), these structures were sequentially reduced to secondary amine and formed hydrated salts with inorganic acids by the same group.[155] Unexpectedly, these derived POCs demonstrated excellent proton conductivities on the order of 10^{-3} S cm^{-1} even at high relative humidity. The molecular level analysis disclosed a necessarily three-dimensional conduction pathway mechanism for proton transfer (Fig. 27**b**). This preliminary result extends the potential application of POCs in solid state electrolyte.

Furthermore, Andrew Gewirth and co-workers adopted a new type of POCs that generated through enyne metathesis reactions to act as solid electrolyte in LIBs (Fig. 28).[156] Together with LiTFSI and DME (1, 2-dimethoxyethane) as co-existing components, this new fabricated nanocomposite exhibited lithium ionic conductivity also on the order of 10^{-3} S cm^{-1} with excellent oxidative stability up to 4.7 V vs Li/Li$^+$. Detailed investigation indicated that the confined space of POCs may provide highly coordinated environment for LiTFSI and DME, thus contributing to its excellent ionic conductivity and stability. Although it's not a solid-state electrolyte system in the strict sense, however, this study shows great potential of POCs materials as solid-state electrolyte candidates in near future. In practical, the POCs structures can be decorated with functional organic group to form ionic frameworks that facilitate Li$^+$ ion transport without using solvent as additive, where a real solid-state electrolyte shall be furnished based on the POCs materials.

5.2. HOFs-based SSEs

Hydrogen-organic frameworks (HOFs) are assembled from organic molecules based on certain hydrogen bonding interactions and possessing 1D to 3D channels. Due to the widely existing hydrogen bonding connections in the structure, it makes HOFs as ideal materials for conducting through diverse proton transfer pathways. Besides, the open channels of HOFs allow water as proton carriers to achieve conductivity and its excellent stability against humidity conditions also makes HOFs a promising material for proton conduction.

In 2016, Ghosh et. al. reported a kind of HOF based on arene sulfonates and guanidinium ions (Fig. 29**a**).[157] Owing to the ionic backbones, these structures exhibit ultrahigh proton conductivities with representative values of 0.75×10^{-2} S cm^{-1} and 1.8×10^{-2} S cm^{-1} under humidified conditions, which is the highest value to date in organic-based porous materials. Later, Chen et. al. presented a porphyrin-based porous HOF for proton conduction (Fig. 29**b**).[158] The 3D intersected channels with exposed porphyrins endows this structure with abundant proton donors/acceptors sites. These features makes this HOF a proton conductivity of 3.4×10^{-2} S cm^{-1} that can be applicable for proton conducting materials. Recently, Ben et. al. adopted acid-base combination strategy to successfully assemble a series of HOFs (Fig. 29**c**).[159] They found that the water content in the channels is the key factor to influence the proton conduction performance. Finally, a high proton conductivity of 2.2×10^{-2} S cm^{-1}was achieved at ambient and high humid conditions. Nevertheless, the HOFs as a new-rising materials are still in the preliminary stage for kinds of applications, including solid-state electrolyte study. The next facing challenge is to transplant the proton conductivity to Li$^+$ ion conductivity and solve the compatibility between the interfaces. In addition, careful attention need to be paid on the electrochemical stability of the HOFs for their practical application in batteries. In general, the research of HOFs for ionic

conductivities is still in its infancy, the solid- state electrolyte related applications are rarely explored. Given the great advantages of HOFs, this type of molecular frameworks should attract more attention and holds wide opportunity for battery materials.

6. Summary and Outlook

Searching for high performanceSSEs is essential for the development of next generation lithium metal batteries with high energy density and reliable safety. Compared to tranditional polymer and inorganic SSEs, CPMs with high surface area, well-defined structure, and versatile functionality have shown great potential to fabricate high-performance SSEs in recent years. In this review, the latest progress of CPMs-based SSEs for lithium metal batteries, including MOFs, COFs, zeolites, POCs and HOFs, has been systematically elucidated. The significant progress and strategies for achieving high-performance CPMs-based SSEs can be summarized into the following three main categories:

(1) Pristine CPMs SSEs. Grafting the CPMs with anions of the lithium salts would result in a single Li^+ conductor with an extremely high Li^+ transference number (> 0.8), which has been intensively investigated to suppress the polarization effect. In addition, there are some intrinsically cationic and anionic frameworks of CPMs have been explored to boost the ionic conductivity up to $\sim 10^{-3}$ S cm^{-1}. Furthermore, the strong mechanical strength of the pristine CPMs SSEs might be helpful to suppress the growth of lithium dendrites, while the flexibility and interfacial compatibility remain to be solved.
(2) CPMs/IL-based SSEs. The CPMs loaded with nonflammable and nonvolatile ILs would lead to an excellent interfacial wettability with the electrodes, and the ionic conductivity can reach up to $\sim 10^{-3}$ S cm^{-1} depends on the loading amount of IL and inner interactions, which offers great opportunities for designing high-performance SSEs.
(3) CPMs/polymer-based SSEs. Similar to the inorganic ceramic/polymer composites SSEs, introducing polymer to CPMs significantly enhances the flexibility of the SSEs and therefore improves the interfacial contact with the electrodes, which leads to a much improved battery cycling performance. The CPMs/polymer-based SSEs are normally prepared by either physical mixing the polymer with CPM particles or chemical grafting the polymers on CPMs, which exhibits a high ionic conductivity up to $\sim 10^{-3}$ S cm^{-1} and a moderate Li^+ transference number of 0.4~0.6.
(4) CPMs/multicomponent-based SSEs. In consideration of the complementary roles of ILs, polymers, and inorganic ceramic, the hetergenous interfaces among multicomponents as well as electrodes/SSEs interfaces could be effectively resolved, of which the ionic conductivity could be reached up to $\sim 10^{-3}$ S cm^{-1} at the room temperature and the electrochemical window could expand to above 6.0 V.

Finally, the comprehensive performance comparison for various CPMs-based SSEs is visualized in the radar plot in Fig. 30. Despite these many advantages offered by the compositional and structural versatility of CPMs as well as the recent progress has been made, the application of CPMs in high-performance SSEs for lithium metal batteries is still an emerging hotspot and encounters many challenges. Therefore, great efforts are still needed on the following aspects to overcome the obstacles and promote the development of the CPMs-based SSEs:

(1) The ionic conduction mechanism in the channels of CPMs need to be further clarified. There are lots of puzzles to be explored, such as the impacts of the crystalline size, morphology, and orientation of the CPM particles on the ionic conductivity and the actual ion transport pathways.
(2) The incorporation of CPMs with ILs and polymers to form composite SSEs has been proven to yield improved performance for lithium metal batteries. There are many more contacting interfaces, such as the interfaces between CPMs and ILs or polymers, making the actual ion transport pathways and conduction mechanism more complicated, which need to be inverstigated in depth with the aid of advanced characterization technologies and theoretical calculations.
(3) Relatively low ionic conductivity is still an obstacle for operating solid-state lithium metal batteries at room-temperature. Hence, novel CPMs with high ionic conductivity should be explored, such as the POCs and HOFs that have already exihibited high proton conductivity. With the understanding of the ion conduction mchanism on the multiple interfaces among CPMs, ILs, and polymers, the quickest and continuous Li^+ transport pathway should be constructed in the CPMs-based composite SSEs.
(4) The electrochemial and chemical stability of the CPMs upon battery cycling need to be studied, which will allow us to screen out the situable CPMs-based SSEs in the furture. For instance, the CPMs that have chemically inner ligands might be preferable.
(5) The cost in synthesizing CPMs can be a concern. Thus, the search of inexpensive ligands and low-cost, envrionmental friendly large-scale preparation techniques are urgent needed for their practical appliations.
(6) Developing more advanced characterization techniques and simulations. These methods would make great progress toward elucidating phenomena such as ion transport mechanisms and interfacial properties, which may offer new insights to understand the structure-property-performance relationships of the CPMs-based SSEs.

Author Contributions

Luyi Chen, Kui Ding, Kang Li and Qifeng Zheng wrote the manuscript, Zhongliang Li and Xueliang Zhang proofread the manuscript, Qifeng Zheng, Yue-Peng Cai and Ya-Qian Lan revised the manuscript.

Table 1, Table 2, Table 3, Table 4, Table 5, Table 6, Table 7

Table 1
Summary of some common MOFs in this review.

MOFs	Ligands	Porous parameter (nm)	Open metal sites (Y or N)
MOF-5	H_2bdc	0.78	N
MOF-525	H_4tcpp	1.84	N
HKUST-1	H_3btc	1.1	Y
ZIF-8 (MAF-4)	2-methylimidazole	0.74 (cage: 1.81)	N
UIO-66	H_2bdc	0.75, 1.2	Y
UIO-67	H_2bpdc	1.2, 2.3	Y
MIL-53(Al)	H_2bdc	0.7	Y
MIL-100-Al	H_3btc	2.5, 2.9	Y
MIL-100-Cr		(windows: 0.6,	
MIL-100-Fe		0.9)	
MIL-121	H_2btec	1.84	N
MIL-125	2-amino-terephthalic	0.6, 1.25	N
InOF	H_4THBA	0.68 × 0.74	N
$Cu_2(BPY)_2$(NDIDS)	NDIDS	-	N
MOF-688	TFPM	0.86	N
Cu-MOF-74	H_4dobdc	0.8	Y
MIT-20	H_2btdd	2.25	N
Al-Td-MOF-1	1,4-dihydroxybenzene	0.55	N
Li-AOIA	H_4AOIA	-	Y

Table 2
Summary of MOF ion conductors.

MOFs	Ligands	Lithium salts	Ionic conductivity	Activation energy	t_{Li+}	Electrochemical window	Ref.
Mg_2(dobdc)	H_4dobdc	$LiO^iPr+LiBF_4$	3.1×10^{-4} S cm^{-1} at 27°C	0.15 eV	-	-	[34]
Mg_2(dobpdc)	H_4dobpdc	$Mg(OPhCF_3)_2$+Mg $(TFSI)_2$	2.5×10^{-4} S cm^{-1} at 30°C	0.13 eV	-	-	[35]
UIO-66	H_2bdc	LiO*t*Bu	1.8×10^{-5} S cm^{-1} at 25°C	0.18 eV	-	-	[36]
MIL-121	H_4btec	$LiClO_4$	9.1×10^{-5} S cm^{-1} at 50°C	0.28 eV	-	-	[37]
EHU1(Sc, M)	H_2pmdc	$LiBF_4$	4.2×10^{-4} S cm^{-1} at 25°C	0.25 eV	-	-	[38]
MIL-100(Al)	H_3btc	LiCl	1.9×10^{-4} S cm^{-1} at 60°C	0.30 eV	-	-	[39]
InOF	H_4THBA	LiTFSI	1.49×10^{-3} S cm^{-1} at 25°C	0.19 eV at 25°C	0.78 at 25°C	-	[40]
CPM-s3	M_2dsoba, $M^+ = Na^+$, K^+, Cs^+	-	1.25×10^{-3} S cm^{-1} at 22°C	-	-	-	[41]
$Cu_2(BPY)_2$(NDIDS)	NDIDS	$LiClO_4$	2.3×10^{-4} S cm^{-1} at 60°C	0.167 eV	-	-	[42]
MOF-688	TFPM	LiTFSI	3.4×10^{-4} S cm^{-1} at 20°C	-	0.87 at 20°C	-	[43]
MIT-20	H_2btdd	$LiBF_4$	4.8×10^{-4} S cm^{-1}	0.16 eV	0.66	-	[44]
MOF-*MX*	H_4ttpm	LiCl	2.4×10^{-5} S cm^{-1}		0.69	-	[45]
UIO-66-LiSS	H_2bdc	-	6.0×10^{-5} S cm^{-1} at 25°C, 7.8×10^{-4} S cm^{-1} (EC/PC)	0.21 eV	0.88	5.2 V	[46]
Al-Td-MOF-1	1,4-dihydroxybenzene	-	5.7×10^{-5} S cm^{-1} at 25°C	-	-	-	[47]
Li-AOIA, Li-TMCA	H_4AOIA, H_4TMCA	$LiBF_4$	1.09×10^{-5} S cm^{-1} and 2.93×10^{-6} S cm^{-1} at 25°C	-	-	-	[48]

Table 3
Summary of MOF/IL-based SSEs.

ILs	MOFs	Ionic conductivity	Activation energy	t_{Li+}	Electrochemical window	Ref.
$[Na_{0.1}EMIM_{0.9}]$[TFSI]	ZIF-8	8.4×10^{-6} S cm^{-1} at 25°C	0.28 eV	-		[52]
[EMIM][$N(CN)_2$]	PCN-777	4.4×10^{-3} S cm^{-1} at 25°C	0.20 eV at 25°C	-	-	[57]
[EMIM][TFSI]	ZIF-8	-	-	-		[60]
Li-[EMIM][TFSI]	ZIF-8	2.09×10^{-6} S cm^{-1} at 25°C	0.21 eV	0.45	4.7 v	[63]
$[Li_{0.2}EMIM_{0.8}]$[TFSI]	MOF-525	3.4×10^{-4} S cm^{-1} at 30°C	-	0.36		
Li-[EMIM][TFSI]	UIO-66	3.2×10^{-4} S cm^{-1} at 25°C	-	0.33 at 25°C		[66]
[EMIM][TFSI]	UIOSLi	3.3×10^{-4} S cm^{-1} at 25°C	-	-		[67]
[Bmpyr][TFSI]	UIOSNa	3.6×10^{-4} S cm^{-1} at 25°C	-	-	5.5 V	[68]
[EMIM][TFSI]	UIO-66@67	6.5×10^{-3} S cm^{-1} at 25°C	-	0.63 at 25°C	5.2 V	[69]
[EMIM][TFSI]	HKUST-1	1.82×10^{-4} S cm^{-1} at 25°C	-	-	-	[70]
Grafting-[EMIM][TFSI]	ZIF-90-g-IL	1.17×10^{-4} S cm^{-1} at 30°C	-	0.44 at 60°C	-	[74]

Table 4
Summary of MOF/polymer-based SSEs

Polymers	MOFs	Ionic conductivity	t_{Li+}	Electrochemical window	Ref.
PEO	MOF-5	3.16×10^{-5} S cm^{-1} at 25°C	-	4.57 V at 60°C	[80]
	ZIF-8	2.2×10^{-5} S cm^{-1} at 30°C	0.36 at 60°C	> 5 V at 60°C	[81]
	UIO-66-NH_2	3.1×10^{-5} S cm^{-1} at 25°C	0.72	4.97 V	[82]
	UIO-66-NH_2	3.56×10^{-4} S cm^{-1} at 60°C	-	> 4.5 V at 60°C	[83]
	UIO-66-NH_2@SiO_2	$\approx 1.0 \times 10^{-4}$ S cm^{-1} at 60°C	0.68 at 60°C	-	[84]
	HKUST-1	3.5×10^{-4} S cm^{-1} at 50°C	0.38 at 50°C	4.71 V at 50°C	[86]
	Al-MOF	2.09×10^{-5} S cm^{-1} at 30°C	0.46 at 30°C	4.7 V at 30°C	[87]
	Al-TPA-MOF	1.0×10^{-4} S cm^{-1} at 60°C	-	-	[88]
	Ni_3-$(BTC)_2$	1.4×10^{-4} S cm^{-1} at 30°C,	0.4 at 70°C	-	[90]
	NMS	1.66×10^{-5} S cm^{-1} at 25°C	0.378 at 25°C	4.9 V at 25°C	[91]
	Mg-TMA	7.02×10^{-4} S cm^{-1} at 25°C	0.58 at 50°C	-	[92]
	Ce-MOF	3.0×10^{-5} S cm^{-1} at 30°C	0.75 at 60°C	4.5 V at 60°C	[93]
PVDF	MOF-688	3.4×10^{-4} S cm^{-1} at 20°C	0.87 at 25°C	-	[43]
	Cu(BDC)	2.4×10^{-4} S cm^{-1} at 30°C	0.61 at 30°C	~5 V at 30°C	[99]
	Mg-MOF-74	3.43×10^{-4} S cm^{-1} at 25°C	0.66		[100]
	LiUIO-66	2.07×10^{-4} S cm^{-1} at 25°C	0.84	4.52 V	[101]
PTFE			up to 0.65	-	[103]

(*continued on next page*)

Table 4 (*continued*)

Polymers	MOFs	Ionic conductivity	t_{Li+}	Electrochemical window	Ref.
	HKUST-1,	0.38×10^{-3} S cm^{-1},			
	UIO-66,	0.18×10^{-3} S cm^{-1},			
	UIO-67,	0.65×10^{-3} S cm^{-1},			
	MIL-100-Al,	1.22×10^{-3} S cm^{-1},			
	MIL-100-Cr,	0.23×10^{-3} S cm^{-1},			
	MIL-100-Fe,	0.9×10^{-3} S cm^{-1},			
	MOF-5	0.13×10^{-3} S cm^{-1} at 25°C.			
	Cu-MOF-74	$\sim 10^{-3}$ S cm^{-1}	0.82	4.9 V	[104]
	ZIF-8	1.05×10^{-4} S cm^{-1} at 25°C	0.52 at 25°C	4.7 V at 25°C	[105]
	hollow ZIF-67@ZIF-8	1.35×10^{-3} S cm^{-1} at 25°C	0.82 at 25°C	5.31 V at 25°C	[106]
	glassy ZIF-4	1.61×10^{-4} S cm^{-1} at 30°C	0.885 at 30°C	4.0 V at 30°C	[107]
PVA	UIO-66	3.16×10^{-5} S cm^{-1} at 30°C	0.79 at 30°C	4.9 V at 30°C	[109]
PSS	HKUST-1	5.53×10^{-4} S cm^{-1} at 25°C	-	-	[110]
PEGDA	UIO-66-NH_2	4.31×10^{-5} S cm^{-1} at 30°C	-	5.5 V at 28°C	[94]
	ZIF-8	9.96×10^{-5} S cm^{-1} at 30°C	0.16	>4 V	[96]
	UIO-66-NH-MET	2.26×10^{-4} S cm^{-1} at 25°C	0.44	>5.4 V	[97]
PVDF-HFP	UIO-66	$>1 \times 10^{-3}$ S cm^{-1} at 20°C	0.66 at 25°C	4.4 V	[112]
	Zr-MA-Li^+	6.62×10^{-4} S cm^{-1} at 25°C	0.63	4.6 V	[113]
	MIL-101(Cr)-DETA-Li	7.13×10^{-4} S cm^{-1} at 30°C	0.87	4.7 V	[114]
	Zr-BPDC-2SO_3H	7.88×10^{-4} S cm^{-1} at 25°C	0.88	5.1 V	[115]
P(TFEMA-*ran*-PEGMA)	MOF-5	1.44×10^{-5} S cm^{-1} at 30°C	0.51	5.38 V	[116]

Table 5
Summary of MOF/multicomponent-based SSEs

Multicomponent	MOFs	Ionic conductivity	t_{Li+}	Electrochemical window	Ref.
LiTFSI in [EMIM][TFSI]/PEO	UIO-66	1.3×10^{-4} S cm^{-1} at 30°C	0.35	4.5 V at 25°C	[117]
[EMIM][TFSI]/ PVDF-HFP	UIO-66-2COOH	1.06×10^{-3} S cm^{-1} at 25°C	-	-	[119]
Li-[EMIM][TFSI]/PEO	hollow-ZIF	1.41×10^{-4} S cm^{-1} at 25°C	0.41	5.0 V at 60°C	[120]
[$EMIM_{0.83}Li_{0.17}$][TFSI]/cross-linked PEO	ZIF-8	4.26×10^{-4} S cm^{-1} at 30°C	0.67	-	[121]
[$EMIM_{0.8}Li_{0.2}$][TFSI]/PEO	HKUST-1	1.2×10^{-4} S cm^{-1} at 30°C	-	-	[122]
[BMIM][BF_4]/PVDF-HFP	CuBTC	8.7×10^{-3} S cm^{-1} at 380 K	-	6.1 V	[123]
PI/PEGDA-BMA	ZIF-8	4.7×10^{-4} S cm^{-1}	0.68	-	[124]
PAN/PEO	UIO-66	2.89×10^{-4} S cm^{-1} at 60°C	0.52	4.7 V	[125]
LLZO/[EMIM][TFSI]	UIO-67	1.0×10^{-4} S cm^{-1}	-	5.2 V	[126]
LLZN/PVDF-HFP/PEO	HKUST-1	2.00×10^{-4} S cm^{-1}	0.62	4.92 V	[127]
LAGP/PEO	ZIF-67	2.4×10^{-4} S cm^{-1} at 30°C	-	-	[128]

Table 6
Summary of COFs-based SSEs.

COFs	Lithium salts/Solvents	Ionic conductivity	Activation energy	t_{Li+}	Electrochemical window	Ref.
CD-COFs-Li	$LiPF_6$/EC-DMC	2.7×10^{-3} S cm^{-1} at 30 °C	-			[136]
PEG-Li^+@CD-COF-Li	$LiClO_4$/PEG	2.6×10^{-5} S cm^{-1} at 30 °C	-	0.2		[129]
PEG-Li^+@COF-5	$LiClO_4$/PEG	3.49×10^{-5} S cm^{-1} at 120 °C	-			
ICOF-2	PC/	3.05×10^{-5} S cm^{-1} at 25 °C	0.80 eV	-		[130]
Li-CON-TFSI	LiTFSI/-	2.09×10^{-4} S cm^{-1} at 70 °C	0.34 eV	0.61	3.8 V	[140]
Li^+@TPB-BMTP-COF	$LiClO_4$/-	6.04×10^{-6} S cm^{-1} at 40 °C	0.87 eV	-		[132]
H-ImCOF	$LiClO_4$/PC	4.0×10^{-5} S cm^{-1} at 25 °C	-	0.21		[137]
H-Li-ImCOFs	-/PC	5.3×10^{-3} S cm^{-1} at 25 °C	0.12 eV	0.88	2-5 V	
CH_3-Li-ImCOF	-/PC	8.0×10^{-5} S cm^{-1} at 25 °C	0.27 eV	0.93	2-4.5 V	
CF_3-Li-ImCOF	-/PC	7.2×10^{-3} S cm^{-1} at 25 °C	0.10 eV	0.81	2-4.5 V	
TpPa-SO_3Li	-/-	2.7×10^{-5} S cm^{-1} at 25 °C	0.18 eV	0.9	-	[142]
COF-PEO-9-Li	LiTFSI	1.33×10^{-3} S cm^{-1} at 200 °C	-	-	2.5-4.2 V	[133]
LiCON-3	-/EC	9.06×10^{-6} S cm^{-1} at 20 °C	0.13 eV	0.92	1.6-4.3 V	[141]
dCOF-ImTFSI-60	LiTFSI	7.05×10^{-3} S cm^{-1} at 150 °C	0.28 eV	0.72 at 30 °C	5.32 V	[143]
PVDF/H-COF-1@10	$LiClO_4$/EC-DMC	2.5×10^{-4} S cm^{-1} at 25 °C	-	0.71		[145]
Q-COF	LiTFSI	1.5×10^{-4} S cm^{-1} at 60 °C	0.19 eV at 25 °C	0.72 at 60 °C	5.6 V	[135]

Table 7
Summary of other types of CPMs for SSEs.

CPMs	Components	Ionic conductivity Proton	Li ion	Activation energy	Ref.
Zeolites	Na-zeolite A	2.9×10^{-3} S cm^{-1} at 600°C	-	-	[148]
	Zeolite/PEO	-	10^{-7} S cm^{-1} at 20°C	-	[149]
	Zeolite X (LiX) membrane	-	2.7×10^{-4} S cm^{-1} at 25°C	0.07 eV	[151]
	SSZ-13/Polymer electrolyte	-	5.3×10^{-2} S cm^{-1} at 70°C	-	[152]
	ZSM-5	-	3.0×10^{-3} S cm^{-1} at 25°C	-	[153]
Porous organic cages	CC3	6.4×10^{-6} S cm^{-1} at 30°C	-	-	[154]
	RCC3	10^{-3} S cm^{-1} at 30°C	-	-	[155]
	Td_A	-	10^{-3} S cm^{-1} at 25°C	0.16 eV	[156]
Hydrogen organic frameworks	HOF-GS-10	0.75×10^{-2} S cm^{-1} at 25°C	-	0.49 eV	[157]
	HOF-GS-11	1.8×10^{-2} S cm^{-1} at 25°C	-	0.14 eV	
	HOF-6	3.4×10^{-6} S cm^{-1} at 27°C	-	-	[158]
	CPOS-1	1.0×10^{-2} S cm^{-1} at 60°C	-	0.61 eV	[159]
	CPOS-2	2.2×10^{-2} S cm^{-1} at 60°C	-	0.93 eV	

Declaration of Competing Interest

The authors declare no conflict of interest.

Acknowledgements

The authors thank the financial supports of the National Natural Science Foundation of China (No. 22005108), Natural Science Foundation of Guangdong Province (No. 2019A1515011460, 2019B1515120027), Key Research and Development (R&D) Program of Guangdong Province (2020B0101030005), and China Postdoctoral Science Foundation (2021M691090).

References

[1] M. Li, J. Lu, Z. Chen, K. Amine, 30 years of lithium-ion batteries, Adv. Mater. 30 (2018), 1800561.
[2] J.B. Goodenough, K.S. Park, The Li-ion rechargeable battery: A perspective, J. Am. Chem. Soc. 135 (2013) 1167–1176.
[3] M. Armand, J.M. Tarascon, Building better batteries, Nature 451 (2008) 652–657.
[4] J.M. Tarascon, M. Armand, Issues and challenges facing rechargeable lithium batteries, Nature 414 (2001) 359–367.
[5] M.M. Thackeray, C. Wolverton, E.D. Isaacs, Electrical energy storage for transportation-approaching the limits of, and going beyond, lithium-ion batteries, Energy Environ. Sci. 5 (2012) 7854–7863.
[6] X. Shen, X.-Q. Zhang, F. Ding, J.-Q. Huang, R. Xu, X. Chen, C. Yan, F.-Y. Su, C.-M. Chen, X. Liu, et al., Advanced electrode materials in lithium batteries: Retrospect and prospect, Energy Mater. Adv. 2021 (2021) 1–15.
[7] J. Liu, Z.N. Bao, Y. Cui, E.J. Dufek, J.B. Goodenough, P. Khalifah, Q.Y. Li, B. Y. Liaw, P. Liu, A. Manthiram, et al., Pathways for practical high-energy long-cycling lithium metal batteries, Nat. Energy. 4 (2019) 180–186.
[8] D.C. Lin, Y.Y. Liu, Y. Cui, Reviving the lithium metal anode for high-energy batteries, Nat. Nanotechnol. 12 (2017) 194–206.
[9] X. Zhang, Y.A. Yang, Z. Zhou, Towards practical lithium-metal anodes, Chem. Soc. Rev. 49 (2020) 3040–3071.
[10] C.C. Fang, X.F. Wang, Y.S. Meng, Key issues hindering a practical lithium-metal anode, Trends Chem. 1 (2019) 152–158.
[11] J.G. Zhang, W. Xu, J. Xiao, X. Cao, J. Liu, Lithium metal anodes with nonaqueous electrolytes, Chem. Rev. 120 (2020) 13312–13348.
[12] Y.L. Jie, X.D. Ren, R.G. Cao, W.B. Cai, S.H. Jiao, Advanced liquid electrolytes for rechargeable Li metal batteries, Adv. Funct. Mater. 30 (2020), 1910777.
[13] F.N. Jiang, S.J. Yang, H. Liu, X.B. Cheng, L. Liu, R. Xiang, Q. Zhang, S. Kaskel, J. Q. Huang, Mechanism understanding for stripping electrochemistry of Li metal anode, SusMat 1 (2021) 506–536.
[14] X.B. Cheng, R. Zhang, C.Z. Zhao, Q. Zhang, Toward safe lithium metal anode in rechargeable batteries: A review, Chem. Rev. 117 (2017) 10403–10473.
[15] B. Jiang, Y. Wei, J. Wu, H. Cheng, L. Yuan, Z. Li, H. Xu, Y. Huang, Recent progress of asymmetric solid-state electrolytes for lithium/sodium-metal batteries, Energy Chem. 3 (2021), 100058.
[16] S.X. Xia, X.S. Wu, Z.C. Zhang, Y. Cui, W. Liu, Practical challenges and future perspectives of all-solid-state lithium-metal batteries, Chem 5 (2019) 753–785.
[17] J. Wan, J. Xie, D.G. Mackanic, W. Burke, Z. Bao, Y. Cui, Status, promises, and challenges of nanocomposite solid-state electrolytes for safe and high performance lithium batteries, Mater. Today Nano 4 (2018) 1–16.
[18] D. Zhou, D. Shanmukaraj, A. Tkacheva, M. Armand, G.X. Wang, Polymer electrolytes for lithium-based batteries: Advances and prospects, Chem 5 (2019) 2326–2352.
[19] Y. Zheng, Y.Z. Yao, J.H. Ou, M. Li, D. Luo, H.Z. Dou, Z.Q. Li, K. Amine, A.P. Yu, Z. W. Chen, A review of composite solid-state electrolytes for lithium batteries: Fundamentals, key materials and advanced structures, Chem. Soc. Rev. 49 (2020) 8790–8839.
[20] J.C. Bachman, S. Muy, A. Grimaud, H.H. Chang, N. Pour, S.F. Lux, O. Paschos, F. Maglia, S. Lupart, P. Lamp, et al., Inorganic solid-state electrolytes for lithium batteries: Mechanisms and properties governing ion conduction, Chem. Rev. 116 (2016) 140–162.
[21] Y. Kato, S. Hori, T. Saito, K. Suzuki, M. Hirayama, A. Mitsui, M. Yonemura, H. Iba, R. Kanno, High-power all-solid-state batteries using sulfide superionic conductors, Nat. Energy. 1 (2016) 16030.
[22] P.V. Wright, An anomalous transition to a lower activation energy for dc electrical conduction above the glass-transition temperature, J. Polym. Sci. Polym. Phys. Ed. 14 (1976) 955–957.
[23] H.C. Wang, L. Sheng, G. Yasin, L. Wang, H. Xu, X.M. He, Reviewing the current status and development of polymer electrolytes for solid-state lithium batteries, Energy Storage Mater. 33 (2020) 188–215.
[24] J. Lopez, D.G. Mackanic, Y. Cui, Z. Bao, Designing polymers for advanced battery chemistries, Nat. Rev. Mater. 4 (2019) 312–330.
[25] W. Liu, S.W. Lee, D.C. Lin, F.F. Shi, S. Wang, A.D. Sendek, Y. Cui, Enhancing ionic conductivity in composite polymer electrolytes with well-aligned ceramic nanowires, Nat. Energ 2 (2017) 17035.
[26] W.-H. Huang, X.-M. Li, X.-F. Yang, X.-X. Zhang, H.-H. Wang, H. Wang, The recent progress and perspectives on metal- and covalent-organic framework based solid-state electrolytes for lithium-ion batteries, Mater. Chem. Front. 5 (2021) 3593–3613.
[27] R. Zhao, Y. Wu, Z. Liang, L. Gao, W. Xia, Y. Zhao, R. Zou, Metal–organic frameworks for solid-state electrolytes, Energy Environ. Sci. 13 (2020) 2386–2403.
[28] Y.B. Huang, J. Liang, X.S. Wang, R. Cao, Multifunctional metal-organic framework catalysts: Synergistic catalysis and tandem reactions, Chem. Soc. Rev. 46 (2017) 126–157.
[29] J.J. Jiao, W. Gong, X.W. Wu, S.P. Yang, Y. Cui, Multivariate crystalline porous materials: Synthesis, property and potential application, Coord. Chem. Rev. 385 (2019) 174–190.
[30] H. Zeng, M. Xie, T. Wang, R.J. Wei, X.J. Xie, Y. Zhao, W. Lu, D. Li, Orthogonal-array dynamic molecular sieving of propylene/propane mixtures, Nature 595 (2021) 542–548.
[31] F.Z. Jin, J.J. Liu, Y. Chen, Z.J. Zhang, Tethering flexible polymers to crystalline porous materials: A win-win hybridization approach, Angew. Chem. Int. Ed. 60 (2021) 14222–14235.
[32] J.W. Zhou, B. Wang, Emerging crystalline porous materials as a multifunctional platform for electrochemical energy storage, Chem. Soc. Rev. 46 (2017) 6927–6945.
[33] X. Li, K.P. Loh, Recent progress in covalent organic frameworks as solid-state ion conductors, ACS Materials Lett. 1 (2019) 327–335.
[34] B.M. Wiers, M.-L. Foo, N.P. Balsara, J.R. Long, A solid lithium electrolyte via addition of lithium isopropoxide to a metal-organic framework with open metal sites, J. Am. Chem. Soc. 133 (2011) 14522–14525.

This work firstly reported the design of MOF/PEO-based SSE.

[35] M.L. Aubrey, R. Ameloot, B.M. Wiers, J.R. Long, Metal-organic frameworks as solid magnesium electrolytes, Energy Environ. Sci. 7 (2014) 667–671.
[36] R. Ameloot, M. Aubrey, B.M. Wiers, A.P. Gomora-Figueroa, S.N. Patel, N.P. Balsara, J.R. Long, Ionic conductivity in the metal-organic framework UiO-66 by dehydration and insertion of lithium tert-butoxide, Chem. Eur. J. 19 (2013) 5533–5536.
[37] R. Zettl, S. Lunghammer, B. Gadermaier, A. Boulaoued, P. Johansson, H.M. R. Wilkening, I. Hanzu, High Li^+ and Na^+ conductivity in new hybrid solid electrolytes based on the porous MIL-121 metal organic framework, Adv. Energy Mater. 11 (2021), 2003542.
[38] J. Cepeda, S. Perez-Yanez, G. Beobide, O. Castillo, E. Goikolea, F. Aguesse, L. Garrido, A. Luque, P.A. Wright, Scandium/alkaline metal-organic frameworks: Adsorptive properties and ionic conductivity, Chem. Mater. 28 (2016) 2519–2528.

[39] S. Ma, L. Shen, Q. Liu, W. Shi, C. Zhang, F. Liu, J.A. Baucom, D. Zhang, H. Yue, H. B. Wu, et al., Class of solid-like electrolytes for rechargeable batteries based on metal-organic frameworks infiltrated with liquid electrolytes, ACS Appl. Mater. Interfaces 12 (2020) 43824–43832.
[40] X. Duan, Y. Ouyang, Q. Zeng, S. Ma, Z. Kong, A. Chen, Z. He, T. Yang, Q. Zhang, Two carboxyl-decorated anionic metal-organic frameworks as solid-state electrolytes exhibiting high Li^+ and Zn^{2+} conductivity, Inorg. Chem. 60 (2021) 11032–11037.
[41] A.N. Hong, H. Yang, A. Zhou, X. Bu, P. Feng, Roles of alkali metals and ionic networks in directing the formation of anionic metal-organic frameworks, Cryst. Growth Des. 20 (2020) 6668–6676.
[42] D.K. Panda, K. Maity, A. Palukoshka, F. Ibrahim, S. Saha, Li^+ ion-conducting sulfonate-based neutral metal-organic framework, ACS Sustainable Chem. Eng. 7 (2019) 4619–4624.
[43] W. Xu, X. Pei, C.S. Diercks, H. Lyu, Z. Ji, O.M. Yaghi, A metal-organic framework of organic vertices and polyoxometalate linkers as a solid-state electrolyte, J. Am. Chem. Soc. 141 (2019) 17522–17526.

This work firstly reported the synthesize of anionic MOF (MOF-688) for SSE.

[44] S.S. Park, Y. Tulchinsky, M. Dinca, Single-ion Li^+, Na^+, and Mg^{2+} solid electrolytes supported by a mesoporous anionic Cu-Azolate metal-organic framework, J. Am. Chem. Soc. 139 (2017) 13260–13263.
[45] E.M. Miner, S.S. Park, M. Dinca, High Li^+ and Mg^{2+} conductivity in a Cu-Azolate metal-organic framework, J. Am. Chem. Soc. 141 (2019) 4422–4427.
[46] H. Yang, B. Liu, J. Bright, S. Kasani, J. Yang, X. Zhang, N. Wu, A single-ion conducting UiO-66 metal-organic framework electrolyte for all-solid-state lithium batteries, ACS Appl. Energy Mater. 3 (2020) 4007–4013.
[47] S. Fischer, J. Roeser, T.C. Lin, R.H. DeBlock, J. Lau, B.S. Dunn, F. Hoffmann, M. Froeba, A. Thomas, S.H. Tolbert, A metal-organic framework with tetrahedral aluminate sites as a single-ion Li^+ solid electrolyte, Angew. Chem. Int. Ed. 57 (2018) 16683–16687.
[48] K. Nath, A. Bin Rahaman, R. Moi, K. Maity, K. Biradha, Porous Li-MOF as a solid-state electrolyte: Exploration of lithium ion conductivity through bio-inspired ionic channels, Chem. Commun. 56 (2020) 14873–14876.
[49] I.J. Villar-Garcia, S. Fearn, G.F. De Gregorio, N.L. Ismail, F.J.V. Gschwend, A.J. S. McIntosh, K.R.J. Lovelock, The ionic liquid-vacuum outer atomic surface: A low-energy ion scattering study, Chem. Sci. 5 (2014) 4404–4418.
[50] F. Ren, J.W. Wang, F.W. Xie, K. Zan, S. Wang, S.J. Wang, Applications of ionic liquids in starch chemistry: A review, Green Chem. 22 (2020) 2162–2183.
[51] K. Karuppasamy, J. Theerthagiri, D. Vikraman, C.J. Yim, S. Hussain, R. Sharma, T. Maiyalagan, J. Qin, H.S. Kim, Ionic liquid-based electrolytes for energy storage devices: A brief review on their limits and applications, Polymers 12 (2020) 918.
[52] K. Fujie, K. Otsubo, R. Ikeda, T. Yamada, H. Kitagawa, Low temperature ionic conductor: Ionic liquid incorporated within a metal-organic framework, Chem. Sci. 6 (2015) 4306–4310.
[53] S. Zhang, J. Zhang, Y. Zhang, Y. Deng, Nanoconfined ionic liquids, Chem. Rev. 117 (2017) 6755–6833.
[54] W. Silva, M. Zanatta, A.S. Ferreira, M.C. Corvo, E.J. Cabrita, Revisiting ionic liquid structure-property relationship: A critical analysis, Int. J. Mol. Sci. 21 (2020) 7745.
[55] D.R. MacFarlane, M. Forsyth, P.C. Howlett, M. Kar, S. Passerini, J.M. Pringle, H. Ohno, M. Watanabe, F. Yan, W.J. Zheng, et al., Ionic liquids and their solid-state analogues as materials for energy generation and storage, Nat. Rev. Mater. 1 (2016) 1–15.
[56] G. Ori, F. Villemot, L. Viau, A. Vioux, B. Coasne, Ionic liquid confined in silica nanopores: Molecular dynamics in the isobaric-isothermal ensemble, Mol. Phys. 112 (2014) 1350–1361.
[57] Y. Yoshida, K. Fujie, D.W. Lim, R. Ikeda, H. Kitagawa, Superionic conduction over a wide temperature range in a metal-organic framework impregnated with ionic liquids, Angew. Chem. Int. Ed. 58 (2019) 10909–10913.
[58] X.C. Huang, Y.Y. Lin, J.P. Zhang, X.M. Chen, Ligand-directed strategy for zeolite-type metal-organic frameworks: Zinc(ii) imidazolates with unusual zeolitic topologies, Angew. Chem. Int. Ed. 45 (2006) 1557–1559.
[59] K.S. Park, Z. Ni, A.P. Cote, J.Y. Choi, R. Huang, F.J. Uribe-Romo, H.K. Chae, M. O'Keeffe, O.M. Yaghi, Exceptional chemical and thermal stability of zeolitic imidazolate frameworks, Proc. Natl. Acad. Sci. U. S. A. 103 (2006) 10186–10191.
[60] K. Fujie, T. Yamada, R. Ikeda, H. Kitagawa, Introduction of an ionic liquid into the micropores of a metal-organic framework and its anomalous phase behavior, Angew. Chem. Int. Ed. 53 (2014) 11302–11305.
[61] V. Nozari, C. Calahoo, J.M. Tuffnell, P. Adelhelm, K. Wondraczek, S.E. Dutton, T. D. Bennett, L. Wondraczek, Sodium ion conductivity in superionic IL-impregnated metal-organic frameworks: Enhancing stability through structural disorder, Sci. Rep. 10 (2020) 3532.
[62] J.M. Tuffnell, J.K. Morzy, N.D. Kelly, R. Tan, Q. Song, C. Ducati, T.D. Bennett, S. E. Dutton, Comparison of the ionic conductivity properties of microporous and mesoporous mofs infiltrated with a Na-ion containing IL mixture, Dalton Trans. 49 (2020) 15914–15924.
[63] X. Qi, D. Cai, X. Wang, X. Xia, C. Gu, J. Tu, Ionic liquid-impregnated ZIF-8/polypropylene solid-like electrolyte for dendrite-free lithium-metal batteries, ACS Appl. Mater. Interfaces 14 (2022) 6859–6868.
[64] Z. Wang, R. Tan, H. Wang, L. Yang, J. Hu, H. Chen, F. Pan, A metal-organic-framework-based electrolyte with nanowetted interfaces for high-energy-density solid-state lithium battery, Adv. Mater. 30 (2018), 1704436.
[65] W. Morris, B. Volosskiy, S. Demir, F. Gandara, P.L. McGrier, H. Furukawa, D. Cascio, J.F. Stoddart, O.M. Yaghi, Synthesis, structure, and metalation of two new highly porous zirconium metal-organic frameworks, Inorg. Chem. 51 (2012) 6443–6445.
[66] J.F. Wu, X. Guo, Nanostructured metal-organic framework (MOF)-derived solid electrolytes realizing fast lithium ion transportation kinetics in solid-state batteries, Small 15 (2019), 1804413.
[67] P. Chiochan, X. Yu, M. Sawangphruk, A. Manthiram, A metal organic framework derived solid electrolyte for lithium–sulfur batteries, Adv. Energy Mater. 10 (2020), 2001285.
[68] X. Yu, N.S. Grundish, J.B. Goodenough, A. Manthiram, Ionic liquid (IL) laden metal-organic framework (IL-MOF) electrolyte for quasi-solid-state sodium batteries, ACS Appl. Mater. Interfaces 13 (2021) 24662–24669.
[69] A.E. Abdelmaoula, J. Shu, Y. Cheng, L. Xu, G. Zhang, Y. Xia, M. Tahir, P. Wu, L. Mai, Core-shell MOF-in-MOF nanopore bifunctional host of electrolyte for high-performance solid-state lithium batteries, Small Methods 5 (2021), 2100508.

This work reported the first employ of MOF-in-MOF filling with ionic liquid for SSE.

[70] M. Li, T. Chen, S. Song, Y. Li, J. Bae, HKUST-1@IL-Li solid-state electrolyte with 3D ionic channels and enhanced fast Li^+ transport for lithium metal batteries at high temperature, Nanomaterials 11 (2021) 736.
[71] M. Vazquez, M. Liu, Z. Zhang, A. Chandresh, A.B. Kanj, W. Wenzel, L. Heinke, Structural and dynamic insights into the conduction of lithium-ionic-liquid mixtures in nanoporous metal-organic frameworks as solid-state electrolytes, ACS Appl. Mater. Interfaces 13 (2021) 21166–21174.
[72] B.J. Siwick, H.J. Bakker, On the role of water in intermolecular proton-transfer reactions, J. Am. Chem. Soc. 129 (2007) 13412–13420.
[73] P.J. Celis-Salazar, M. Cai, C.A. Cucinell, S.R. Ahrenholtz, C.C. Epley, P.M. Usov, A. J. Morris, Independent quantification of electron and ion diffusion in metallocene-doped metal-organic frameworks thin films, J. Am. Chem. Soc. 141 (2019) 11947–11953.
[74] Z. Lei, J. Shen, J. Wang, Q. Qiu, G. Zhang, S.-S. Chi, H. Xu, S. Li, W. Zhang, Y. Zhao, et al., Composite polymer electrolytes with uniform distribution of ionic liquid-grafted ZIF-90 nanofillers for high-performance solid-state Li batteries, Chem. Eng. J. 412 (2021), 128733.

This work pioneered the synthesize of ionic liquid-grafted ZIF-90 for SSE.

[75] S.J. Tan, X.X. Zeng, Q. Ma, X.W. Wu, Y.G. Guo, Recent advancements in polymer-based composite electrolytes for rechargeable lithium batteries, Electrochem. Energy Rev. 1 (2018) 113–138.
[76] K.S. Ngai, S. Ramesh, K. Ramesh, J.C. Juan, A review of polymer electrolytes: Fundamental, approaches and applications, Ionics 22 (2016) 1259–1279.
[77] A. Arya, A.L. Sharma, Polymer electrolytes for lithium ion batteries: A critical study, Ionics 23 (2017) 497–540.
[78] L.-Z. Fan, H. He, C.-W. Nan, Tailoring inorganic-polymer composites for the mass production of solid-state batteries, Nat. Rev. Mater. 6 (2021) 1003–1019.
[79] Q. Zhao, X. Liu, S. Stalin, K. Khan, L.A. Archer, Solid-state polymer electrolytes with in-built fast interfacial transport for secondary lithium batteries, Nat. Energy. 4 (2019) 365–373.
[80] C. Yuan, J. Li, P. Han, Y. Lai, Z. Zhang, J. Liu, Enhanced electrochemical performance of poly(ethylene oxide) based composite polymer electrolyte by incorporation of nano-sized metal-organic framework, J. Power Sources 240 (2013) 653–658.

This work firstly reported the design of MOF/PEO-based SSE.

[81] Z. Lei, J. Shen, W. Zhang, Q. Wang, J. Wang, Y. Deng, C. Wang, Exploring porous zeolitic imidazolate frame work-8 (ZIF-8) as an efficient filler for high-performance poly(ethyleneoxide)-based solid polymer electrolytes, Nano Res. 13 (2020) 2259–2267.
[82] H. Huo, B. Wu, T. Zhang, X. Zheng, L. Ge, T. Xu, X. Guo, X. Sun, Anion-immobilized polymer electrolyte achieved by cationic metal-organic framework filler for dendrite-free solid-state batteries, Energy Storage Mater. 18 (2019) 59–67.
[83] X. Qing, J. Li, Z. Wang, M. Chen, J. Lin, X. Lin, A functionalized metal organic framework-laden nanoporous polymer electrolyte for exceptionally stable lithium electrodeposition, Chem. Commun. 56 (2020) 15533–15536.
[84] N. Angulakshmi, Y. Zhou, S. Suriyakumar, R.B. Dhanalakshmi, M. Satishrajan, S. Alwarappan, M.H. Alkordi, A.M. Stephan, Microporous metal-organic framework (MOF)-based composite polymer electrolyte (CPE) mitigating lithium dendrite formation in all-solid-state-lithium batteries, ACS Omega 5 (2020) 7885–7894.
[85] S.S.Y. Chui, S.M.F. Lo, J.P.H. Charmant, A.G. Orpen, I.D. Williams, A chemically functionalizable nanoporous material $[Cu_3(TMA)_2(H_2O)_3]_n$, Science 283 (1999) 1148–1150.
[86] C.-C. Sun, A. Yusuf, S.-W. Li, X.-L. Qi, Y. Ma, D.-Y. Wang, Metal organic frameworks enabled rational design of multifunctional PEO-based solid polymer electrolytes, Chem. Eng. J. 414 (2021), 128702.
[87] Z. Zhang, J.H. You, S.J. Zhang, C.W. Wang, Y. Zhou, J.T. Li, L. Huang, S.G. Sun, Metal organic framework nanorod doped solid polymer electrolyte with decreased

crystallinity for high-performance all-solid-state lithium batteries, ChemElectroChem 7 (2020) 1125–1134.
[88] S. Suriyakumar, S. Gopi, M. Kathiresan, S. Bose, E.B. Gowd, J.R. Nair, N. Angulakshmi, G. Meligrana, F. Bella, C. Gerbaldi, et al., Metal organic framework laden poly(ethylene oxide) based composite electrolytes for all-solid-state Li-S and Li-metal polymer batteries, Electrochim. Acta. 285 (2018) 355–364.
[89] Z. Ge, J. Li, J. Liu, Enhanced electrochemical performance of all-solid-state sodium-sulfur batteries by PEO-$NaCF_3SO_3$-MIL-53(Al) solid electrolyte, Ionics 26 (2020) 1787–1795.
[90] S. Suriyakumar, M. Kanagaraj, N. Angulakshmi, M. Kathiresan, K.S. Nahm, M. Walkowiak, K. Wasiński, P. Półrolniczak, A.M. Stephan, Charge-discharge studies of all-solid-state Li/$LiFePO_4$ cells with PEO-based composite electrolytes encompassing metal organic frameworks, RSC Adv. 6 (2016) 97180–97186.
[91] Q. Han, S. Wang, Z. Jiang, X. Hu, H. Wang, Composite polymer electrolyte incorporating metal-organic framework nanosheets with improved electrochemical stability for all-solid-state Li metal batteries, ACS Appl. Mater. Interfaces 12 (2020) 20514–20521.
[92] D.E. Mathew, S. Gopi, M. Kathiresan, A.M. Stephan, S. Thomas, Influence of mof ligands on the electrochemical and interfacial properties of PEO-based electrolytes for all-solid-state lithium batteries, Electrochim. Acta. 319 (2019) 189–200.
[93] X. Wu, K. Chen, Z. Yao, J. Hu, M. Huang, J. Meng, S. Ma, T. Wu, Y. Cui, C. Li, Metal organic framework reinforced polymer electrolyte with high cation transference number to enable dendrite-free solid state Li metal conversion batteries, J. Power Sources 501 (2021), 229946.
[94] Z. Wang, S. Wang, A. Wang, X. Liu, J. Chen, Q. Zeng, L. Zhang, W. Liu, L. Zhang, Covalently linked metal-organic framework (MOF)-polymer all-solid-state electrolyte membranes for room temperature high performance lithium batteries, J. Mater. Chem. A 6 (2018) 17227–17234.
[95] Q. Zhang, B. Liu, J. Wang, Q. Li, D. Li, S. Guo, Y. Xiao, Q. Zeng, W. He, M. Zheng, et al., The optimized interfacial compatibility of metal-organic frameworks enables a high-performance quasi-solid metal battery, ACS Energy Lett. 5 (2020) 2919–2926.
[96] Z. Lei, Q. Qiu, J. Shen, X. Ao, B. Zhang, Y. Guo, J. Wang, Y. Deng, C. Wang, Room-temperature solid-state lithium metal batteries using metal organic framework composited comb-like methoxy poly(ethylene glycol) acrylate solid polymer electrolytes, Macromol. Mater. Eng. 306 (2021), 2100336.
[97] H. Wang, Q. Wang, X. Cao, Y. He, K. Wu, J. Yang, H. Zhou, W. Liu, X. Sun, Thiol-branched solid polymer electrolyte featuring high strength, toughness, and lithium ionic conductivity for lithium-metal batteries, Adv. Mater. 32 (2020), 2001259.
[98] Y.X. Wu, Y. Li, Y. Wang, Q. Liu, Q.G. Chen, M.H. Chen, Advances and prospects of PVDF based polymer electrolytes, J. Energy Chem. 64 (2022) 62–84.
[99] J. Yu, T. Guo, C. Wang, Z. Shen, X. Dong, S. Li, H. Zhang, Z. Lu, Engineering two-dimensional metal-organic framework on molecular basis for fast Li^+ conduction, Nano Lett. 21 (2021) 5805–5812.
[100] D.D. Han, Z.Y. Wang, G.L. Pan, X.P. Gao, Metal-organic-framework-based gel polymer electrolyte with immobilized anions to stabilize a lithium anode for a quasi-solid-state lithium-sulfur battery, ACS Appl. Mater. Interfaces 11 (2019) 18427–18435.
[101] F. Zhu, H. Bao, X. Wu, Y. Tao, C. Qin, Z. Su, Z. Kang, High-performance metal-organic framework-based single ion conducting solid-state electrolytes for low-temperature lithium metal batteries, ACS Appl. Mater. Interfaces 11 (2019) 43206–43213.
[102] S. Reichman, A. Ulus, E. Peled, PTFE-based solid polymer electrolyte membrane for high-temperature fuel cell applications, J. Electrochem. Soc. 154 (2007) B327–B333.
[103] L. Shen, H.B. Wu, F. Liu, J.L. Brosmer, G. Shen, X. Wang, J.I. Zink, Q. Xiao, M. Cai, G. Wang, et al., Creating lithium-ion electrolytes with biomimetic ionic channels in metal-organic frameworks, Adv. Mater. 30 (2018), 1707476.
[104] S. Yuan, J.L. Bao, J. Wei, Y. Xia, D.G. Truhlar, Y. Wang, A versatile single-ion electrolyte with a Grotthuss-like Li conduction mechanism for dendrite-free Li metal batteries, Energy Environ. Sci. 12 (2019) 2741–2750.
[105] C. Sun, J.H. Zhang, X.F. Yuan, J.N. Duan, S.W. Deng, J.M. Fan, J.K. Chang, M. S. Zheng, Q.F. Dong, ZIF-8-based quasi-solid-state electrolyte for lithium batteries, ACS Appl. Mater. Interfaces 11 (2019) 46671–46677.
[106] Z. Liu, P. Liu, L. Tian, J. Xiao, R. Cui, Z. Liu, Significantly enhancing the lithium-ion conductivity of solid-state electrolytes via a strategy for fabricating hollow metal-organic frameworks, Chem. Commun. 56 (2020) 14629–14632.
[107] G. Jiang, C. Qu, F. Xu, E. Zhang, Q. Lu, X. Cai, S. Hausdorf, H. Wang, S. Kaskel, Glassy metal-organic-framework-based quasi-solid-state electrolyte for high-performance lithium-metal batteries, Adv. Funct. Mater. 31 (2021), 2104300.
[108] S. Alipoori, S. Mazinani, S.H. Aboutalebi, F. Sharif, Review of PVA-based gel polymer electrolytes in flexible solid-state supercapacitors: Opportunities and challenges, J. Energy Storage 27 (2020), 101072.
[109] C. Zhang, L. Shen, J. Shen, F. Liu, G. Chen, R. Tao, S. Ma, Y. Peng, Y. Lu, Anion-sorbent composite separators for high-rate lithium-ion batteries, Adv. Mater. 31 (2019), 1808338.
[110] Y. Guo, Y. Ying, Y. Mao, X. Peng, B. Chen, Polystyrene sulfonate threaded through a metal-organic framework membrane for fast and selective lithium-ion separation, Angew. Chem. Int. Ed. 55 (2016) 15120–15124.
[111] T. Liu, Z.W. Chang, Y.B. Yin, K. Chen, Y. Zhang, X.B. Zhang, The PVDF-HFP gel polymer electrolyte for Li-O_2 battery, Solid State Ionics 318 (2018) 88–94.
[112] X. Lu, H. Wu, D. Kong, X. Li, L. Shen, Y. Lu, Facilitating lithium-ion conduction in gel polymer electrolyte by metal-organic frameworks, ACS Materials Lett. 2 (2020) 1435–1441.
[113] Q. Zhang, Y. Xiao, Q. Li, J. Wang, S. Guo, X. Li, Y. Ouyang, Q. Zeng, W. He, S. Huang, Design of thiol-lithium ion interaction in metal-organic framework for high-performance quasi-solid lithium metal batteries, Dalton Trans. 50 (2021) 2928–2935.
[114] D. Li, J. Wang, S. Guo, Y. Xiao, Q. Zeng, W. He, L. Gan, Q. Zhang, S. Huang, Molecular-scale interface engineering of metal-organic frameworks toward ion transport enables high-performance solid lithium metal battery, Adv. Funct. Mater. 30 (2020), 2003945.
[115] Q. Zeng, J. Wang, X. Li, Y. Ouyang, W. He, D. Li, S. Guo, Y. Xiao, H. Deng, W. Gong, et al., Cross-linked chains of metal-organic framework afford continuous ion transport in solid batteries, ACS Energy Lett. 6 (2021) 2434–2441.
[116] W. Wen, Z. Wang, A. Wang, Q. Zeng, P. Chen, X. Wen, Z. Li, Z. Li, W. Liu, L. Zhang, A metal-organic framework-5-incorporated all-solid-state composite polymer electrolyte membrane with enhanced performances for high-safety lithium-ion batteries, Energy Technol. 9 (2020), 2000808.
[117] J.-F. Wu, X. Guo, MOF-derived nanoporous multifunctional fillers enhancing the performances of polymer electrolytes for solid-state lithium batteries, J. Mater. Chem. A 7 (2019) 2653–2659.
[118] L. Liu, C. Sun, Flexible quasi-solid-state composite electrolyte membrane derived from a metal-organic framework for lithium-metal batteries, ChemElectroChem 7 (2020) 707–715.
[119] Q. Zhang, D. Li, J. Wang, S. Guo, W. Zhang, D. Chen, Q. Li, X. Rui, L. Gan, S. Huang, Multiscale optimization of Li-ion diffusion in solid lithium metal batteries via ion conductive metal-organic frameworks, Nanoscale 12 (2020) 6976–6982.
[120] Y. Hu, T. Feng, L. Xu, L. Zhang, L. Luo, A hollow porous metal-organic framework enabled polyethylene oxide based composite polymer electrolytes for all-solid-state lithium batteries, Batteries & Supercaps 202100303 (2021).
[121] Y. Xia, N. Xu, L. Du, Y. Cheng, S. Lei, S. Li, X. Liao, W. Shi, L. Xu, L. Mai, Rational design of ion transport paths at the interface of metal-organic framework modified solid electrolyte, ACS Appl. Mater. Interfaces. 12 (2020) 22930–22938.
[122] Z. Wang, H. Zhou, C. Meng, W. Xiong, Y. Cai, P. Hu, H. Pang, A. Yuan, Enhancing ion transport: Function of ionic liquid decorated mofs in polymer electrolytes for all-solid-state lithium batteries, ACS Appl. Energy Mater. 3 (2020) 4265–4274.
[123] R. Dutta, A. Kumar, Probing the ionic transport dynamics in ionic liquid incorporated CuBTC-metal-organic framework based PVdF-HFP nanocomposite membranes, Solid State Sci 100 (2020), 106115.
[124] G. Wang, P. He, L.Z. Fan, Asymmetric polymer electrolyte constructed by metal-organic framework for solid-state, dendrite-free lithium metal battery, Adv. Funct. Mater. 31 (2020), 2007198.
[125] Z. Li, S. Wang, J. Shi, Y. Liu, S. Zheng, H. Zou, Y. Chen, W. Kuang, K. Ding, L. Chen, et al., A 3D interconnected metal-organic framework-derived solid-state electrolyte for dendrite-free lithium metal battery, Energy Storage Mater 47 (2022) 262–270.
[126] Z. Wang, Z. Wang, L. Yang, H. Wang, Y. Song, L. Han, K. Yang, J. Hu, H. Chen, F. Pan, Boosting interfacial Li^+ transport with a MOF-based ionic conductor for solid-state batteries, Nano Energy 49 (2018) 580–587.
[127] J. Sun, X. Yao, Y. Li, Q. Zhang, C. Hou, Q. Shi, H. Wang, Facilitating interfacial stability via bilayer heterostructure solid electrolyte toward high-energy, safe and adaptable lithium batteries, Adv. Energy Mater. 2000709 (2020).
[128] R. Zhao, L. Gao, M. Song, Y. Ye, Z. Liang, J. Bian, J. Zhu, S. Li, R. Zou, Y. Zhao, Stabilization of nasicon-type electrolyte against Li anode via an ionic conductive MOF-incorporated adhesive interlayer, ACS Energy Lett. 6 (2021) 3141–3150.
[129] Z. Guo, Y. Zhang, Y. Dong, J. Li, S. Li, P. Shao, X. Feng, B. Wang, Fast ion transport pathway provided by polyethylene glycol confined in covalent organic frameworks, J. Am. Chem. Soc. 141 (2019) 1923–1927.
[130] Y. Du, H. Yang, J.M. Whiteley, S. Wan, Y. Jin, S.-H. Lee, W. Zhang, Ionic covalent organic frameworks with spiroborate linkage, Angew. Chem. Int. Ed. 55 (2016) 1737–1741.

This work pioneered the synthesize of ionic COF for SSE.

[131] A.P. Cote, A.I. Benin, N.W. Ockwig, M. O'Keeffe, A.J. Matzger, O.M. Yaghi, Porous, crystalline, covalent organic frameworks, Science 310 (2005) 1166–1170.
[132] Q. Xu, S. Tao, Q. Jiang, D. Jiang, Ion conduction in polyelectrolyte covalent organic frameworks, J. Am. Chem. Soc. 140 (2018) 7429–7432.

This work firstly reported the design of COF/PEO-based SSE.

[133] G. Zhang, Y.-l. Hong, Y. Nishiyama, S. Bai, S. Kitagawa, S. Horike, Accumulation of glassy poly(ethylene oxide) anchored in a covalent organic framework as a solid-state Li^+ electrolyte, J. Am. Chem. Soc. 141 (2019) 1227–1234.
[134] Z. Liu, K. Zhang, G. Huang, B. Xu, Y.L. Hong, X. Wu, Y. Nishiyama, S. Horike, G. Zhang, S. Kitagawa, Highly processable covalent organic framework gel electrolyte enabled by side-chain engineering for lithium-ion batteries, Angew. Chem. Int. Ed. 61 (2022), 202110695.

[135] C. Niu, W. Luo, C. Dai, C. Yu, Y. Xu, High-voltage-tolerant covalent organic framework electrolyte with holistically oriented channels for solid-state lithium metal batteries with nickel-rich cathodes, Angew. Chem. Int. Ed. 60 (2021) 24915–24923.
[136] Y. Zhang, J. Duan, D. Ma, P. Li, S. Li, H. Li, J. Zhou, X. Ma, X. Feng, B. Wang, Three-dimensional anionic cyclodextrin-based covalent organic frameworks, Angew. Chem. Int. Edit. 56 (2017) 16313–16317.
[137] Y. Hu, N. Dunlap, S. Wan, S. Lu, S. Huang, I. Sellinger, M. Ortiz, Y. Jin, S.-h. Lee, W. Zhang, Crystalline lithium imidazolate covalent organic frameworks with high Li-ion conductivity, J. Am. Chem. Soc. 141 (2019) 7518–7525.
[138] S. Kandambeth, A. Mallick, B. Lukose, M.V. Mane, T. Heine, R. Banerjee, Construction of crystalline 2D covalent organic frameworks with remarkable chemical (acid/base) stability via a combined reversible and irreversible route, J. Am. Chem. Soc. 134 (2012) 19524–19527.
[139] S. Mitra, S. Kandambeth, B.P. Biswal, M.A. Khayum, C.K. Choudhury, M. Mehta, G. Kaur, S. Banerjee, A. Prabhune, S. Verma, et al., Self-exfoliated guanidinium-based ionic covalent organic nanosheets (iCONs), J. Am. Chem. Soc. 138 (2016) 2823–2828.
[140] H. Chen, H. Tu, C. Hu, Y. Liu, D. Dong, Y. Sun, Y. Dai, S. Wang, H. Qian, Z. Lin, et al., Cationic covalent organic framework nanosheets for fast Li-ion conduction, J. Am. Chem. Soc. 140 (2018) 896–899.
[141] X. Li, Q. Hou, W. Huang, H.-S. Xu, X. Wang, W. Yu, R. Li, K. Zhang, L. Wang, Z. Chen, et al., Solution-processable covalent organic framework electrolytes for all-solid-state Li-organic batteries, ACS Energy Lett 5 (2020) 3498–3506.
[142] K. Jeong, S. Park, G.Y. Jung, S.H. Kim, Y.H. Lee, S.K. Kwak, S.Y. Lee, Solvent-free, single lithium-ion conducting covalent organic frameworks, J. Am. Chem. Soc. 141 (2019) 5880–5885.

This work firstly synthesized single lithium-ion conducting COF for SSE.

[143] Z. Li, Z.W. Liu, Z. Li, T.X. Wang, F. Zhao, X. Ding, W. Feng, B.H. Han, Defective 2D covalent organic frameworks for postfunctionalization, Adv. Funct. Mater. 30 (2020), 1909267.
[144] Z. Shan, M. Wu, Y. Du, B. Xu, B. He, X. Wu, G. Zhang, Covalent organic framework-based electrolytes for fast Li^+ conduction and high-temperature solid-state lithium-ion batteries, Chem. Mater. 33 (2021) 5058–5066.
[145] D. Dong, H. Zhang, B. Zhou, Y. Sun, H. Zhang, M. Cao, J. Li, H. Zhou, H. Qian, Z. Lin, et al., Porous covalent organic frameworks for high transference number polymer-based electrolytes, Chem. Commun. 55 (2019) 1458–1461.
[146] W. Sun, J. Zhang, M. Xie, D. Lu, Z. Zhao, Y. Li, Z. Cheng, S. Zhang, H. Chen, Ultrathin aramid/COF heterolayered membrane for solid-state li-metal batteries, Nano Lett. 20 (2020) 8120–8126.
[147] Z. Cheng, M. Xie, Y. Mao, J. Ou, S. Zhang, Z. Zhao, J. Li, F. Fu, J. Wu, Y. Shen, et al., Building lithiophilic ion-conduction highways on garnet-type solid-state Li^+ conductors, Adv. Energy Mater. 10 (2020), 1904230.
[148] K. G, S. G, Ionic conductivity in dehydrated zeolites, J. Mater. Sci. 27 (1992) 6036–6040.
[149] N. Munichandraiah, L.G. Scanlon, R.A. Marsh, B. Kumar, A.K. Sircar, Influence of zeolite on electrochemical and physicochemical properties of polyethylene oxide solid-electrolyte, J. Appl. Electrochem. 25 (1995) 857–863.
[150] M. Feuerstein, R.F. Lobo, Mobility of Li cations in X zeolites studied by solid-state NMR spectroscopy, Solid State Ionics 118 (1999) 135–139.
[151] X.W. Chi, M.L. Li, J.C. Di, P. Bai, L.N. Song, X.X. Wang, F. Li, S. Liang, J.J. Xu, J. H. Yu, A highly stable and flexible zeolite electrolyte solid-state Li-air battery, Nature 592 (2021) 551–557.

This work reported the great progress of zeolite-based SSE for Li-air batteries.

[152] H. Jamal, F. Khan, S. Hyun, S.W. Min, J.H. Kim, Enhancement of the ionic conductivity of a composite polymer electrolyte via surface functionalization of SSZ-13 zeolite for all-solid-state Li-metal batteries, J. Mater. Chem. A 9 (2021) 4126–4137.
[153] D. Lee, K.H. Park, S.Y. Kim, J.Y. Jung, W. Lee, K. Kim, G. Jeong, J.S. Yu, J. Choi, M.S. Park, et al., Critical role of zeolites as H_2S scavengers in argyrodite Li_6PS_5Cl solid electrolytes for all-solid-state batteries, J. Mater. Chem. A 9 (2021) 17311–17316.
[154] T. Tozawa, J.T.A. Jones, S.I. Swamy, S. Jiang, D.J. Adams, S. Shakespeare, R. Clowes, D. Bradshaw, T. Hasell, S.Y. Chong, et al., Porous organic cages, Nat. Mater. 8 (2009) 973–978.
[155] M. Liu, L. Chen, S. Lewis, S.Y. Chong, M.A. Little, T. Hasell, I.M. Aldous, C. M. Brown, M.W. Smith, C.A. Morrison, et al., Three-dimensional protonic conductivity in porous organic cage solids, Nat. Commun. 7 (2016) 12750.
[156] A. Petronico, T.P. Moneypenny, B.G. Nicolau, J.S. Moore, R.G. Nuzzo, A. A. Gewirth, Solid-liquid lithium electrolyte nanocomposites derived from porous molecular cages, J. Am. Chem. Soc. 140 (2018) 7504–7509.

This work reported the ground-breaking evolvement of POC-based SSE for LIBs.

[157] A. Karmakar, R. Illathvalappil, B. Anothumakkool, A. Sen, P. Samanta, A.V. Desai, S. Kurungot, S.K. Ghosh, Hydrogen-bonded organic frameworks (HOFs): A new class of porous crystalline proton-conducting materials, Angew. Chem. Int. Ed. 55 (2016) 10667–10671.
[158] W. Yang, F. Yang, T.L. Hu, S.C. King, H.L. Wang, H. Wu, W. Zhou, J.R. Li, H. D. Arman, B.L. Chen, Microporous diaminotriazine-decorated porphyrin-based hydrogen-bonded organic framework: Permanent porosity and proton conduction, Cryst. Growth Des. 16 (2016) 5831–5835.
[159] G.L. Xing, T.T. Yan, S. Das, T. Ben, S.L. Qiu, Synthesis of crystalline porous organic salts with high proton conductivity, Angew. Chem. Int. Ed. 57 (2018) 5345–5349.

Luyi Chen received his Ph.D. degree in polymer physics and chemistry from Sun Yat-sen University in 2017. Recently, he joined in Prof. Yue-peng Cai and Prof. Qifeng Zheng's group as a research scientist in the school of chemistry at the South China Normal University (SCNU). His research interests focus on the design and synthesis of porous materials including porous polymer materials, porous carbon materials, and metal-organic frameworks, and their applications for lithium batteries.

Kui Ding received his Ph.D. degree in chemistry from Shanghai Jiao Tong University in 2020. Thereafter, he joined in Prof. Yue-peng Cai and Prof. Qifeng Zheng's group as a research scientist in the school of chemistry at SCNU. His current research interests focus on the design and synthesis of high-performance electrolytes for rechargeable batteries with high energy density and high safety.

Kang Li is current a research scientist in the school of chemistry at SCNU, China. He received his Ph.D. degree in material physics and chemistry under the supervision of Prof. Cheng-Yong Su from Sun Yat-sen University in 2014. His research interests focus on supramolecular metal-organic materials such as metal-organic frameworks (MOFs), metal-organic gels (MOGs), metal-organic cages (MOCs) and their applications for host-guest recognition, supramolecular catalysis, and energy storage and conversion.

Qifeng Zheng received his BS degree in Chemistry from Xiamen University in 2012, and Ph.D. degree in Materials Science from University of Wisconsin-Madison in 2017. Thereafter, he joined in The University of Tokyo and served successively as a Project Researcher and JSPS Fellow. Since Nov. 2019, he has become a professor of chemistry at SCNU. His research mainly focuses on developing high-performance electrolytes for rechargeable batteries with high energy density and high safety.

Yue-Peng Cai received his Ph.D. degree in 2002 from Sun Yat-Sen University, under the supervision of Prof. Bei-Sheng Kang. He became a professor of chemistry at SCNU since 2004, and served as dean of the School of Chemistry at SCNU since 2019. His current research interests focus on the synthesis of crystalline porous materials (MOFs and COFs) and their applications in energy storage as well as the storage and separation of small molecules.

Ya-Qian Lan received his BS and Ph.D. degree (2009) from Northeast Normal University under the supervision of Prof. Zhong-Min Su. In 2010, he worked as a JSPS postdoctoral fellow at National Institute of Advanced Industrial Science and Technology (AIST, Japan). Since the end of 2012, he has been a professor of chemistry at Nanjing Normal University (NNU, China). He joined SCNU in 2021. His current research interests focus on the synthesis of new crystalline materials and catalytic research related to clean energy applications.